NOTICE

The quality of this microform is heavily dependent upon the quality of the original thesis submitted for microfilming. Every effort has been made to ensure the highest quality of reproduction possible.

If pages are missing, contact the university which granted the degree.

Some pages may have indistinct print especially if the original pages were typed with a poor typewriter ribbon or if the university sent us an inferior photocopy.

AVIS

La qualité de cette microforme dépend grandement de la qualité de la thèse soumise au microfilmage. Nous avons tout fait pour assurer une qualité supérieure de reproduction.

S'il manque des pages, veuillez communiquer avec l'université qui a conféré le grade.

La qualité d'impression de certaines pages peut laisser à désirer, surtout si les pages originales ont été dactylographiées à l'aide d'un ruban usé ou si l'université nous a fait parvenir une photocopie de qualité inférieure.

Canada

FRICTION DAMPED BRACED FRAMES

Parvaneh Baktash

A Thesis
In the
Centre for
Building Studies
Faculty of Engineering

Presented in Partial Fulfillment of the Requirements
for the degree of Doctor of Philosophy at
Concordia University
Montreal, Quebec, Canada

January 1989

ISBN 0-315-49053-5

ABSTRACT

FRICTION DAMPED BRACED FRAMES

Parvaneh Baktash

The design of structures subjected to seismic forces has the objective not only to reduce the risk to life, but also to reduce secondary damage by controlling peak accelerations and deflections.

This study deals with the friction damped braced frame, which possesses many advantages in the seismic design of steel structures.

The system utilizes a friction device in the bracing to dissipate energy mechanically. The joints resist the action of normal service loads and moderate earthquakes, but will slip during high seismic excitation.

Friction devices were incorporated in the following types of braced frame:

- Z-Braced Frames
- K-Braced Frames
- X-Braced Frames

Nonlinear dynamic analysis was performed on these structural systems and the results were compared with the computed response of the following frames without friction dampers:

- Moment Resisting Frames
- Concentric Braced Frames using X-Bracing

K-Bracing, with consideration of post buckling behaviour of braces

- Eccentric Braced Frames

A steel model was designed, and tested on a shaking table. A spring loading device was developed to create a known slip force in the joints. By varying the slip force the model could be made to exhibit the behaviour of a moment resisting frame (zero slip force), a friction damped braced frame, or a concentric braced frame (no slip in the device).

The tests indicated that friction damped braced frames have stable, unpinched hysteretic loops, and the behaviour correlated well with the computer prediction.

A direct method to calculate the optimum slip force is presented, and validated by the theoretical and experimental results.

This study shows the superiority of the optimised friction damped braced frames over the other systems studied.

ACKNOWLEDGEMENTS

ACKNOWLEDGEMENTS

I would like to express my sincere thanks to Professor Cedric Marsh, my supervisor and advisor, for his guidance and help throughout this study.

Additional thanks are due to Mr. J. Zilka, lab technician, who aided me on numerous occasions during the experiments, to Dr. Avtar Pall for his valuable advice, and to Marshall Steel Limited for the steel test model. This research project was made possible through grants from the Natural Sciences and Engineering Research Council of Canada.

TABLE OF CONTENTS

TABLE OF CONTENTS

LIST OF FIGURES

LIST OF FIGURES

LIST OF SYMBOLS

LIST OF SYMBOLS

A	Cross Sectional Area
b	Bay Width
[C]	Damping Matrix
e	Length of Eccentric Beam
E	Modulus of Elasticity
h	Storey Height
H	Building height
K	Stiffness
[K]	Stiffness Matrix
[M]	Mass Matrix
M_p	Limiting Moment
M_p^*	Plastic Moment Capacity of the Flanges of the Beam
P	Load
P_c	Compression Force
P_s	Slip Force
P_t	Tension Force
q	Slip Force per Unit Length
r	Displacement
$\dot{\sigma}$	Velocity
$\ddot{\sigma}$	Acceleration
R	Load in Column
R_x	Load in Column at Distance X
T	Period of Vibration
V	Total Shear Force

V_b	Shear Resisted by the Bracing
V_f	Shear Resisted by the Frame
W_f	Energy Dissipated by Friction
σ°	Ground Acceleration
α, β	Mass, Stiffness Dependent Damping
α	Angle
λ	Critical Damping

CHAPTER 1

INTRODUCTION

INTRODUCTION

1.1- GENERAL

Structures in seismic regions must be designed not only to withstand large lateral forces, so as to reduce the risk of human loss, but also to minimize secondary damage and economic deprivations.

Certain basic requirements are to be fulfilled in the design of earthquake resistant structures. First, the structure should stay elastic under wind forces, and moderate earthquakes. This is met by controlling the storey drift and providing the required strength for the structure. Second, the structure should not collapse during a major earthquake. Inelastic deformations are allowed so long as the structure does not suffer major structural damage which can endanger human life. This is presently required by most codes and the requirement can be met using traditional structural systems. However, it is being increasingly recognized that there is a further requirement to minimize the secondary damage to the building envelope and its furnishings, so as to minimize economic losses.

One of the most effective methods available to absorb the energy fed into the structure is undoubtedly the use of sliding friction joints.

The first requirement is met before slipping occurs. The second requirement is satisfied by giving the frame sufficient strength. To minimize building acceleration, distortion and non-structural damage, energy must be dissipated, and the friction device has been shown to be one of the best methods.

A sliding friction device is made up of steel plates held together by high tension bolts in slotted holes, with flat brake lining pads trapped in between. Slip occurs at a predetermined load, giving the device a rectangular hysteretic loop, as shown in Fig. 1.1 (1). A friction device limits the force in the joint, behaving as a "fuse"; after slipping it acts as a damper. The system is thus ideal for dissipating energy caused by seismic forces.

This chapter gives a general survey of the possible uses of friction devices in buildings, and then discusses the other methods of energy dissipation in buildings. In chapter 2, means of establishing the optimum slip force in friction damped braced frames, FDBF, and coupled braced shearwalls are proposed. In chapter 3, dynamic analyses of various types of bracing with friction dampers are reported, illustrating the optimum slip force. Other types of steel framed and braced building are then compared with the optimised FDBF. Finally, chapter 4 describes static and dynamic tests conducted on a large model of a friction damped braced frame.

1.2- SOME PROPOSED APPLICATIONS OF FRICTION DEVICES IN BUILDINGS

1.2.1- JOINTS BETWEEN CONCRETE SHEAR WALLS

Concrete shear walls are very stiff and they are widely used in tall buildings for their lateral rigidity. They perform well under wind loads and moderate earthquakes, but during high seismic forces their performance is dependent on the material and detailing, as survival relies on the ductility of the structure. Even though concrete shear walls may possess good ductile behaviour (2,3), energy is dissipated by cracking concrete and yielding reinforcing bars, causing permanent damage.

To avoid this damage a friction joint to connect shear walls was et al developed at Concordia University by Pall et al (1). Tests on an earthquake bed were conducted (in 1981), on a model of a shear wall incorporating friction devices (4,5). The efficiency of these devices was demonstrated in comparison with the two extreme cases of isolated walls (zero slip force in the joints), and the monolithic wall (no slip in the joints). The experimental set up is shown in Fig. 1.2 (5).

In a practical application the shear walls are anchored to the foundation and act as independent vertical cantilevers joined by friction devices, in the style of a leaf spring. The sliding joints consist of steel plates, anchored into the edges of the shear walls, to which are bolted plates with slotted holes, shown in Fig. 1.3 (6). The slip load is sufficient to resist wind loads and moderate seismic forces, but under higher lateral inertial forces caused by earthquake, the shear force in the vertical interface causes the joints to slip, extracting energy by friction.

Any set of walls with fix bases which form an "L", "I", or "box" shape can be interconnected by a vertical line of friction devices.

1.2.2- CONNECTIONS OF CURTAIN WALLS AND INFILL PANELS

Frames may support vertical interior or exterior rigid panels for the vertical surfaces, which can contribute to the shear strength and stiffness of the structure. The connection of these panels can be made using friction devices to act as energy absorbing elements. Figure 1.4 shows how sliding panels may incorporate friction joints in horizontal connections or vertical connections.

1.2.3- BASE ISOLATION

If buildings were designed in such a fashion that the ground move independently from the building, the force exerted on the building by the ground motions would be eliminated.

By using sliding friction supports between the foundation and the superstructure, the friction will resist forces due to wind and minor earthquakes but the building will be partly isolated from the ground motion during severe earthquakes, as the force applied to the base of the building will be limited to the slip load. The support may allow the building to move in any direction, and may provide a rising resistance, as the displacement increases, by using ramped or dished friction surfaces as seen in Fig. 1.5 (7) in order to control the maximum movement.

Conventional base isolation systems slide on teflon or roller bearing, control the motion by means of springs, and absorb the energy by lead, rubber or dash-pots. The friction support could clearly be less costly.

It is preferred that there be no uplift so the aspect ratio of the base isolated buildings should be small (height/base width < 3), thus leading to applications mainly in low-rise buildings.

1.2.4- CONNECTIONS IN STEEL FRAMED BUILDINGS

The system which is the concern of this report utilizes friction devices in the connections of the bracing (8,9,10,11). The system was originally developed by Pall and Marsh (8), at Concordia University, where tests have been conducted since 1982. Other research centres which have taken up these

studies, following the lead of Concordia University, are:

- The University of British Columbia (12);
- The University of California, Berkeley (13, 14), using the computer aided design environment Delight Struct. (15); and
- Imperial College, London.

Said studies demonstrate the efficiency of friction damped devices when they are incorporated in braced frame structures.

In order to judge the value of this device it is necessary to understand how traditional steel buildings perform in earthquakes. This will be discussed in the following section.

1.3- THE BEHAVIOUR OF STEEL FRAMED BUILDINGS

1.3.1- MOMENT RESISTING FRAMES (MRF)

A moment resisting frame is a rectangular skeleton frame with rigid joints. These structures have stable ductile behaviour under cyclic loading, and energy dissipation is achieved by plastic bending of the beams.

Ductility is a feature of these structures, and they often have an unpinched hysteretic loop. Fig. 1.6 (16) shows the load-deflection loops for successive cycles of loading on a joint in a moment resisting frame. The consistency of the loops shows that there is no detericration in the joint after a few cycles. However, because of the large deflections after yielding, the stability of these structures is affected by the P-Δ factor, and "damage" is permanent.

1.3.2- BRACED FRAMES

Bracing members are used in framed structures to provide resistance against lateral forces. This type of structure is more economical than a rigid frame, since it is cheaper to resist the lateral forces by braces than by the moment resistance of the frame alone.

Single braced moment resisting frames are initially stiff, but after bucking or yielding of the braces, they behave as ductile frames.

Axially loaded members under the action of cyclic tension and compression have only a limited capacity for energy dissipation, due to their deteriorating hysteretic loops. Fig. 1.7 shows the typical pinched loops for a single brace (25).

A number of studies have been made on braced frames, both experimental and theoretical (18,19,20,21,22,23,24,25). The cyclic inelastic behaviour involves yielding in tension and buckling in compression of the individual bars. The force-displacement relationship has been divided into seven zones, as shown in Fig. 1.8 (24). Successive cycles have characteristics similar to the first cycle, except for the new starting point, the reduction in the buckling load, and the increasing deflection of the building.

Fig. 1.9 (25) shows the behaviour of a cross-braced frame in which each brace behaves in the manner described, illustrating the reduced capacity after a few cycles. Failure of a cross braced frame occurs when one brace ruptures in tension.

As a result of many uncertainties in the evaluation of the response of these structures, designs have been developed which combine the ductility of moment resistant frames and the stiffness of braced frames. In Japan, the braces are often designed to carry a portion of the lateral forces (18), while the remainder of the lateral forces is carried by the moment resistance of the frame.

1.3.3.- ECCENTRICALLY BRACED RIGID FRAMES (EBF)

Various types of eccentric braced frames have been suggested in which energy is dissipated by local yielding at the eccentric joint. Fujimoto et al (26) studied an eccentric K-braced frame, seen in Fig. 1.10 (a), where the braces (diagonals) are offset at the beam centre and energy is dissipated by yielding in the central section of the beam. This system gave an unpinched hysteretic loop, but large deflections caused considerable damage to the floor slab.

Hisatoku et al (27) suggested the frame shown in Fig. 1.10 (b). An unpinched hysteretic loop is obtained for reversals of yielding in the vertical studs, but severe distortions occurred at the mid-span of the beam.

In the eccentric braced frame developed by Roeder and Popov, the intersection of the diagonals with the horizontal beams is offset from the column, as seen in Fig. 1.11 (28). The energy is dissipated by shear yielding in the web of the beam between the brace and the column (18,19,20,28). Braces are required to be strong enough not to buckle, and are usually designed with a 50% margin, making them much stronger that would be required for wind forces only (19). Stiffeners are required to avoid shear instability in the web (Fig. 1.12). As in all systems which rely on the yielding of the structure to absorb energy, there will be large permanent deformations caused by the seismic forces, requiring major repairs. Figure 1.13 shows the damaged beam after severe cyclic loading.

1.3.4- FRICTION DAMPED BRACED MOMENT RESISTANT FRAMES (FDBF)

In friction damped braced frames, which form the subject of this study, each brace is connected by a friction joint which will slip at a predetermined value of the shear force. It is designed not to slip under the action of wind forces or minor earthquakes, but, under severe seismic activity, it will slip and dissipate energy while maintaining a constant resisting force. The shear resistance of the building rises as the moment resisting frame is brought into action. This increasing resistance is linear up to the first yield in the frame. Up to this point the frame is elastic and no permanent damage has been done to the structure. It is for this condition that the slip forces are optimized. Any yielding of the frame provides an additional source of energy dissipation, giving a margin of security not available in other framing schemes.

Friction joints may be used in any type of braced frame. Those examined in this study are:

I. Tension-compression braces (K or Z bracing):

The device is active in tension and compression and the braces are designed not to buckle. Figure 1.14 shows some arrangements in which the sliding occurs either along the diagonals themselves or along the beams or columns.

II. Tension only braces (X bracing):

To provide a system requiring only tension members, a mechanism was proposed by Pall and Marsh (8), Fig. 1.15, in which, when slip occurs due to tension in one of the braces, the four link mechanism is activated, thereby forcing the other diagonal within the mechanism to slip simultaneously, and thus causing the second brace to shorten. On reversing the load, the other brace accepts the tension. In this kind of tension bracing, the energy is dissipated in both half cycles, while acting in tension only.

III. Coupled braced frames:

Independent bays of braced frames can be connected together by sliding friction devices, shown in Fig. 1.16. The concept is similar to that of coupled concrete shear walls.

1.4- OBJECTIVES OF THE RESEARCH

It is evident that an energy dissipating device that relies on mechanical means such as friction is to be preferred to one in which structural damage must be suffered to provide the required damping. That sufficient energy can be dissipated by friction before any yielding occurs, so as to give the same control over the building motions as is achieved by the more destructive means of damping, has been demonstrated by Pall and Marsh (8). It was now necessary to find a means of establishing the optimum value for the slip force, and to compare the resulting design with the best of the current framing methods, under various earthquake conditions.

The study has thus three main objectives:

1. To establish that an optimum slip load can be rationally derived, and to demonstrate the validity of the values predicted, by both theoretical and experimental means.

2. To make theoretical comparisons with other structural systems, showing the relative behaviour of the friction damped system.

3. To conduct static and dynamic tests on joints and braced frames to provide information on the actual behaviour.

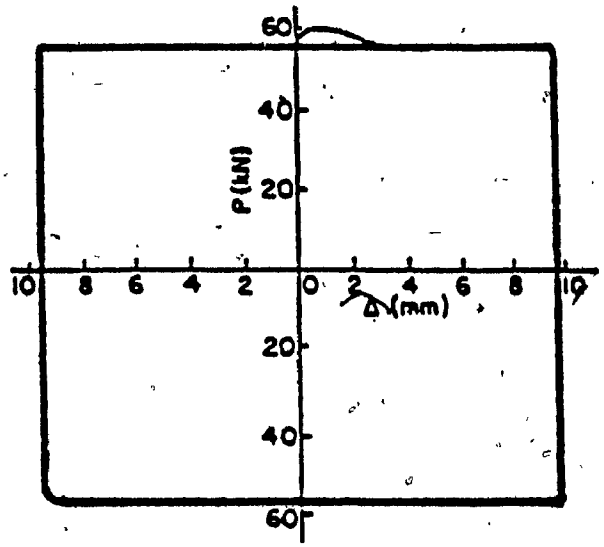

FIG. 1.1 Hysteretic Loops of Friction Joints Using Brake Lining Pads (1)

FIG. 1.2 Overall View of the Model of Shear Wall Incorporating Friction Joints (5)

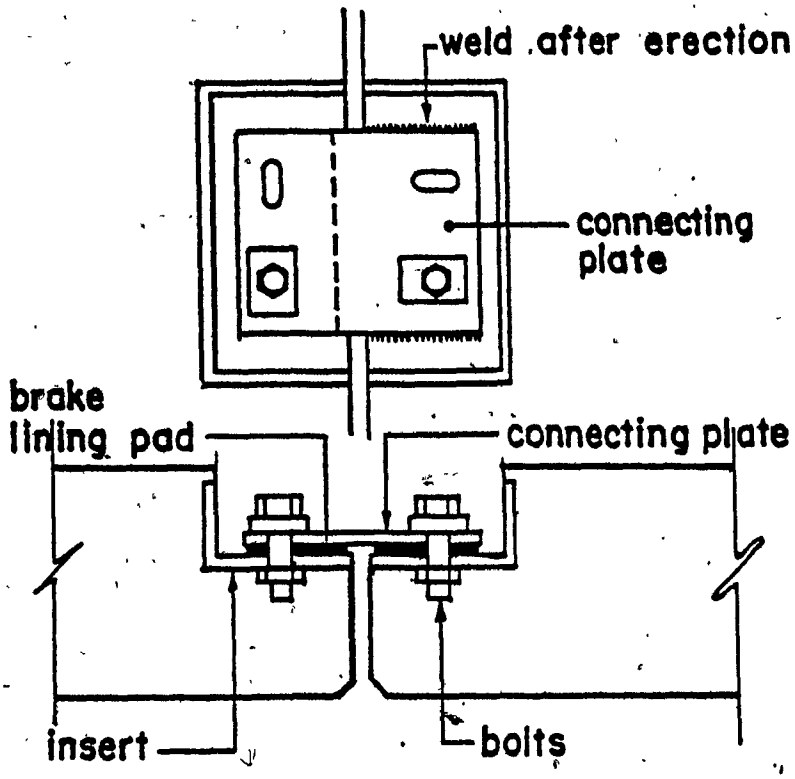

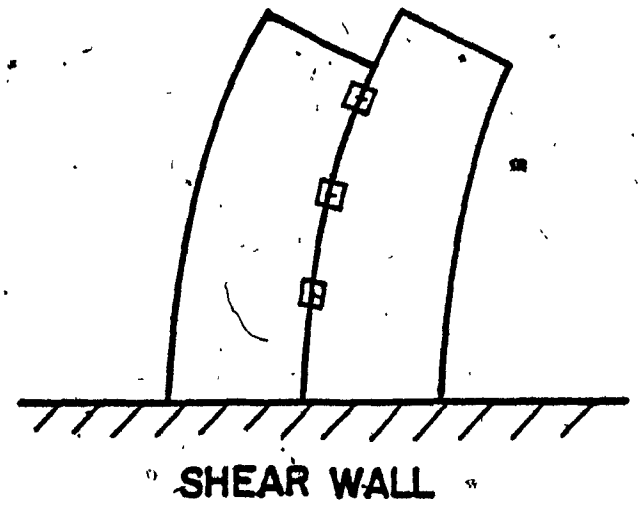

FIG. 1.3 Friction Joints in Coupled Shear Walls (6)

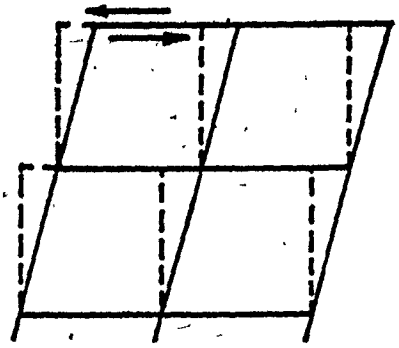

CONNECTIONS TO STRUCTURE SLIDING HORIZONTALLY

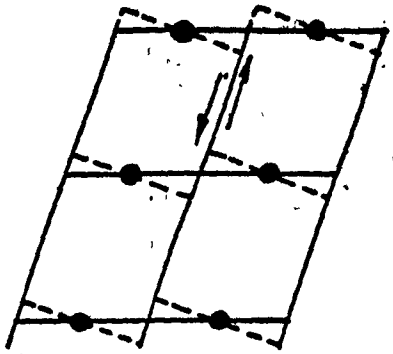

CONNECTIONS BETWEEN PANELS SLIDING VERTICALLY

FIG. 1.4 Sliding Panels

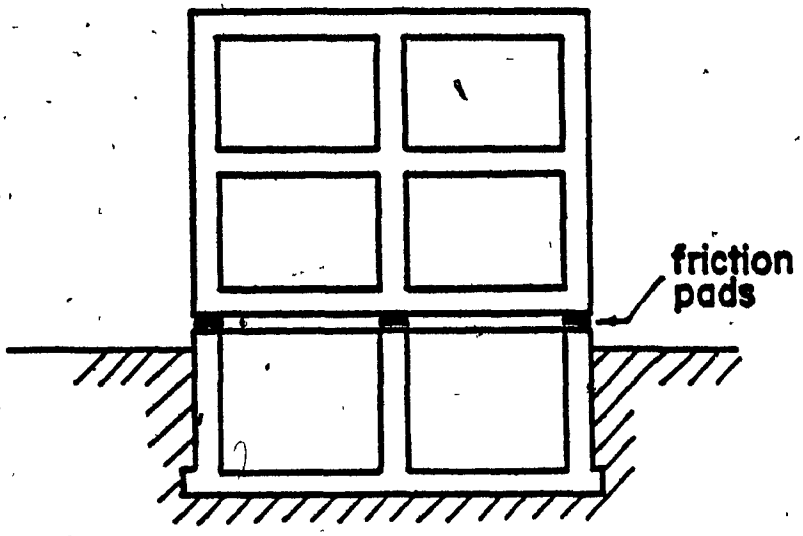

SLIDING SUPPORTS FOR LOW RISE BUILDINGS

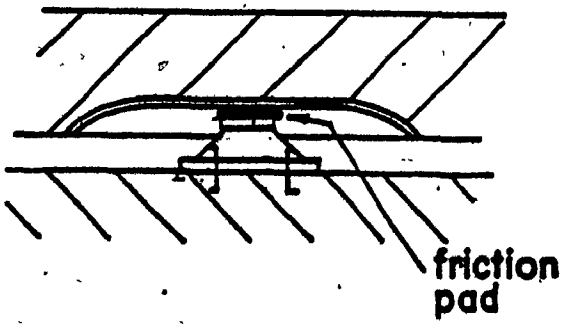

- DISHED SLIDING SUPPORT

FIG 1.5 Low Rise Building Incorporating Sliding Friction Support (7)

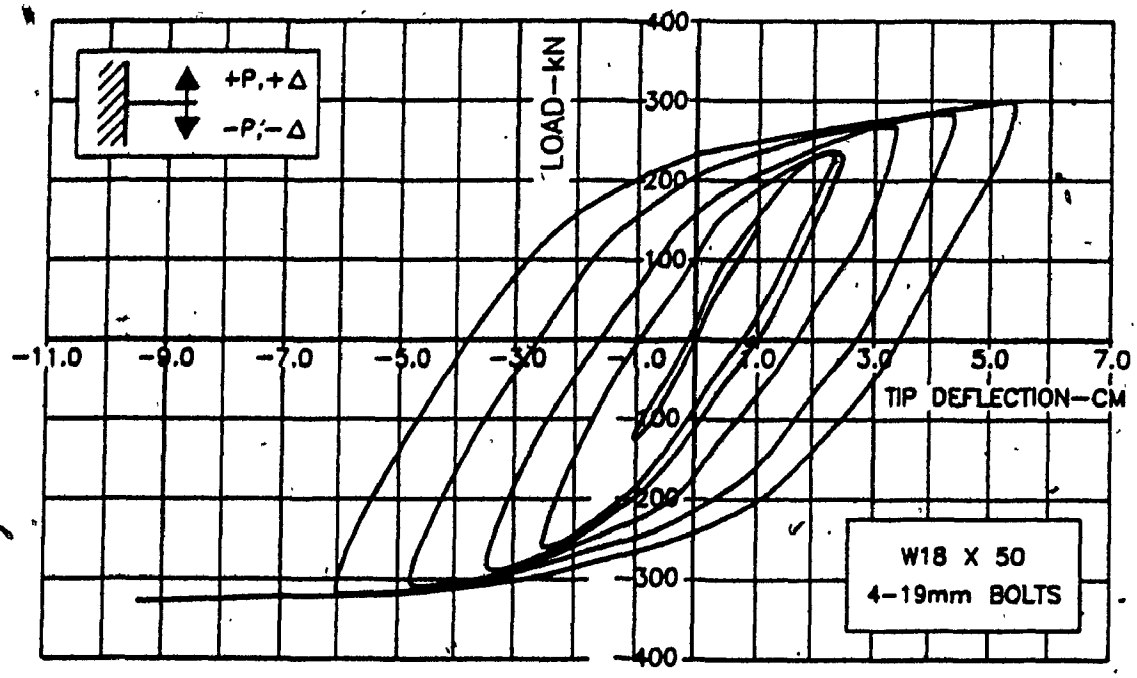

(a)

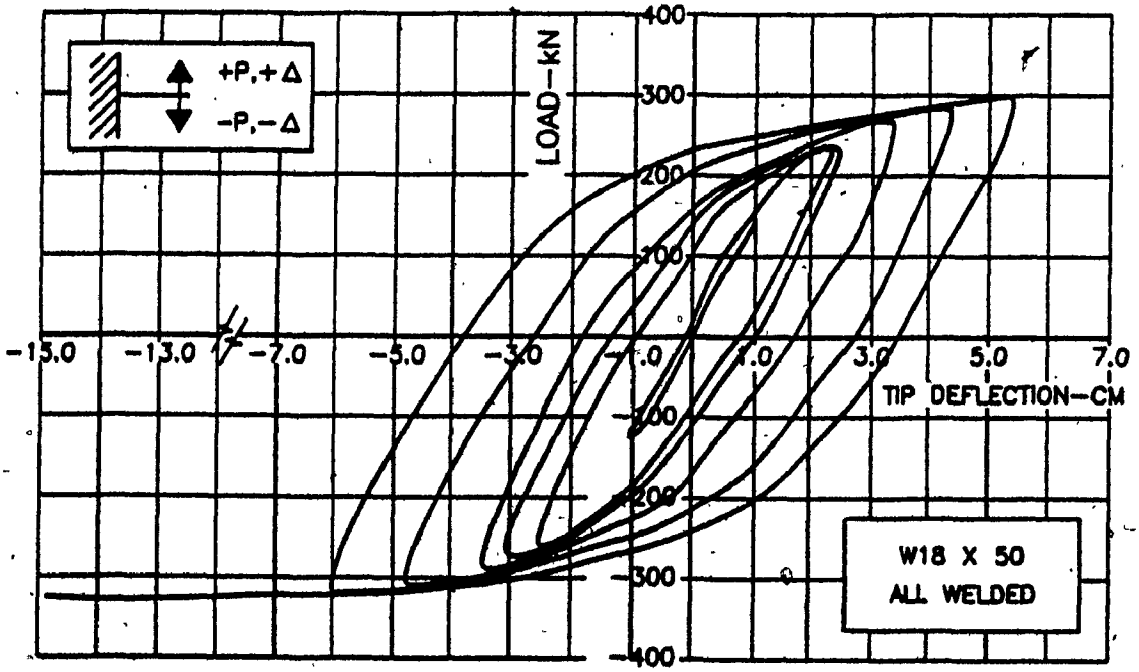

(b)

FIG. 1.6 Load Deflection Hysteretic Loops for 2.44m W18 x 50 Cantilevers Simulating
a) Exterior Connection with Welded Flanges and Bolted Web,
b) All Welded Connections (16).

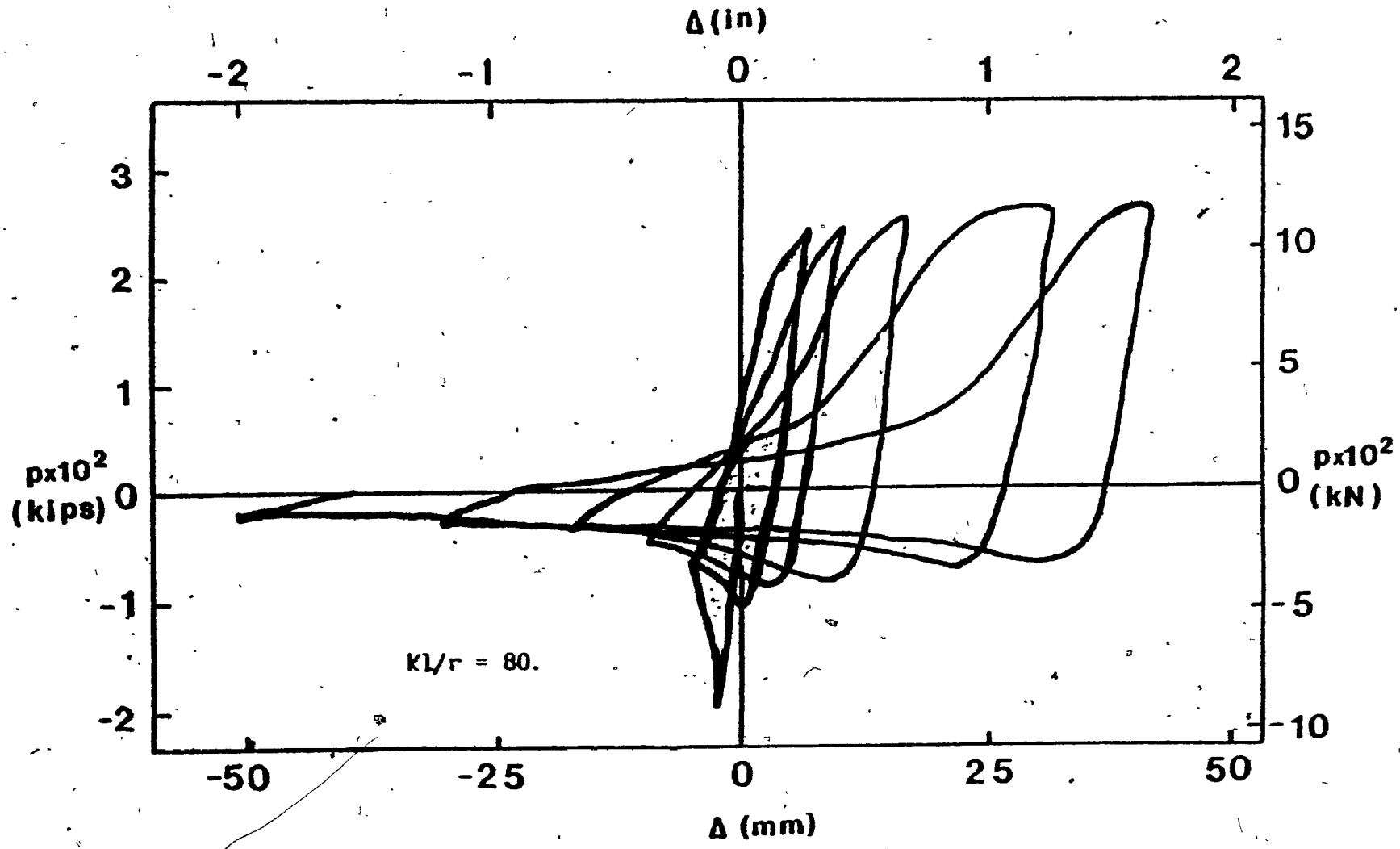

FIG. 1.7 Typical Experimental Load/Axial Deformation Relationship for a Slender Bar (25)

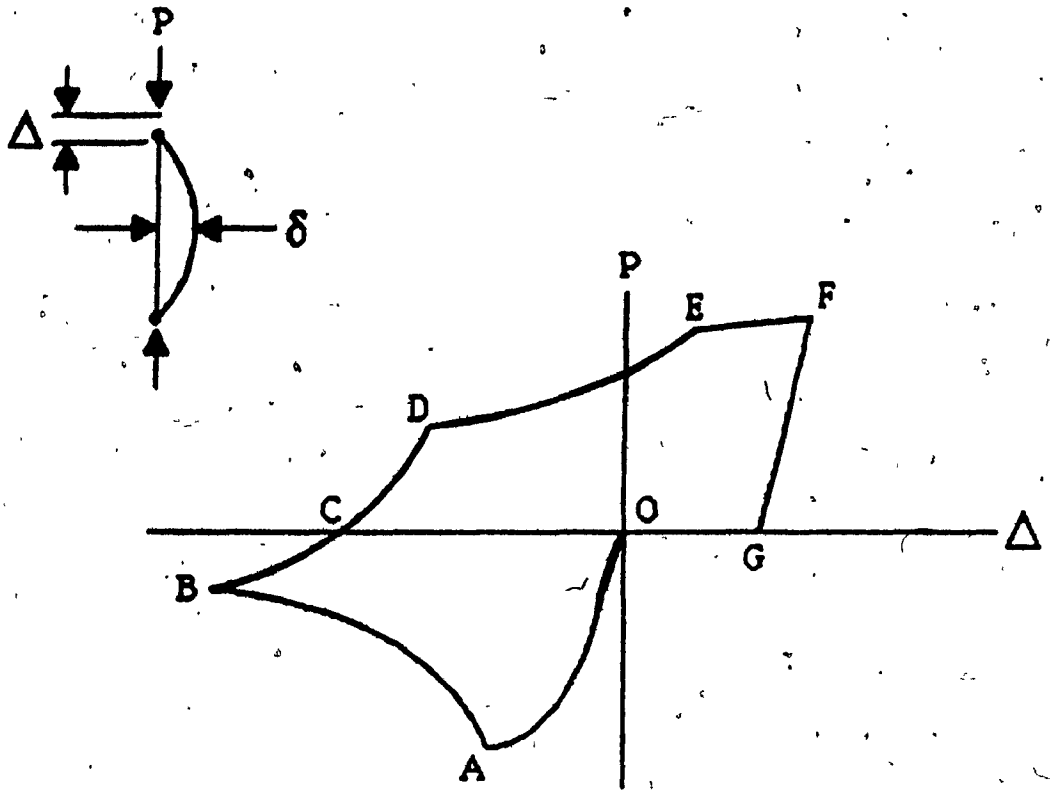

A) HYSTERETIC BEHAVIOR

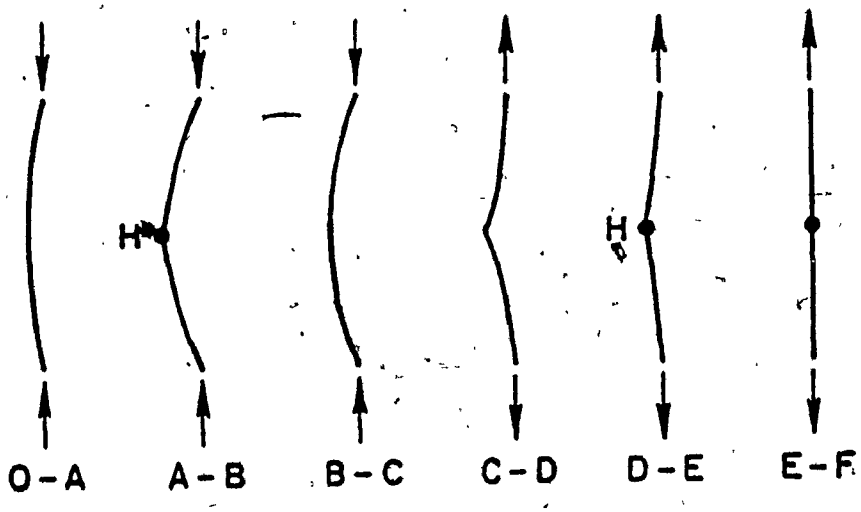

B) ZONES OF BEHAVIOR

FIG. 1.8 Typical Theoretical Load/Axial Deformation Relationship for a Slender Bar (24)

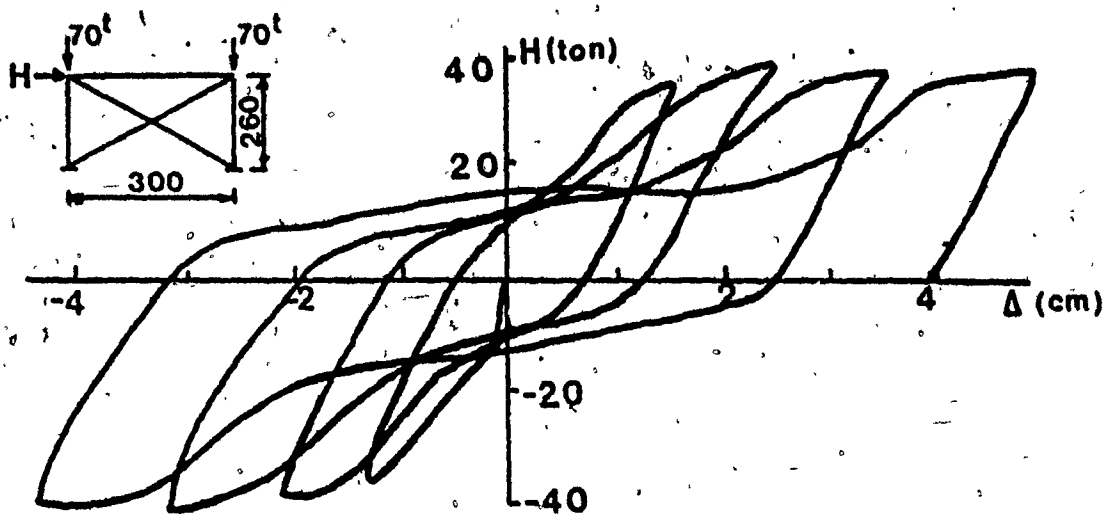

FIG. 1.9 Typical Pinched Hysteresis Loops for a Cross-Braced Frame (17)

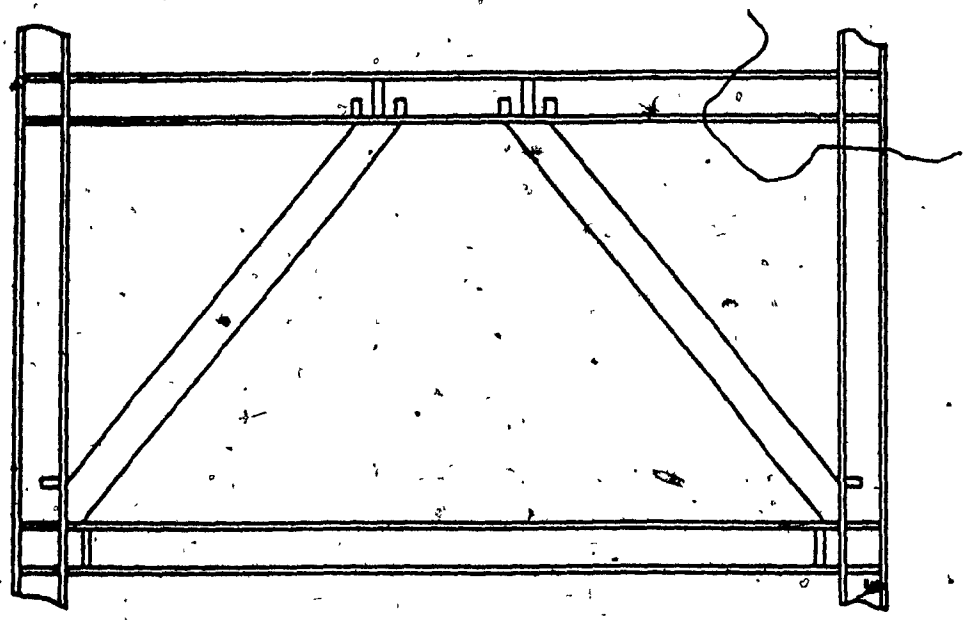

(a)

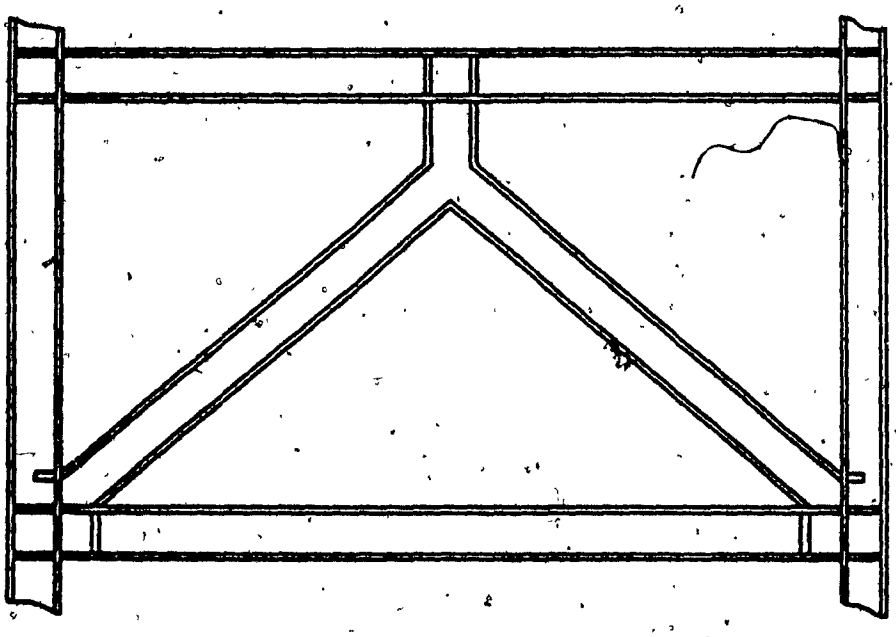

(b)

FIG. 1.10 Types of Eccentric K-Braced Frames (26, 27)

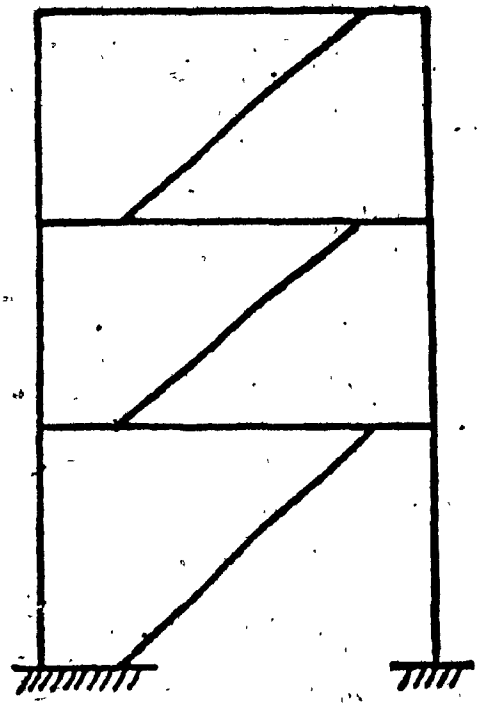

FIG. 1.11 Eccentric Z-Braced Frame (28)

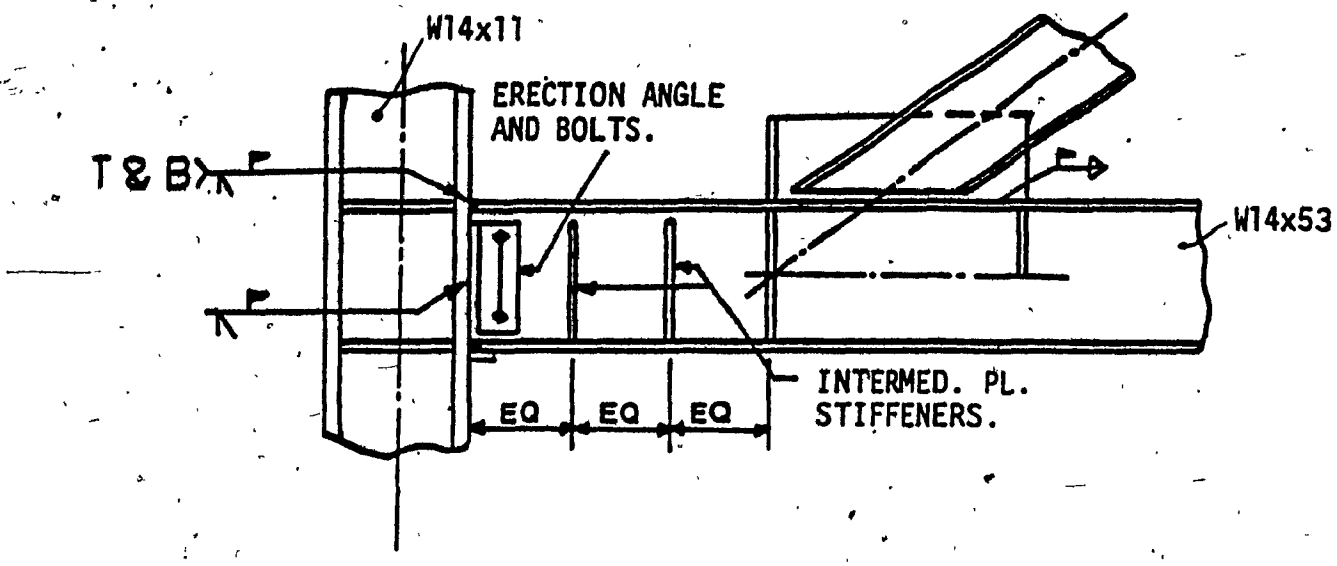

FIG. 1.12 Eccentric Braced Frame (Suggested Detail for a Shear Link with Web Stiffeners) (19)

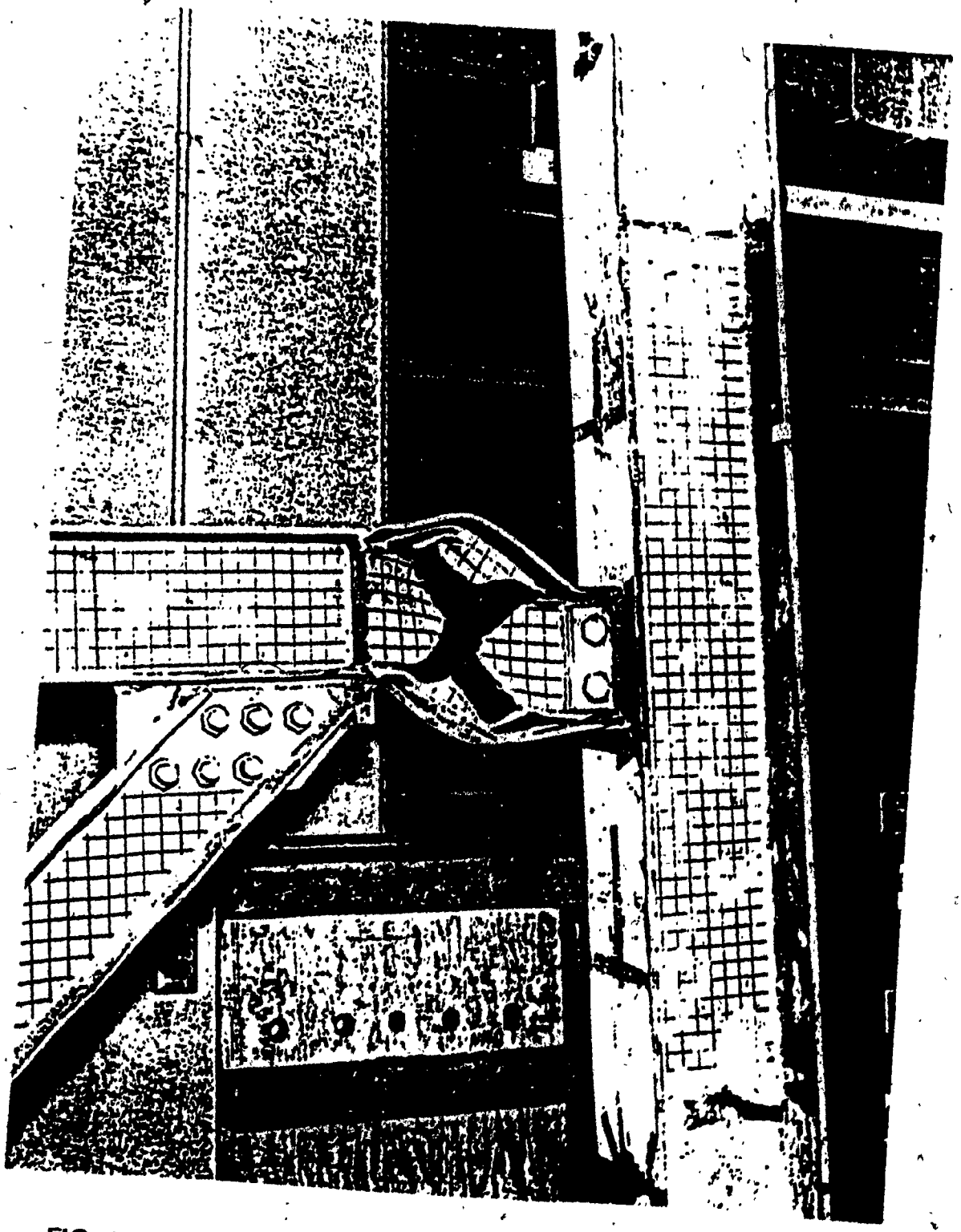

FIG. 1.13 Photograph of the Torn Eccentric Element (19)

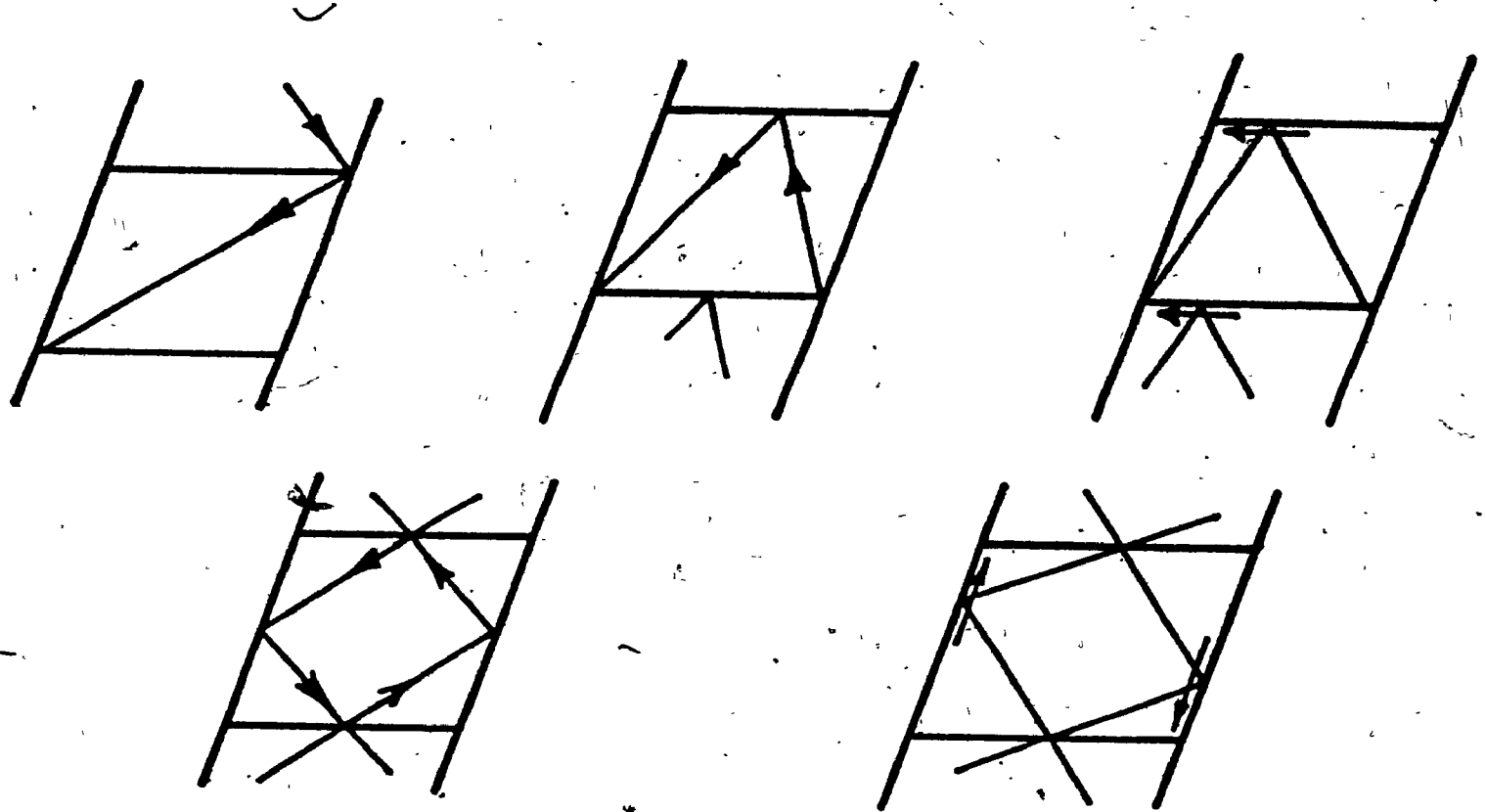

FIG. 1.14 Some Arrangements for Friction Joints in Tension - Compression Bracing

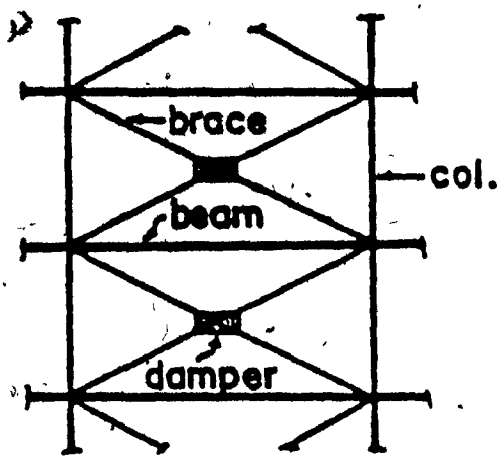

a) Location of Friction Device (damper)

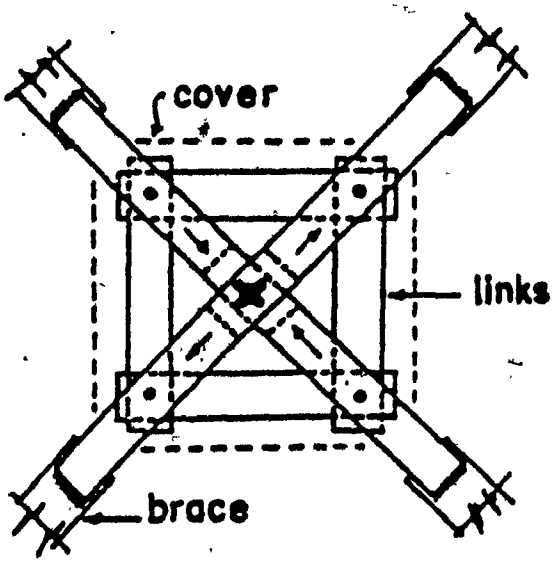

b) Mechanism of Friction Device

FIG. 1.15 Friction Damped Braced Frame (Tension Only Bracing) (8)

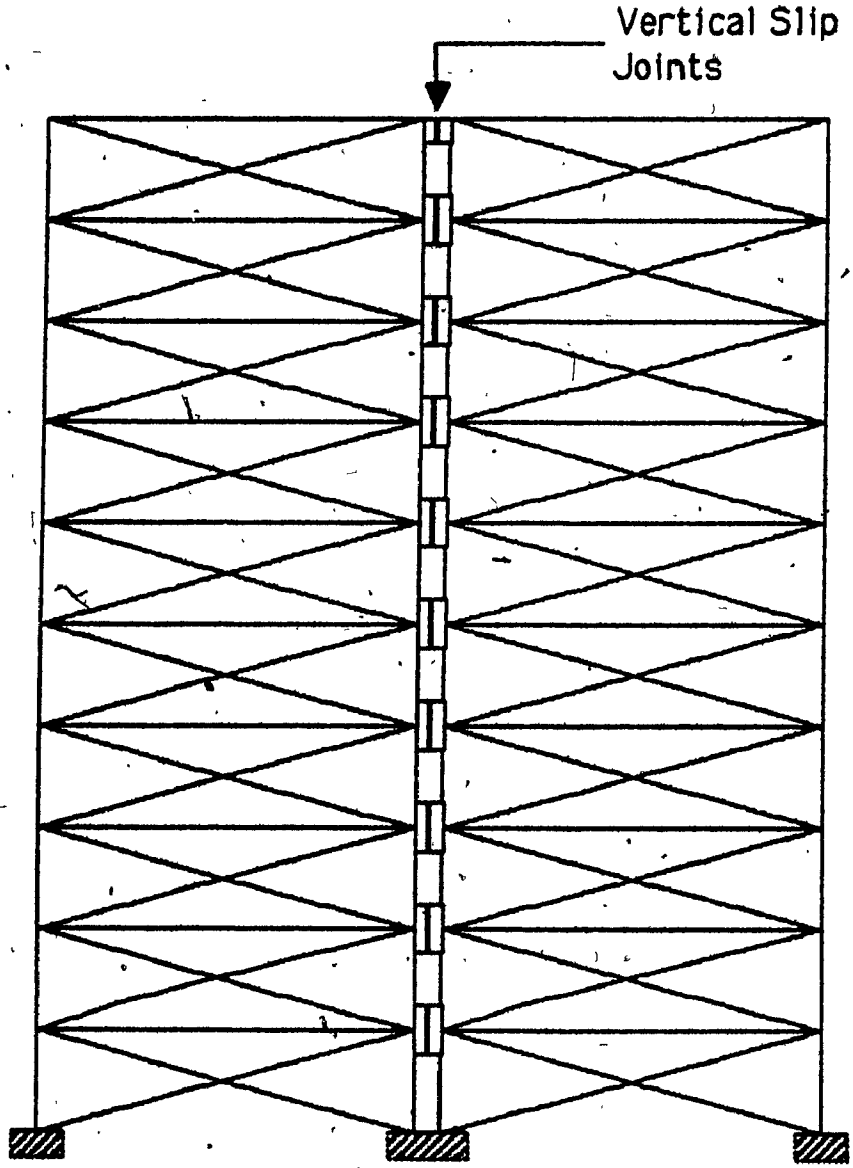

FIG 1.16 Coupled braced frames

CHAPTER 2

OPTIMISATION

2. OPTIMISATION

2.1- GENERAL

In this chapter a method is derived to determine the optimum slip load, based on the maximum energy that can be dissipated while the system is still elastic, i.e. up to yielding in the structural frame. The method is expected to provide a useful design tool for preliminary design, since it does not require computer analysis.

2.2- OPTIMUM SLIP LOADS

2.2.1- BRACED FRAMES

The force/deflection relationship for a framed structure with slipping bracing is assumed to be rigid up to first slipping of the bracing connection and then to be linearly rising as the resistance of the frame is brought into action. The energy dissipated as the friction joint slips is given by the product of the slip force and the distance travelled. To determine that slip force which will best serve the purpose of reducing the amplitude of the response of the structure requires a decision on the nature of the values to be optimized.

It is assumed that a moment resisting frame has been designed to resist wind forces and other specified live loads. Diagonal bracing is then introduced into the frame with a view to improving the response to seismic forces. As the bracing is much more rigid than the frame action, the full wind force must now be resisted by the bracing. If the bracing connections

slip at a predetermined force, allowing the frame action to come into play, it is assumed that the lateral forces can be increased until, at some location in the frame, the yield moment is reached. Up to this point the frame remains elastic and no permanent damage is done. The bracings are designed not to yield or buckle under the action of the slip force.

There are two approaches to optimization:

1. For a given earthquake motion, the slip force is adjusted such that the response of the structure is minimized in terms of deflection. In this case the slip force is a function of the type and intensity of the earthquake, and will vary with the specified ground motion. It is related to the elastic properties of the structure, not to its strength, as no yielding is expected to occur.

The only means of obtaining such an optimum slip force is by trial runs on a computer, using a programme such as DRAIN 2D (29), with the specified earthquake as input.

2. With the given frame, a slip force is chosen such that the maximum amount of energy will have been dissipated when the yield moment is reached at some locations in the frame. By this approach it is anticipated that the intensity of the earthquake that the structure can resist, without causing permanent damage, will be maximized.

The optimum slip force is then a property of the structure, unrelated to the type or intensity of seismic activity.

If, for the given frame, for the maximum intensity of earthquake that can be resisted without yielding, the two approaches give the same slip force, then the following simple procedure of maximizing energy dissipation on the basis of a static analysis becomes a very attractive preliminary design method.

Consider a single storey of a multi-bay framed structure with one or more bays of bracing. After the braces have slipped, let:

V_b = shear resisted by the bracing

V_f = shear resisted by the frame

The total shear is then:

$$V = V_b + V_f \qquad 2.2.1.1$$

The building frame provides a shear resistance that is limited to some pre-established value. It is also assumed that the columns can resist the applied moments and axial forces for all conditions of loading and structural behaviour.

Let the rigidity of the frame be K, such that the shear resisted by the frame action is given by:

$$V_f = K\Delta \qquad 2.2.1.2$$

Where Δ = shear deflection of the storey.

Elastic deformation prior to slipping is neglected.

In the quarter cycle from first slipping to reaching the limiting shear force in the frame, the shear force resisted by the frame rises from zero to V_f, while the shear force resisted by the bracing remains constant at V_b, Fig. 2.1.

The slip travel is proportional to the shear deformation of the frame after slipping occurs. The force resisted by the frame is $(V - V_b)$ and the deflection is thus:

$$\Delta = (V - V_b)/K \qquad 2.2.1.3$$

The energy dissipated by friction is then:

$$W_f = V_b \Delta = V_b (V - V_b)/K \qquad 2.2.1.4$$

This is a maximum when:

$$V_b = V/2 \qquad 2.2.1.5$$

At the limit of elastic behaviour, the total shear force is shared equally between the bracing and the frame, thus:

$$V_b = V_f = V/2 \qquad 2.2.1.6$$

Because the purpose of friction devices is to prevent permanent damage, the limiting value of V_f across a multi-bay storey is deemed to be that which causes first yield, or a fully plastic moment if preferred.

For a simple, single bay frame, using the simplifying assumption of a point of contraflexure at mid-height of the columns in each storey, and based on a weak beam/strong column design, the shear force resisted by the frame action is related to the limiting moment in the beams by:

$$2M_p = V_f.h \qquad 2.2.1.7$$

Where h is the storey height, and M_p is the limiting moment in the beam.

The shear force at which the bracing connections slip is then:

$$V_b = V_f = 2M_p/h \qquad 2.2.1.8$$

This optimum slip condition, as defined, is a structural property. For earthquakes of lesser intensity than that which will cause incipient yielding of the beams, the slip force is not optimum in the sense that it will minimize the response, but it will ensure that the structure remains elastic.

At the extreme deflection, the energy that has been dissipated by friction is given by:

$$W_f = V_f^2/K \qquad 2.2.1.9$$

This is double the elastic energy due to the shear distortion in the frame.

The shear force is shared equally between the braces and the frame at first yield. If the building continues to deflect, the energy absorbed by the yield hinges will be added to that dissipated by the friction joints. Should a sufficient number of hinges be formed to make the frame a mechanism, the total rate of energy dissipation will be double that of the friction joints at the storey where the mechanism is formed.

If a rigid frame is already of sufficient strength to withstand the forces from a specified intensity of earthquake, and it is planned to add bracing with friction joints to minimize the accelerations (deflections) during an earthquake, then the simple analysis for the value of the optimum slip load does not apply directly. On the other hand, this reasoning shows that the optimum slip force would give equal sharing of the shear force, created by the design earthquake, between the two systems. The optimum slip force in this case is determined by computer analysis for the specified earthquake intensity, as the maximum shear force is not initially known.

The preceding reasoning was based on the limiting extreme excursion. For much of the period of an earthquake the building behaves elastically, and does not call on the friction devices. The question arises as to whether the static optimum value is valid for the random action of the building during an earthquake. In the following chapter dynamic analysis is used to provide an answer.

It is to be observed that in a braced frame, with friction joints in the bracing, there are two structural systems acting in parallel, and the manner in which they share the lateral shear force can be optimised. In moment resisting frames which incorporate eccentric joints, there is only one system, which has a limiting shear capacity, and an optimizing procedure of the type discussed is not possible.

2.2.2- COUPLED BRACED FRAMES

Coupled braced frames, similar in concept to coupled shearwalls in concrete, may be composed of two braced frames joined by friction joints, as illustrated in Fig. 2.2.

In this case the shear force and base moment are shared by the two frames equally, but the distribution of stresses between the two central columns varies with the slip force.

If no slipping occurs, there is no load in the two central columns.

If there is no connection between the columns, the load in column at the base is:

$$R = VH/2b \qquad 2.2.2.1$$

in which:

R = load in the column

V = shear force

H = building height

b = bay width

If the inner columns are connected by friction devices, then:

Load in the outer columns, at distance x from top, is:

$$R_{ox} = Vx/2b \qquad 2.2.2.2$$

Load in the inner columns, is:

$$R_{ix} = (Vx/2b - qx) \qquad 2.2.2.3$$

in which, q = slip force per unit length of the joint between two central columns.

The axial displacement of a point at a distance x from the top is:

$$\Delta = (1/AE) \int^{H} (V/2b - q)\, x\, dx$$

$$= [(V/2b) - q]\, (H^2 - x^2)/2AE \qquad 2.2.2.4$$

in which, E = the modulus of elasticity,

A = the cross sectional area of the inner column.

Energy dissipated by friction is:

$$W_f = 2 \int^H q\Delta dx \qquad 2.2.2.5$$

$$= [2q(V/2b - q)/2AE] \int^H (H^2 - x^2)\, dx$$

$$= [V/2b - q)\, q\, 2H^3/3AE \qquad 2.2.2.6$$

For W_f maximum:

$$dW_f/dq = (V/2b - 2q)\, 2H^3/3AE = 0 \qquad 2.2.2.7$$

giving:

$$q = V/4b \qquad 2.2.2.8$$

If the limiting value of V is determined by the available compressive capacity of the outer columns, R_o, then the optimum slip force becomes:

$$q = R_o/2H \qquad 2.2.2.9$$

This, again, is a structural property.

The energy dissipated by friction in one quarter cycle is:

$$W_f = R_o^2 H/6AE \qquad 2.2.2.10$$

This is equal to twice the elastic strain energy in the central columns at maximum deflection. If the area of each of the outer columns is twice the area of the inner columns, the energy dissipated is equal to the total elastic energy in the columns.

The columns and bracing should be designed to resist at least the moments and shear forces developed at the time when the friction joints have all slipped. For higher earthquake intensities, the behaviour will depend on the relative resistance of the frames to shear and overall moment, with no clearly defined reserve source of energy dissipation as there is in the friction damped braced frame.

Because the behaviour of these braced frames parallels that of shear walls, which have already been studied (4, 5), no further analyses were pursued.

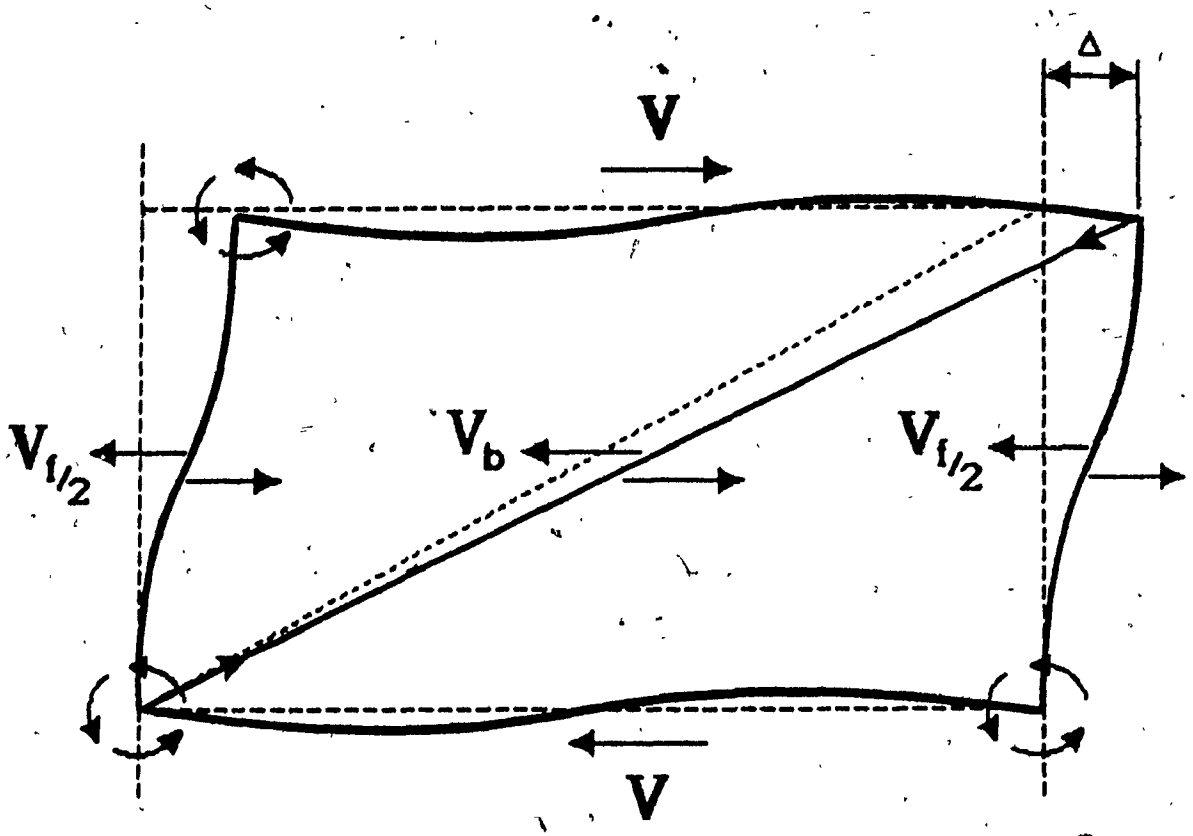

FIG. 2.1 Deformation of One Storey of a Braced Frame

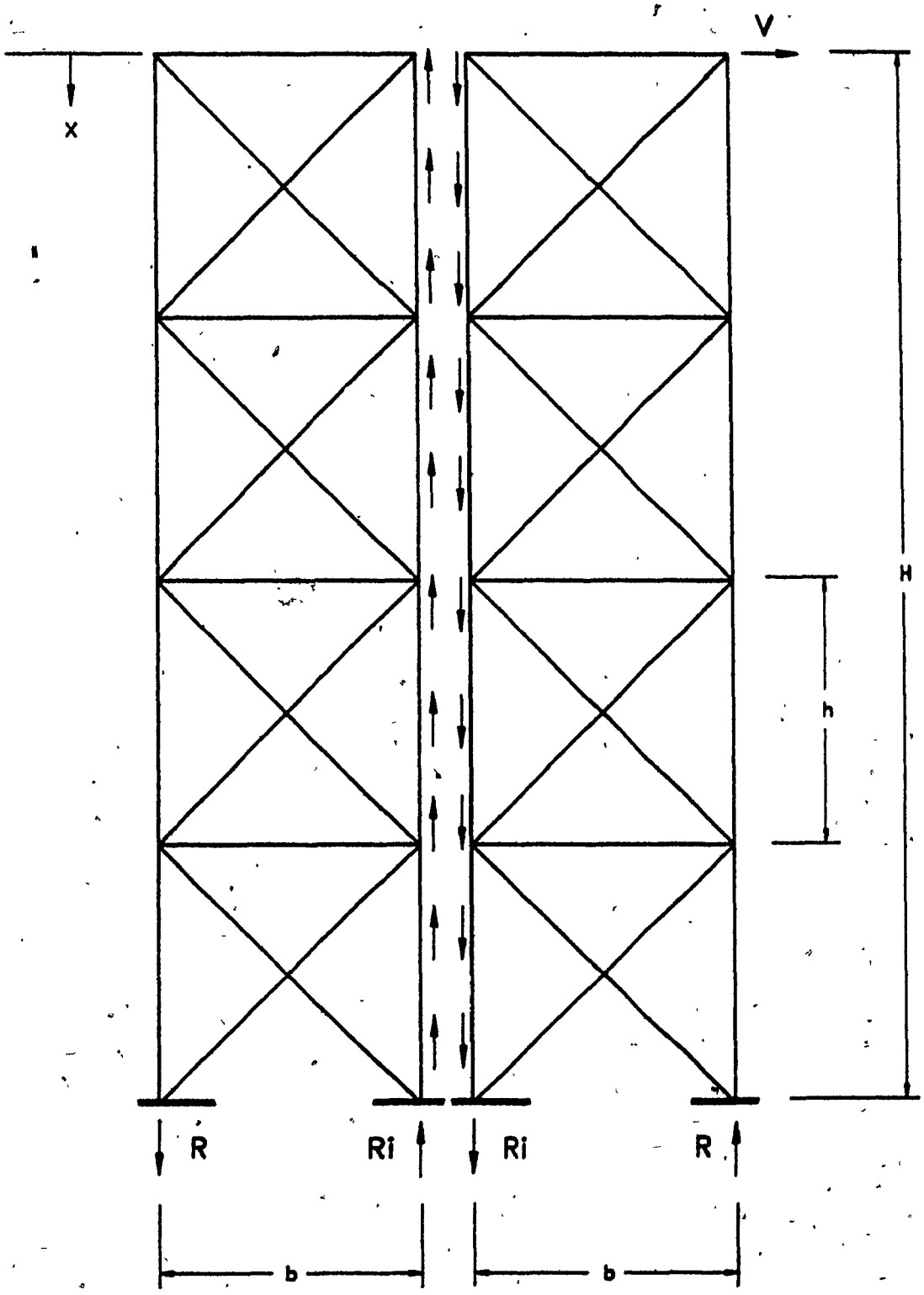

FIG. 2.2 Coupled Braced Frames Utilizing Friction Joints.

CHAPTER 3

INELASTIC DYNAMIC ANALYSIS

CHAPTER 3

INELASTIC DYNAMIC ANALYSIS

3.1- INTRODUCTION:

This chapter deals with the dynamic analysis of various structural framing systems using the computer program DRAIN-2D(30). Three types of friction damped frame, three structural systems without damping, and an eccentrically braced frame were analyzed, Fig. 3.1(a) to (d).

3.2- DRAIN-2D DYNAMIC PROGRAM:

This program performs a plane frame inelastic dynamic analysis for structures subjected to a base excitation. The program employs a step by step procedure, and at the end of each time step it checks the yield state of each element. The tangent stiffness modifications and the equilibrium corrections for any imbalance due to any change in the yield state are applied at the end of each time step. The time step is kept constant throughout the analysis and no iteration is used, except the equilibrium corrections and the change in the tangent stiffness matrix at the end of each time step. These corrections are made to prevent the accumulation of imbalances and divergences. The exact solution could be approached if a sufficiently small time increment was used, but to keep down the cost of the analysis it is desirable to find the largest time step which gives a reasonable solution.

The program has most of the subroutines required for the analysis of a structure in the linear and non-linear ranges and also permits the addition of new inelastic elements to the program. The elements in the existing DRAIN-2D program of interest in this study are:

1) Brace type element which yields or buckles, Fig. 3.2.
2) Beam-column element which includes the interaction between the bending moment and the axial force.
3) Beam element which considers only yielding due to bending.
4) Shear yield element for the eccentric bracing system.
5) Post-buckling brace element which considers the post-buckling behaviour of the braces, Fig. 3.3(30).

3.3- ANALYSIS

3.3.1- PROCEDURE

Step-by-step integration procedure is perhaps the most powerful method available for nonlinear analysis. In this method, the response is found for short equal time increments Δt, and the calculated response at the end of each interval is considered as the initial condition for the next interval. The procedure is continued step by step from the beginning of loading to any desired time.

At any instant of time 't', the equation of dynamic equilibrium can be written as:

$$[M]\{\ddot{dr}\} + [C_T]\{\dot{dr}\} + [K_T]\{dr\} = \{dp\} \qquad 3.1$$

where $\{\ddot{dr}\}$, $\{\dot{dr}\}$, and $\{dr\}$ are the increments of acceleration, velocity, and displacement, respectively, at the nodes; $\{dp\}$ is the increment in applied loading, [M] is the mass matrix, and $[C_T]$ and $[K_T]$ are the tangent values of the damping and stiffness matrices for the structure in its current state. For a finite time step, Δt, the above equation can be written as:

$$[M]\{\Delta\ddot{r}\} + [C_T]\{\Delta\dot{r}\} + [K_T]\{\Delta r\} = \{\Delta P\} \qquad 3.2$$

in which $\{\Delta\ddot{r}\}$, $\{\Delta\dot{r}\}$, $\{\Delta r\}$, and $\{\Delta P\}$ are the finite increments of acceleration, velocity, displacement and load respectively. The tangent stiffness and damping matrices are defined at the beginnning of the time intervals. $\{\Delta P\}$ is the increment of load and is equal to:

$$\{-\Delta P\} = -[M]\{1\}\Delta\ddot{x} \qquad 3.3$$

in which [M] is the mass matrix and $\Delta\ddot{x}$ is the increment of the ground acceleration. The method of Drain-2D is based on a constant acceleration within a time step (29).

3.3.2- TIME STEP

The accuracy of the time history analysis depends on the ratio of the time step and the period of vibration, and greater accuracy can be expected as the integration time step is reduced. However, to reduce the computation time, it is desirable to choose as long a time step as possible. It was

found that for some structures, due to a sudden yield of structural elements, smaller time steps were required.

In general, the time step should be no longer than one tenth of the fundamental period (31). If the frequency content of the acceleration is high, a much smaller time step is required. In the analysis a time step of 0.1 second was utilized for MRF and CBF and 0.05 second for EBF and FDBF.

3.3.3- DAMPING

Basically, the viscous damping results from a combination of mass and stiffness dependent effects, so that:

$$[C] = \alpha[M] + \beta[K] \qquad 3.4$$

In which [C] is the viscous damping matrix; [M] is the mass matrix; and [K] is the stiffness matrix. In the step-by-step analysis this could be taken as the current tangent stiffness matrix, at any time step 't', or the original elastic stiffness. This is a matter of engineering judgement and many analysts prefer to base their analysis on the stiffness-dependent part rather than on the original elastic stiffness.

The values of α and β are to be found from two given critical damping ratios that correspond to two frequencies of vibration.

If only mass dependent damping is assumed, then:

$$\alpha = 4\pi\lambda_i/T_i \qquad 3.5$$

in which λ_i is the critical damping in a mode with period T_i.

If only stiffness dependent damping is assumed, then:

$$\beta = \lambda_i T_i/\pi \qquad 3.6$$

No damping was assumed in the analyses that follow, but it is possible to make comparative runs to establish damping factors equivalent to those provided by friction joints, as discussed in Section 3.9.

3.3.4- INPUT MOTION

The main characteristics of a ground motion affecting the dynamic response of a structure are frequency content, intensity and duration. The frequency characteristics of a given ground motion depend on the resonance or quasi-resonance phenomenon, which occurs when the frequency of the input motion approaches the natural frequency of the structure. Intensity is used as a characteristic measure of the amplitude of the acceleration pulses in a record in terms of the ground acceleration 'g'. The duration of a ground motion is the length of the exciting motion with relatively large amplitude pulses.

In time history analysis of any structure, it is important, but difficult, to choose a ground motion close to that which the structure will experience on a specific site. Variability in the character of the ground

motion makes it desirable to consider a number of representative examples to determine the possible maximum response of a particular structure. Different records, with the same intensity but different frequency spectra, may give different structural responses.

Two different base excitations were used for the time history analysis:

i) The first seven seconds of El-Centro 1940 (N.S. component), because this time period contains almost all of the peak accelerations. Following this excitation, a two second period of zero acceleration was introduced to show the behaviour of the structure after the earthquake.

ii) The most severe segment of 1952 Kern County (Taft), California, occurring between third and tenth seconds, followed by two seconds of zero acceleration.

The earthquake record of El-Centro 1940 (N.S. component) was scaled by factors of 0.5, 1.0, 1.5 and 2.0, to give peak ground accelerations of 0.16g, 0.32g, 0.48g and 0.64g, respectively. The record of Taft earthquake was scaled by factors of 1.0, 2.0 and 4.0 to give peak ground accelerations of 0.16g, 0.32g and 0.64g, respectively.

3.4- FRAME DIMENSIONS AND PROPERTIES

Steel with a yield strength of 250 MPa was used throughout.

The frame chosen for the analysis was that described by Workman (23) for the basic moment resisting frame, MRF, shown in Fig. 3.1(b). Because of the extensive use made of this model in the literature, it provides an excellent standard for comparative studies.

Into this basic frame, different types of bracing were introduced. Those relying on yielding and buckling of the braces to absorb energy were:

Fig.3.1(b) Cross bracing (CBF) with a higher yield force in tension than the buckling force in compression, providing a total shear capacity given by the sum of the strengths of the two braces, one in tension and the other in compression.

Fig.3.1(c) K-bracing acting in tension and compression, with the shear force controlled by the buckling strength of the brace in compression.

A system which combines bracing and ductile moment resistance is the eccentric braced frame (EBF) shown in Fig. 3.1(d).

The three friction damped braced frames (FDBF) studied were:

Fig.3.1(e) Z-bracing with braces designed not to buckle.

Fig.3.1(f) Cross-bracing of the tension-only types using the Pall device at the intersection of the braces.

Fig.3.1(g) K-bracing having braces designed not to buckle, with the friction joints sliding along the horizontal beams.

In all the analyses equal mass of 60,000 kg was assigned at each floor of the structural framing.

Different building heights were studied. Tall buildings of 10, 15 and 20 storeys showed little difference in performances, so the 10 storey building was chosen as the minimum that could reasonably represent high buildings.

3.5- PROPORTIONING OF BRACES

3.5.1- FDBF

Because one of the main objectives of the study was to establish that there is an optimum slip force and that it can be readily determined, a design earthquake which would just yield the beams in the optimum frame of the FDBF type was required. This was established as close to 1.0 x El-Centro, for the Workman frame.

For a Z-Braced frame (Fig. 3.4), the limiting shear force is divided equally between the braces and the moment resisting frames. Using equation 2.2.1.8, the horizontal component of the required slip load, P_s, is:

$$P_s \cos \alpha = V_b = 2M_p \qquad 3.6$$

In which M_p = the plastic moment for the beams

h = the storey height

α = the angle between the brace and the beam

As shown in Fig. 3.1 (e), (f), and (g) the slip forces in the braces vary with the plastic moments of the beams. Consequently three different slip forces were utilized in each FDBF based on the following input:

$\alpha = 31°$, h = 3660mm, M_p = 650 kN.m, 500 kN.m, and 410 kN.m,

The slip force for Z-bracing (braces active in tension and compression), Fig. 3.1(e), is obtained from:

$$P_s = V_b/\cos\alpha$$
$$= 2M_p/h\cos\alpha$$

giving P_s = 415 kN, 320 kN, and 260 kN

The slip force in each brace for tension only braces (Fig. 3.1(f)) is obtained from:

$$P_s = V_b/2\cos\alpha$$
$$= M_p/h\cos\alpha$$

giving P_s = 208 kN, 160 kN, and 130 kN.

For K-bracing, which slips horizontally along the beams Fig. 3.1(g), the slip forces are obtained from:

$$P_s = V_b = V_c$$
$$= 2M_p/h$$

giving P_s = 335 kN, 275 kN, and 223 kN

The shear forces in the columns for 1.0 x El-Centro for the FDBF are shown in Fig. 3.1(g). It can be seen that the shear forces carried by the columns are close to the shear forces carried by the friction devices for the lower floors. The horizontal components of the slip forces are the same for the three case (e), (f), and (g).

To check that the values were close to the optimum, analyses were conducted for 1.0 x El-Centro, utilizing the Z-braced frame shown in Fig. 3.1(e). By varying the slip loads, the characteristics of the structure varied from those of a moment resisting frame to those of a fully braced frame. Figure 3.5 shows how the top storey deflection varied with the slip load and how there is a well defined optimum range very close to the theoretical value, $P_s = 2M_p/h \cos\alpha$, with values of slip force being equal to those shown in Fig. 3.1 (e). In reality, there is little difference in response for variations of $\pm$ 15% in the slip force, thus to use the theoretical value is reasonable for design purposes, as the security of the building is not influenced by minor inaccuracies in the installed value.

The slip loads used in the frames, for the following comparative studies of FDBF's, were the optimum values calculated using the simple relationship of equation 2.2.1.8. The loads were optimum for 1.0xEl Centro.

3.5.2- CBF X- AND K-Bracing

For X-bracing, the bracing was the same as that utilized by Workman (23) as shown in Fig. 3.1(b). The assumed behaviour of the braces was the simple model shown in Fig. 3.2(b).

For K-bracing, the braces used by Nilforoushan (30) as shown in Fig. 3.1(c) were utilized. The behaviour of the braces was modeled as illustrated in Fig. 3.3.

3.5.3- EBF

The eccentric braced frame (EBF) is a modern framing system devised to combine the benefits of a braced frame with the ductility of a moment-resisting frame. Energy is absorbed by shear yielding in the region of the beam between the brace connection and the column. The braces are designed not to buckle and the columns not to yield before the shear links in the beams reach, and exceed, their yield state.

The force in the braces as shown in Fig.3.6 is obtained from:

$$P = V_b\,(b - e)/2 \sin \alpha\,(b/2 - e) \qquad 3.7$$

in which P is the force in the eccentric brace, V_b the shear capacity of the beam, α the angle between the beam and the diagonal bracings, b the bay width, and e the length of eccentric beam (shear link).

Plastic hinges are expected to form at both ends of the shear link shortly after the shear yielding. A satisfactory relationship is obtained (20) when:

$$1.1V_b < 2M^*_p/e < 1.3V_b \quad \therefore V_b \approx 1.7\, M^*_p/e \qquad 3.8$$

Using 3.7 this gives:

$$P \approx 1.7\, M^*_p\, (b\text{-}e)/e \sin \alpha\, (b\text{-}2e) \qquad 3.9$$

in which M^*_p = plastic moment capacity from the flanges of the beam section.

There is no method, comparable to that used for the FDBF, by which the EBF can be optimised. It is simply proportioned to resist the design earthquake by making the shear resistance of the link such that it will yield at a force somewhat below that caused by the earthquake. The columns are designed not to yield under the moments created.

The basic beam element in the Drain-2D program was changed by Roeder (20) for energy dissipation by cyclic shear yielding of the eccentric element. This subroutine was used for the analysis of the EBF.

For this study, the EBF was designed for 1.0 x El-Centro to compare the behaviour with the optimum FDBF.

The most important difference between the FDBF and the EBF is that the shear force (across the frame) in the former is divided equally between the brace and the moment-resisting frame, in the optimum condition, while in the latter the entire shear force must be resisted by the bracing. This results in much heavier braces, as can be seen by comparing the sizes in Fig. 3.1(d) and (e).

3.6- FORCE VS. DISPLACEMENT FOR BRACES

3.6.1- FDBF

For simple Z- and K-bracing with friction joints, up to the slipping of the joints, the force displacement relationship is linear. After slipping, the brace force remains constant. Reverse loading is elastic and linear, until slip occurs in the opposite direction, as shown in Fig. 3.7(a). The structure remains elastic so long as the beams have not yielded.

In the analysis the braces in FDBF with Z-and K-bracing were modelled as truss elements in the "Drain-2D" program, with braces yielding in tension and compression as shown in Fig. 3.7 (a).

For the Pall mechanism, there is a small compressive capacity in the bars, P_c, which is assumed to remain constant after buckling. The sum of the tension and compressive forces causes the mechanism to slip. The model for the behaviour of each bar is that shown in Fig. 3.7(b).

For the detailed analysis of the Pall mechanism, existing "Drain-2D" Program was utilized, with braces modelled as combination of truss elements and beam elements as shown in Fig. 3.7(c).

Changes were made by the author to the basic slip model in the state determination and input subroutine. In this element, in the event of slip in one of the braces the other brace in the same bay slips simultaneously. A listing of the element subroutines are given in Appendix A. By introducing this subroutine in "Drain-2D" program, the bracing system can be modelled as simple cross bracing, with braces slipping simultaneously one brace in tension (P_t), and the other brace in compression, P_c.

3.6.2- CBF X- AND K-BRACING

The behaviour of the braces used in X- and K-bracing were discussed earlier in section 3.5.2.

3.7- ANALYSES CONDUCTED

The types of frame and the types and intensities of earthquake for which analyses were conducted are grouped in the manner in which comparative behaviours were studied. This is shown in the following Table.

	Earthquake	
	Type	Intensities
MRF CBF FDBF, (Z-braced)	El-Centro Taft	0.5, 1.0, 2.0 1.0, 2.0, 4.0
EBF FDBF, (Z-braced)	El-Centro Taft	0.5, 1.0, 2.0 1.0, 2.0, 4.0
FDBF, (Z-braced) FDBF, (Pall mechanism)	El-Centro	0.5, 1.0, 2.0
K-braced FDBF, (K-braced)	El-Centro	1.0, 1.5

3.8- FINDINGS FROM COMPARATIVE STUDIES

3.8.1- MRF, CBF, FDBF (Z-BRACED)

Resistance to seismic action has, in the past, been attributed to the ductility of rigid frame buildings, or to the energy dissipated by yielding and buckling in braces. This first program of studies compares the FDBF with more traditional systems.

Deflections

The deflection envelopes for the three framing systems are given in Fig. 3.8, for 0.5, 1.0 and 2.0 x El-Centro.

For 0.5 El-Centro the behaviour represents that of elastic frames, in

which case the MRF has, as expected, the greatest deflection.

In the case of 1.0 x El-Centro, the deflection of the optimised FDBF is much lower than for the other two intensities, the ratio between the deflections for FDBF, CBF and MRF being 0.4:0.8:1.0.

For an intensity factor of 2, the energy absorbed by damage in the MRF and the CBF, is high enough to bring the deflections closer, but that of the FDBF is still only 0.8 of that of the MRF.

The reason why the CBF deflects more than the MRF for 2.0 x El-Centro is due to the yielding of the columns in the CBF.

For Taft type earthquake, resonance led to major damage in the CBF at a factor of 1.0 with the resulting larger deflections, as seen in Fig. 3.9.

The deflection envelopes again show the performance of the optimum FDBF to be markedly superior for intensity factors of 1.0 and 2.0. For the intensity factor of 4, yielding in the beam has closed the difference between FDBF and CBF, but has led to large deflections in the MRF.

Moments

It is useful to refer to Figs. 3.14 to 3.19 (which show the progressive damage as the earthquake intensity increases) to understand how the column moment envelopes given in Fig. 3.10 and 3.11 are created. At the lowest

intensity of earthquake, the braces in the CBF have yielded, causing moment into the column. Because of the greater distortion than that due to joint slipping in the FDBF, the column moments are higher. Again, the optimum slip force for 1.0 x El-Centro and 2.0 x Taft show the FDBF to the best advantage. The ratio of column base moments for 1.0 x El-Centro is 0.5:0.9:1.0, for the FDBF, MRF and CBF respectively. For a factor of 2.0, all the systems are acting predominantly as ductile moment-resisting frames, and the moment envelopes close up a little, but the ratio of the base moments is still 0.55:0.8:1.0.

The consistently superior behaviour of the FDBF for the Taft earthquakes reflects the relationship between the frequency density of the exitation and the natural frequencies of the structure.

Axial Forces in Columns

Column forces are, by nature of the structural action, lower in MRF's than in braced frames, and a comparison can be reasonably made only between the FDBF and the CBF. In Figs. 3.12 and 3.13, the envelopes for the axial forces are shown, and the reduction affected by the FDBF can be noted for all intensities. The atypical envelope for the axial force in the case of the CBF for 0.5 x El-Centro is attributable to the frequency spectrum of the earthquake matching the natural frequency of the structure.

Damage

Damage, by the creation of yield hinges or by yielding of the braces, requires repair. Figures 3.14 to 3.16 for El-Centro, and 3.17 to 3.19 for Taft, show that structural damage occurs in both the MRF and the CBF at the lowest intensities studied, while the joints in the FDBF are slipping but with no structural damage. Only at the highest intensity earthquake does yielding occur in the beam of the FDBF. At this intensity, the MRF is at incipient collapse, as yield mechanisms have been formed in the columns of several storeys, while most beams of the CBF have yielded. The FDBF thus has a further reserve to resist earthquakes of higher intensity than those sufficient to destroy the MRF and CBF types.

Time Histories of Top Deflection

Typical time histories of the top storey deflections are shown in Figs. 3.20 and 3.21 for the three types of framing. The response for the optimum condition of 1.0 x El-Centro is seen in Fig. 3.20, where the reduced motion of the FDBF will clearly lead to lower accelerations and less secondary damage. For 2.0 x El-Centro, the top storey deflections are shown in Fig. 3.21. In this case, all the frames have yielded and the relative behaviour reflects the additional benefit of the FDBF when the slipping friction joints and yielding beams combine to dissipate energy.

General Observations

The slip loads used were such that 1.0 x El-Centro, (0.32g), was close to the maximum intensity that the frame could resist without permanent damage. It had been expected that the same intensity of Taft, i.e. 2.0 x Taft, (0.32g), would provide the same limit. Because of the frequency spectra, however, 2.0 x Taft proved to be less severe than 1.0 x El-Centro for FDBF, with lower deflections and less damage, thus a higher intensity could be resisted without exceeding the elastic range of behaviour.

3.8.2- EBF AND FDBF (Z-BRACED)

The most recent framing system introduced to dissipate energy during seismic activity is the Eccentric Braced Frame (EBF) which utilizes yielding in the shear webs. The following study compares this method with friction devices.

Deflection

Deflection envelopes are shown in Fig. 3.22 for 0.5, 1.0 and 2.0 x El-Centro.

The FDBF was optimised for 1.0 x El-Centro while the EBF was designed to be just-yielding for this condition. As a result, although plastic hinges were formed in the EBF (see Fig. 3.29), the slipping in the FDBF gave higher deflections. However, the differences between the systems were small.

For the Taft type of earthquake, Fig. 3.23 shows that the FDBF deflects less for all intensities. This difference between the responses to El-Centro and Taft is due to the different relationship between the natural frequencies of the structures and the dominant frequencies in the earthquake spectrum.

Moments

In the EBF, the eccentricity creates moments in the beam and columns for all levels of loading and it is natural that the column moments, as shown in Figs. 3.24 and 3.25, are higher than that in the FDBF. At 2.0 x El-Centro, when most of the beams in both systems have yielded, the column moments are, quite naturally, almost equal.

Axial Column Forces

Because the lateral shear force required to slip the joints in the FDBF is only half that required to yield the shear link in the EBF, the axial forces created in the columns is approximately halved, which is clearly seen in Figs. 3.26 and 3.27 for all intensities of earthquake of the El-Centro and Taft types.

Damage

Structural damage, meaning permanent deformation due to yielding, is shown in Figs. 3.28 and 3.29 to occur in the EBF at 1.0 x El-Centro and 1.0 x Taft, while no damage has occurred in the FDBF at 1.0 x El-Centro and 2.0 x Taft.

Movement in Slipping and Yielding Devices

As it is the slipping in the FDBF and the shear distortion in the EBF which absorb energy, it is of interest to compare the actual travel of these devices during an earthquake when both devices are activated. Fig. 3.30 shows the time histories of slipping in the FDBF and the vertical deflection in the EBF for two earthquakes. At the design loading for both systems, i.e. 1.0 X El-Centro, the displacements are comparable (about 12 mm), as seen in Fig. 3.30(a) but the FDBF has less residual deflection.

For 4.0 Taft, (0.64g), Fig. 3.30(b) shows how the EBF suffers larger distortions, 62mm vs. 28mm, with much more residual deflection.

Not only do FDBF's survive earthquakes with less residual deflection, but the rectification of the building requires only slackening and retightening the bolts. To rectify the EBF requires the replacement of the beams.

Time Histories of Top Deflections

The time histories of the top storey deflections are shown in Figs. 3.31 to 3.34. The maximum deflections are comparable for the two systems of framing but the deflection of the FDBF decays more rapidly and the residual value is lower.

3.8:3- FDBF USING TENSION ONLY BRACINGS AND Z-BRACING

To provide a system requiring only tension bracings, a mechanism was proposed by Pall and Marsh (8). When the slip occurs due to tension in one of the braces, it activates the four link mechanism, thereby forcing the other diagonal to slip simultaneously, even if that brace is carrying zero compression load. On reversing the load, the other diagonal accepts the tension. In this kind of bracing which acts in tension only, the energy is dissipated in both half cycles.

For friction damped braced frames using the proposed mechanism, a detailed analysis was carried out in which each element of the brace and the device was individually modeled as shown in Fig. 3.7(c). Elements 1 to 4 and 7 to 10 were modelled as truss elements yielding in tension and buckling in compression. Elements 5 and 6 were modelled as truss elements yielding in tension and compression at a force equal to the slip force. Additional beam elements were superimposed on the truss elements as seen in Fig. 3.7(c), to provide the required bending resistance at the connection between braces inside and outside the four link mechanism (i.e. between elements 1 and 5, 2 and 6, 4 and 5, and 3 and 6). To eliminate any additional axial stiffness caused by these beam elements area of the beam elements was considered to be close to zero. This proved to be costly in computer time, so, instead, the cross-bracing with friction device was modeled as a single equivalent truss element as discussed in section 3.6.1. The forces in the tension and compressive braces in each bay are equal until the compression brace buckles at P_b, after which the force in the compression bar remains constant as the force in the tension bar increases. When the mechanism slips the force in

the tension brace is P_t, given by:

$$P_t = 2P_s - P_c \qquad 3.10$$

in which P_s is the slip force in the device and P_c is the buckling load.

The model was introduced to the programme as a new subroutine. Figure 3.35 shows the deflection envelope using the detailed analysis and the simplified method based on the modified truss element subroutine. It is illustrated that the results of this modified model are very close to the detailed analysis ($\pm$ 5%) with considerable savings in computer time.

K- and Z-bracing act in tension and compression, and are referred to as tension-compression bracing. The Pall mechanism acts essentially in tension and is referred to as tension-only bracing.

A comparison was made between the FDBF with Z-bracing, as used in the early studies, and with the Pall mechanism. The smallest size of brace suggested by Workman was used (Fig. 3.1(f)). As could be expected, the results obtained, seen in Fig. 3.36 to 3.38, showed little difference between the systems.

3.8.4- K-BRACING WITH AND WITHOUT SLIPPING JOINTS

Numerous studies on post buckling behaviour of braces have been done in recent years, mainly by Higginbotham (32), Nilforoushan (30), Singh (33), Marshal (34), and Jain (35). All have stressed that the energy dissipation

capacity of the bracing members is significant and should not be neglected in the dynamic analysis of a braced frame. The post buckling behaviour is based on the model proposed by Jain and Goel (24) which is similar to the model proposed by Nilforoushan (30). This is introduced to the Drain-2D programme as a new subroutine.

To provide a comparison between this method of dissipating energy and the FDBF, analyses were conducted on two K-braced frames, one of which incorporated connections at the K-braced nodes which slipped along the horizontal beams. The frame chosen for analyses was that by Nilforoushan (30), which is similar to the frame utilized by Workman (28), (Fig.3.1).

For the FDBF, the slip force was that obtained in Section 3.5.1. For the normal K-braced frame (KBF), the hysteretic behaviour of the braces was modelled as shown in Fig. 3.3.

The deflection envelopes are compared in Fig. 3.39. It is observed that, for 1.0 x El-Centro, the top storey deflections for FDBF and KBF are nearly the same. This is attributed to the slipping of the friction joints.

At 1.5 x El-Centro the FDBF has only 75% of the deflection suffered by the KBF, due to the higher energy dissipation of the friction joints. Also, the moments in the column are lower for the FDBF, for both loading cases, and are shown in Fig. 3.40. Figure 3.41 shows that the axial forces on the columns are lower for the FDBF, which is again due to the slipping of the friction joints before the braces buckle.

Damage is caused to the diagonals as they buckle, and to the beam as it yields, in the KBF, for 1.0 x El-Centro. At this force level, there is no damage in the FDBF (Fig. 3.42).

Time histories of the top storey deflection are shown in Fig. 3.43 and 3.44 for 7.0 seconds of El-Centro followed by 2.0 seconds of zero acceleration. It is to be observed how the residual oscillations are much lower in the FDBF because it maintains its initial rigidity. The amplitude of these residual oscillations is a function of the last excursions in the earthquake spectrum and the motion of the structure at that time.

3.9- EQUIVALENT DAMPING

The foregoing studies were based on zero damping since it was the comparisons of the behaviours of the structures that were of interest. The FDBF is a structural system which dissipates energy by friction. To see how this compares with viscous damping, a study was done on moment resisting frames by introducing different values of viscous dampings.

Stiffness damping is preferred since it distributes the damping effect throughout the structure, unlike mass dependent damping which distribute the damping effect at mass points.

To find the natural period of vibrations, the TABS Programme (36) was used. The natural period of vibration related to the first mode was found to be 3.36 seconds.

By comparative analysis, it was found that 37% stiffness dependent damping, or 36% original stiffness damping, both relative to the first mode, was required in MRF to give the same deflection as in the FDBF with zero viscous damping for 1.5 x El-Centro.

Analysis of the CBF showed it to be very sensitive to whether original stiffness proportional damping or stiffness dependent damping is used. In original stiffness proportional damping, the damping matrix is related to the original stiffness rather than to the current tangent stiffness matrix at each time step. This can make a substantial difference in CBF, since stiffness degrades rapidly after buckling of the braces. By introducing 5% original stiffness damping for the first mode, with a natural period of vibration of 1.8 seconds, for 1.5 x El-Centro, the top deflection is reduced to 60% of that for zero damping. However, 13% stiffness dependent damping is required to create the same effect.

This means zero damping in FDBF is equivalent to 13% stiffness dependent damping or 5% original stiffness damping in CBF. With 5% original stiffness damping introduced to the FDBF, the required original stiffness damping for CBF increased to 15%, in order to give the same top deflection.

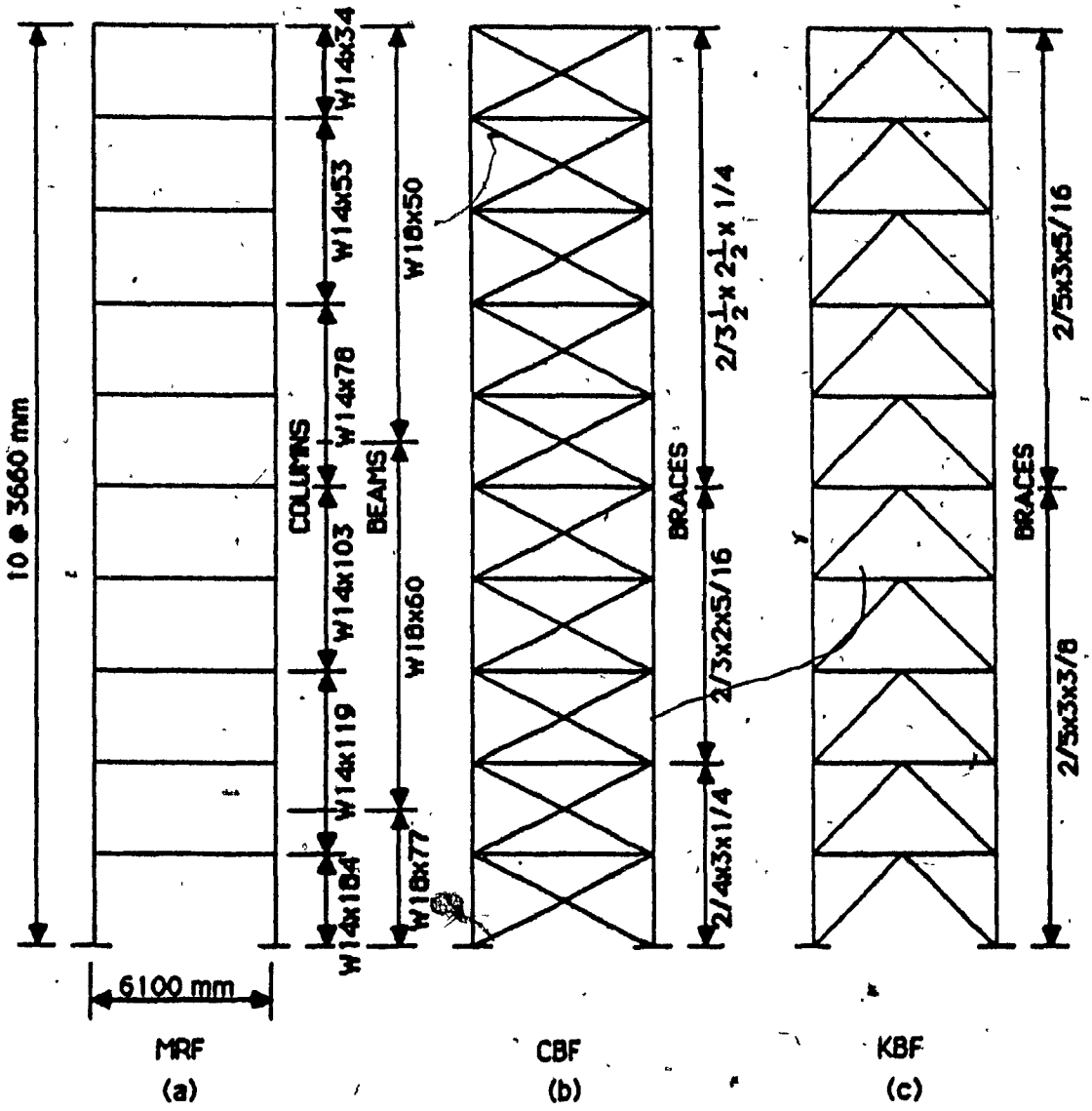

FIG. 3.1 TYPES OF FRAMES ANALYSED

a) Basic moment resisting frame (MRF)
b) Cross braced frame (CBF)
c) 'K' braced frame (KBF)

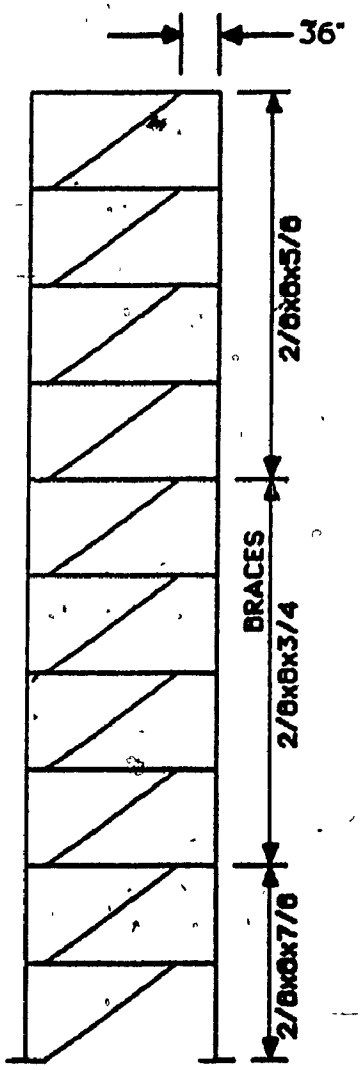

(d)

EBF

FIG. 3.1 (CONTINUED) TYPES OF FRAMES ANALYSED

d) Eccentric braced frame (EBF)

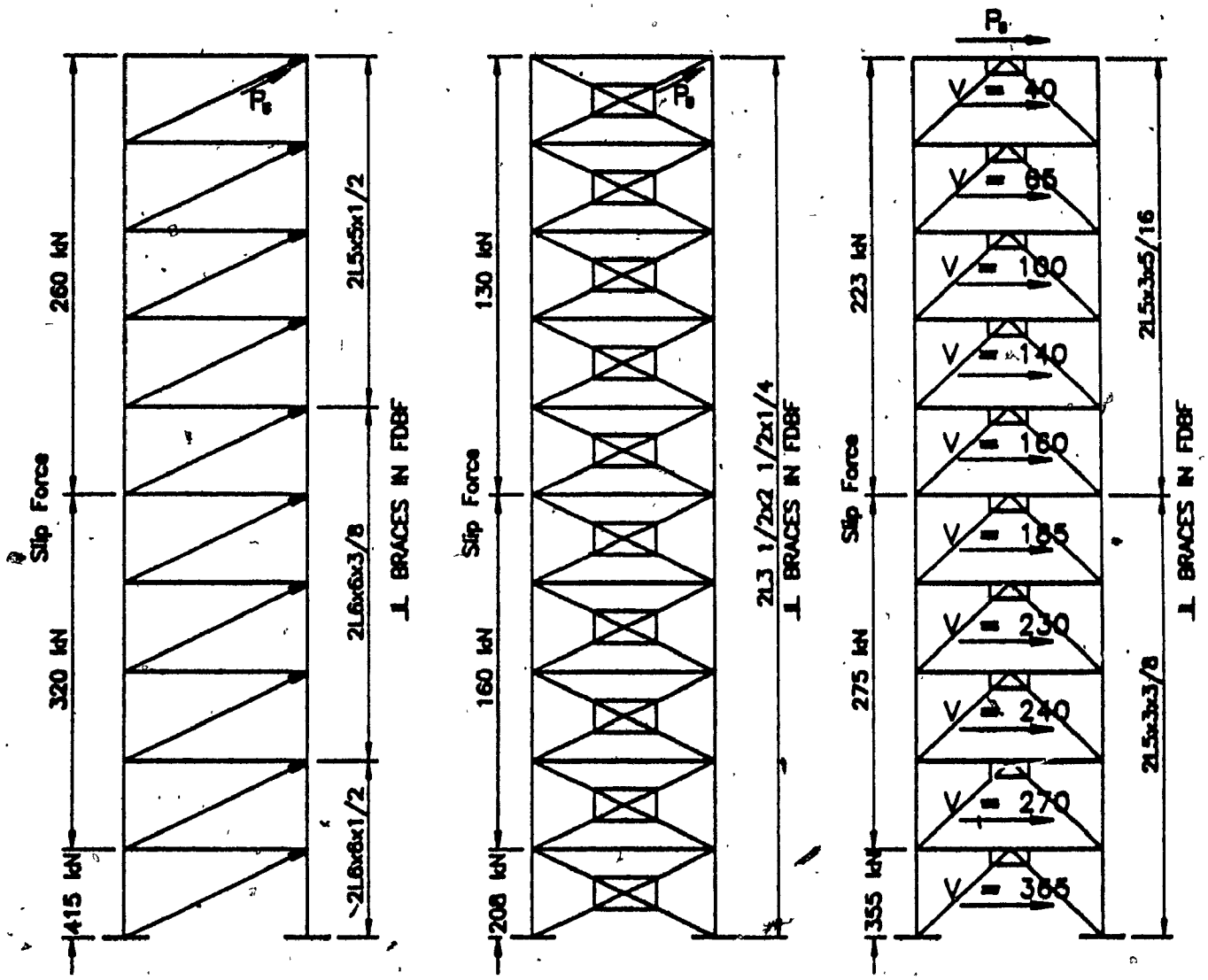

P_s = Slip Force

V = Shear Force in the Columns for 1.0 X El-Centro

Fig 3.1 (CONTINUED) TYPES OF FRAMES ANALYSED

FRICTION DAMPED BRACE FRAMES

e) 'Z' bracing
f) Tension-only Bracing
g) 'K' bracing

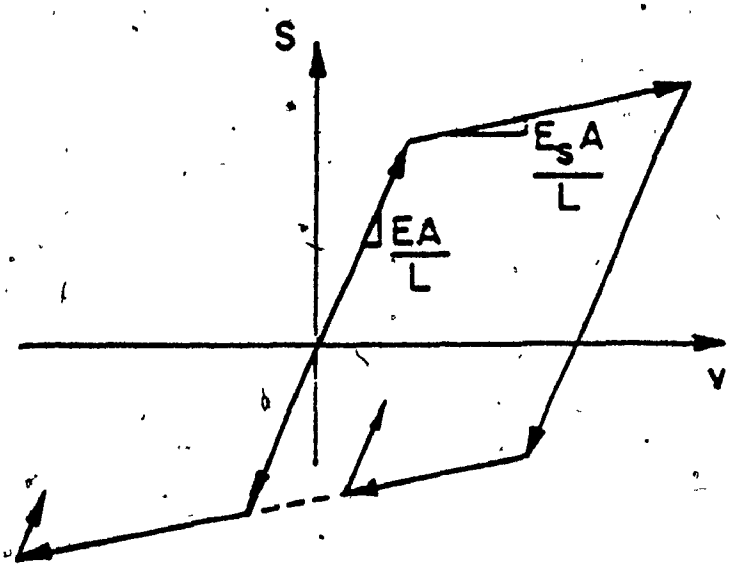

(a) YIELD IN TENSION AND COMPRESSION

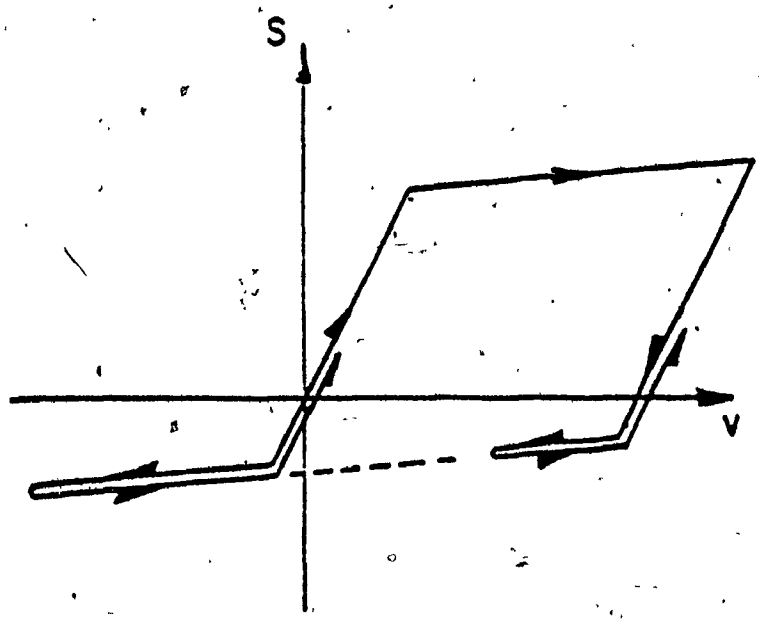

(b) YIELD IN TENSION, BUCKLING IN COMPRESSION

FIG. 3.2 **Simple Axial Force/Displacement Relationships for a Brace**

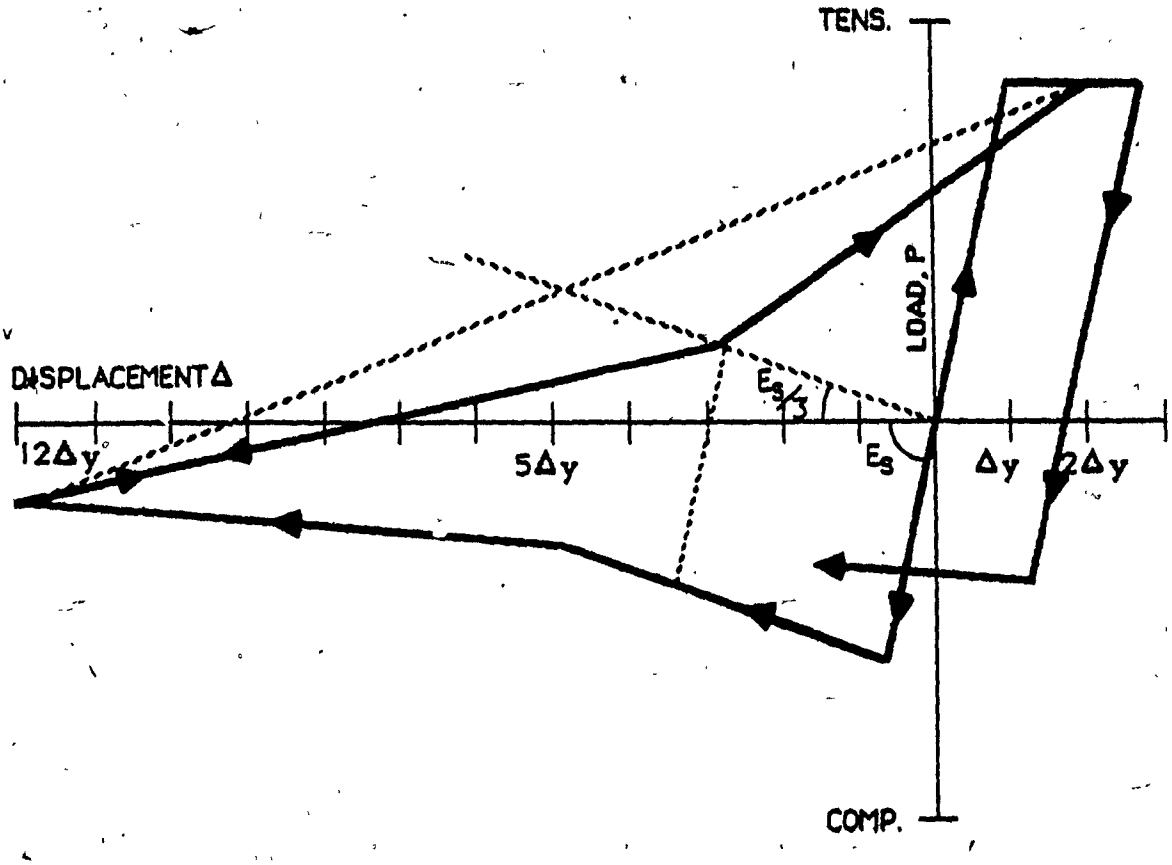

FIG. 3.3 Nilforoushan Model for the Axial Load/Displacement Behaviour of a Brace (30)

FDBF

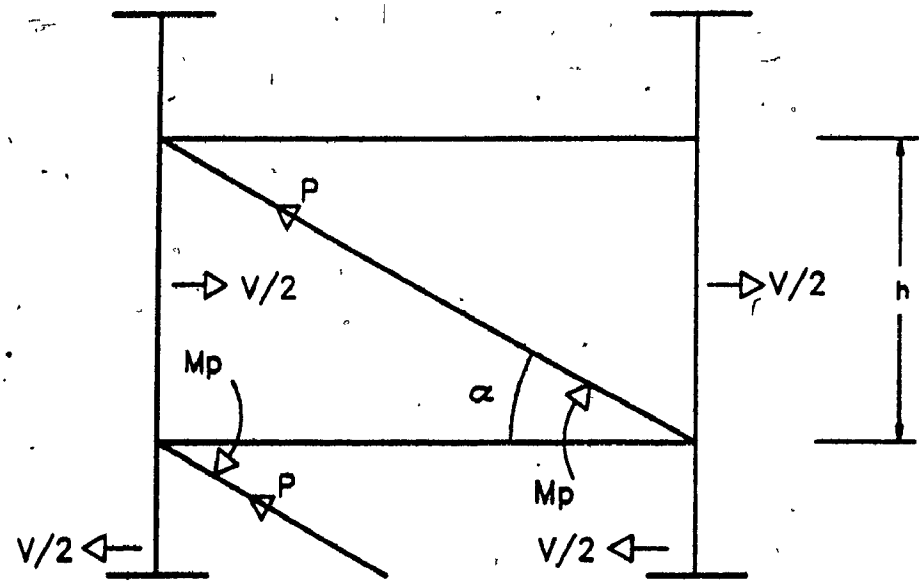

$$P_s = \frac{2M_p}{h \cos \alpha}$$

FIG. 3.4 Brace Force for Optimum Slip Load.

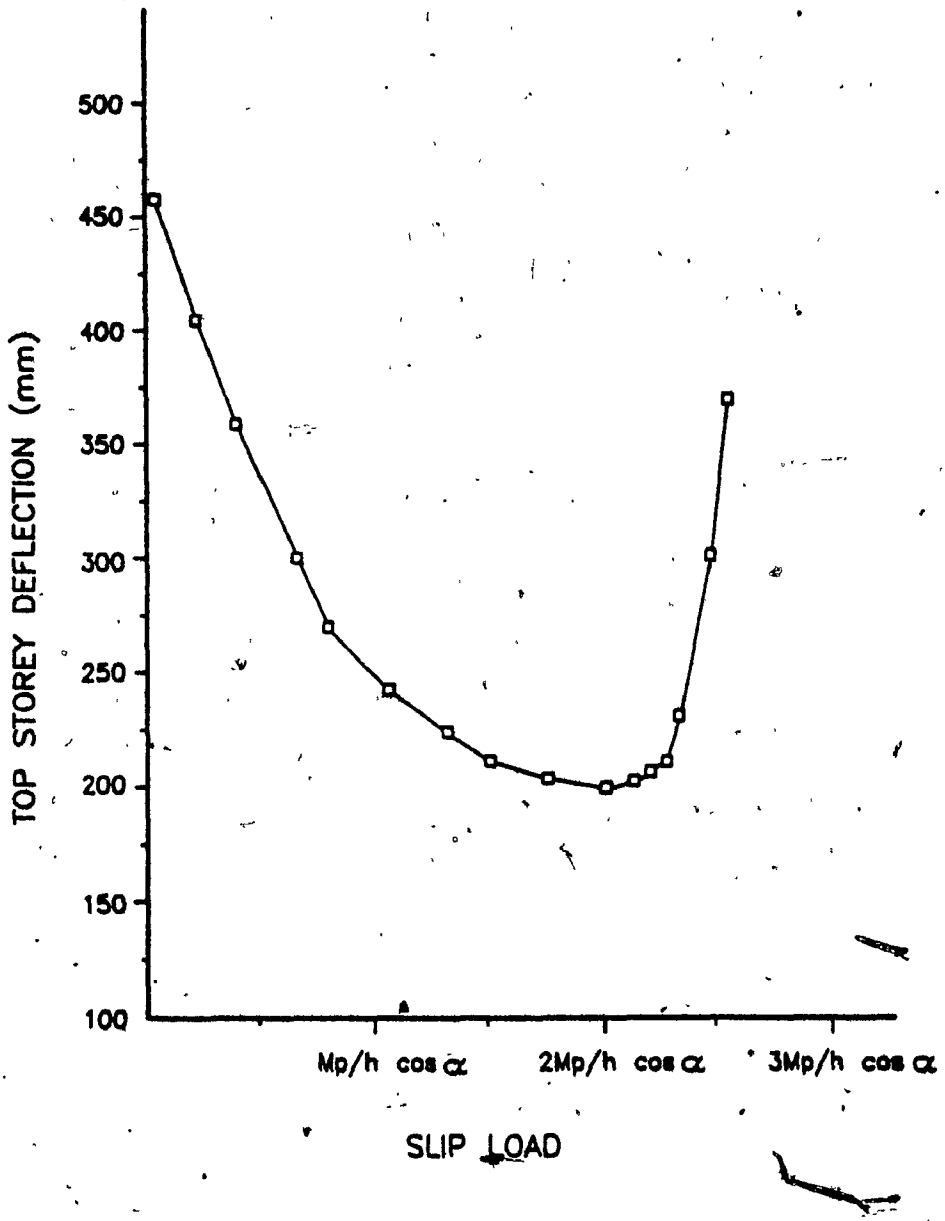

FIG. 3.5 Effect of Slip Load on Top Storey Deflection, 1.0xEl-Centro (0.32g) for Z-Braced Frame.

EBF

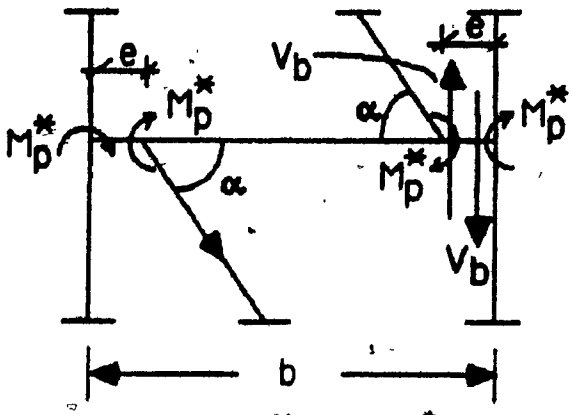

$$P = \frac{1.7M_p^*}{e \sin\alpha} \times \frac{(b-e)}{(b-2e)}$$

FIG. 3.6 Brace Force in Eccentric Braced Frame

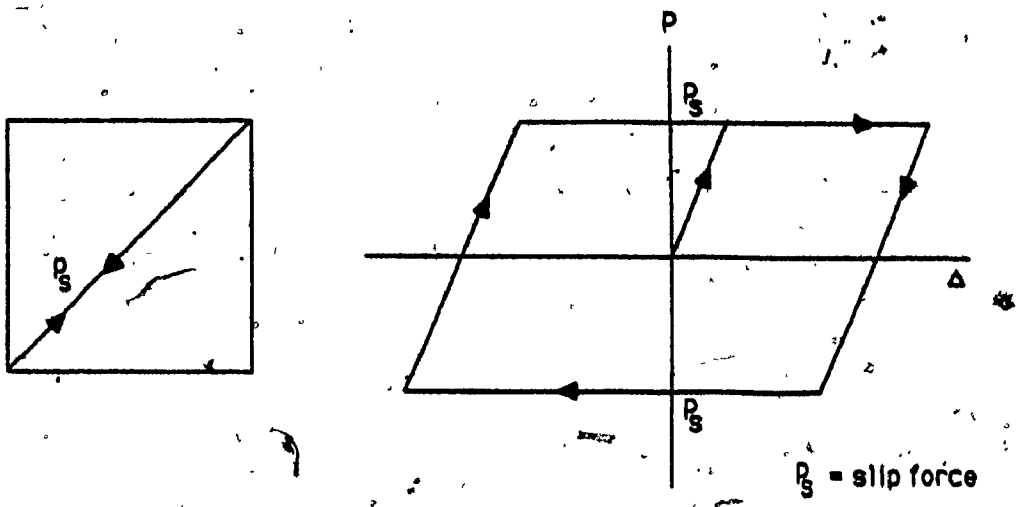

a) Z bracing with slip joints

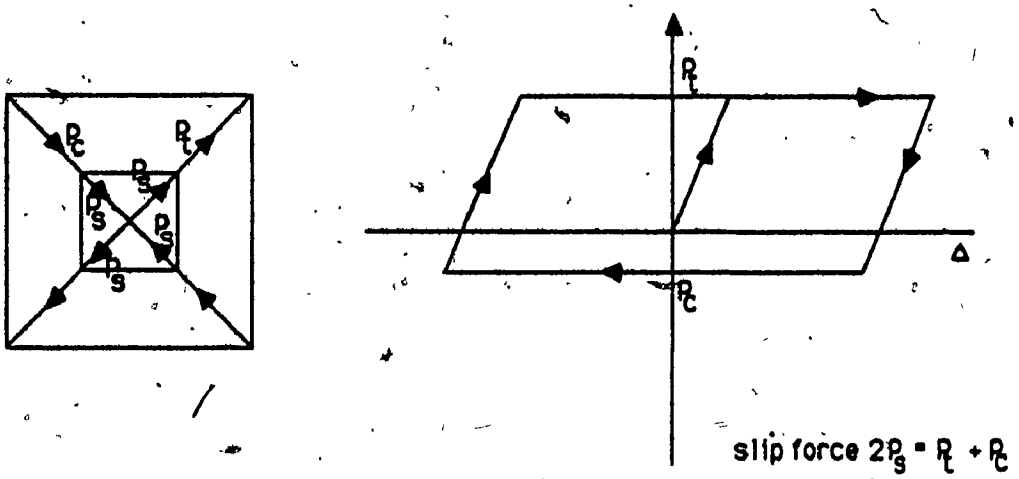

b) Behaviour of a single brace with Pall mechanism

FIG. 3.7 **Axial Force/Displacement Behaviours of Braces in FDBF**

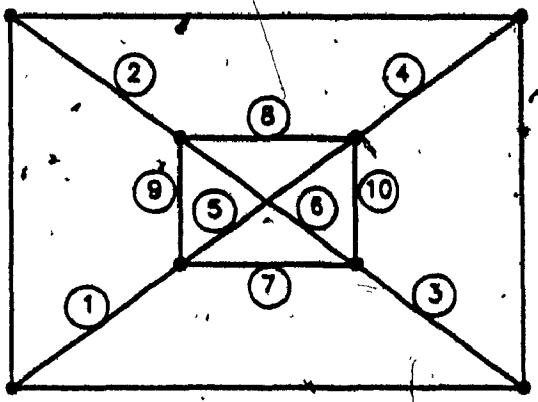

TRUSS ELEMENT

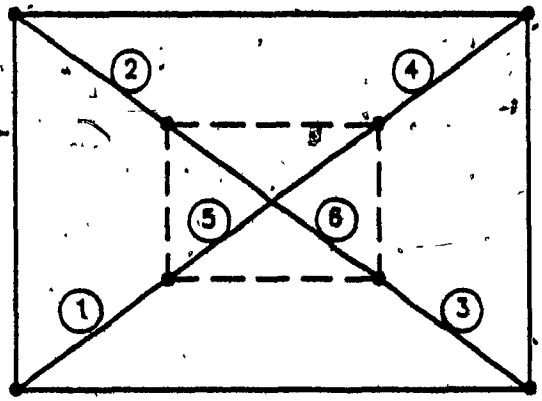

BEAM ELEMENT

LEGEND:

(1) Element No.

• Node

FIG. 3.7 (c) Modelling for Detailed Analysis of FDBF with Tension-only Bracing

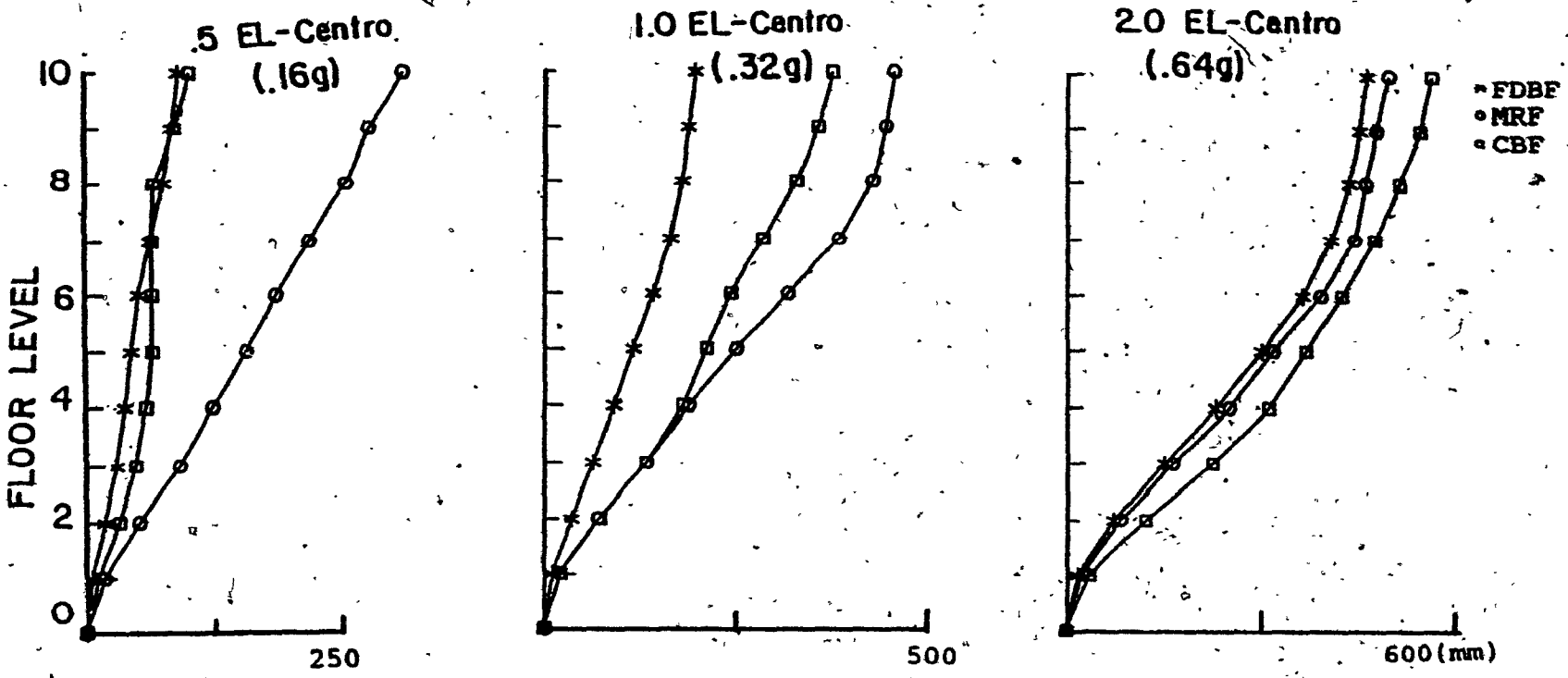

FIG. 3.8 Comparisons between FDBF, MRF, and CBF: Deflection Envelope for El-Centro Excitation

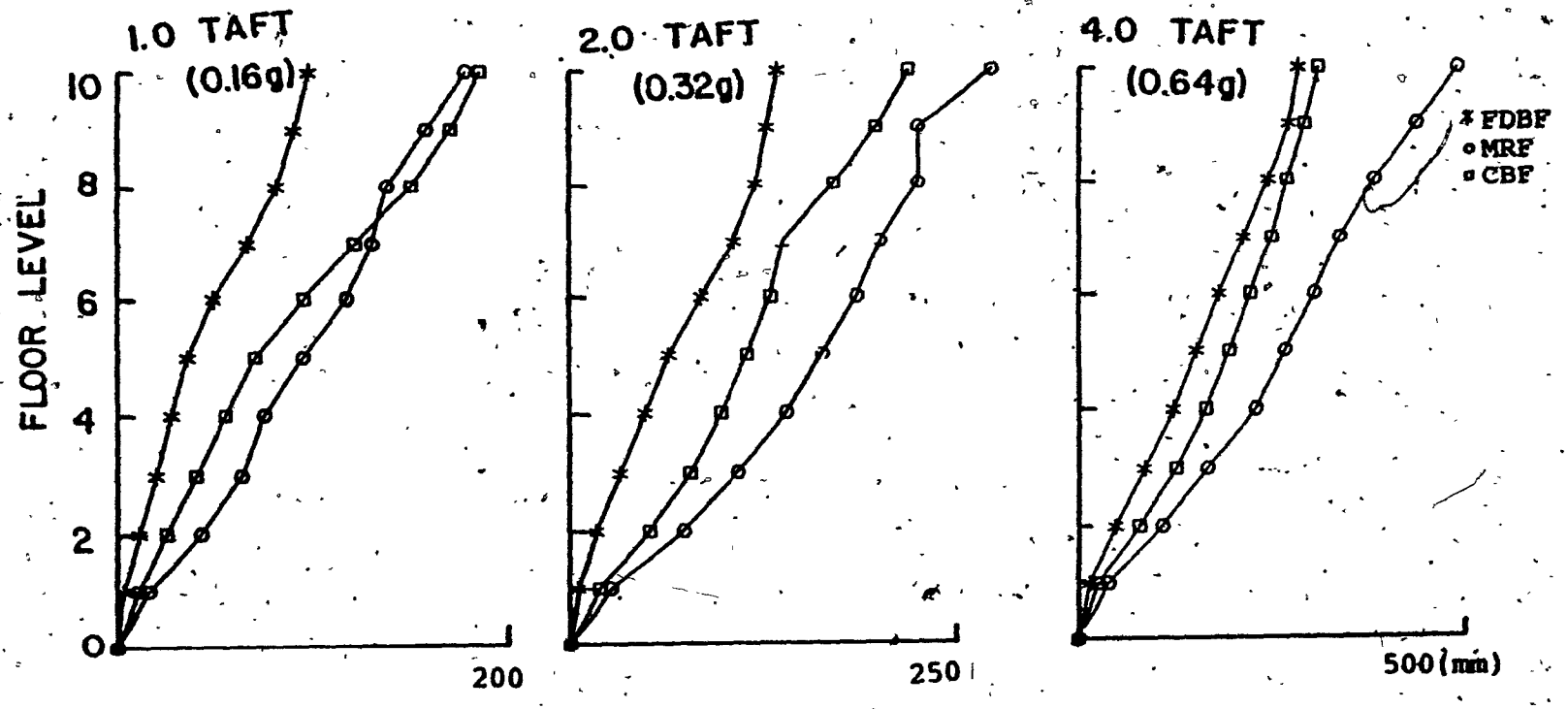

FIG. 3.9 Comparisons between FDBF, MRF, and CBF: Deflection Envelope for Taft Excitation

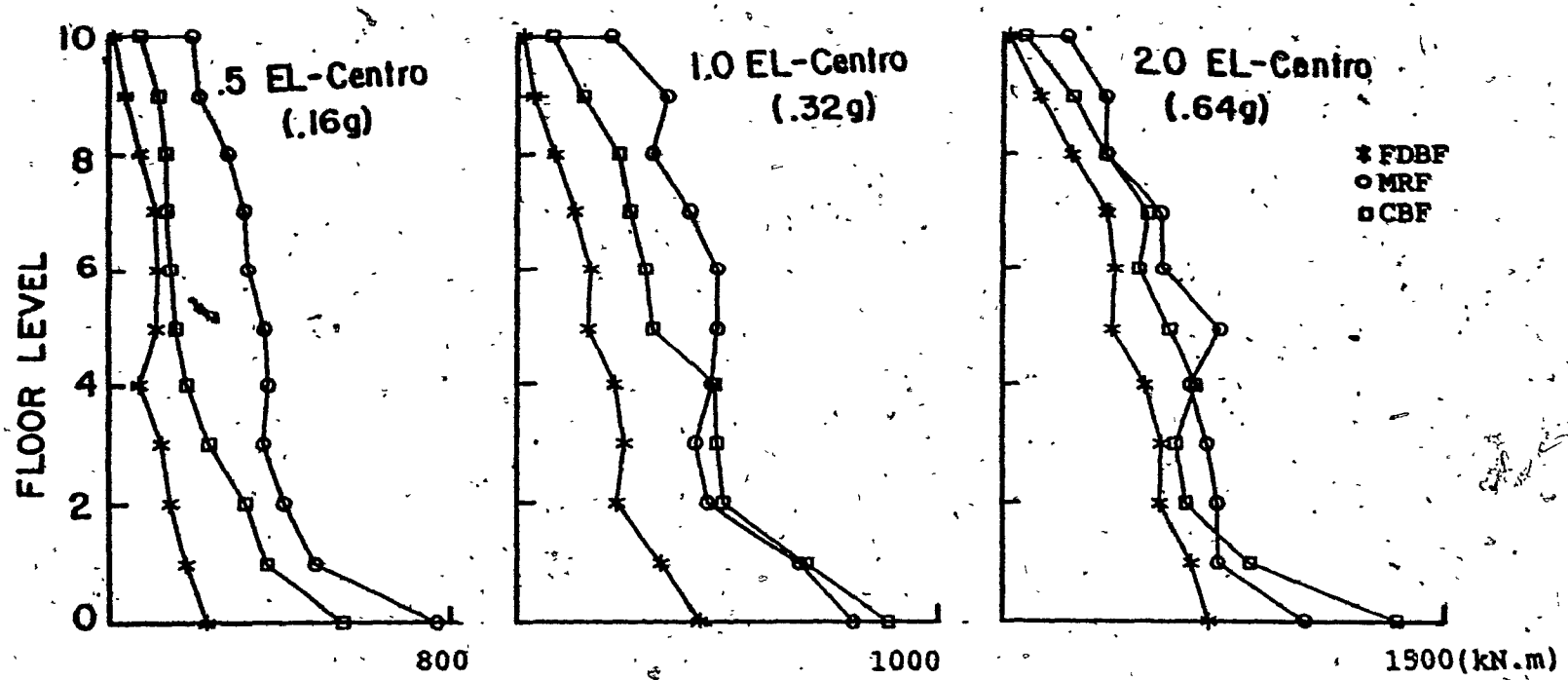

FIG. 3.10 Comparisons between FDBF, MRF, and CBF: Envelope of Moments for El-Centro Excitation

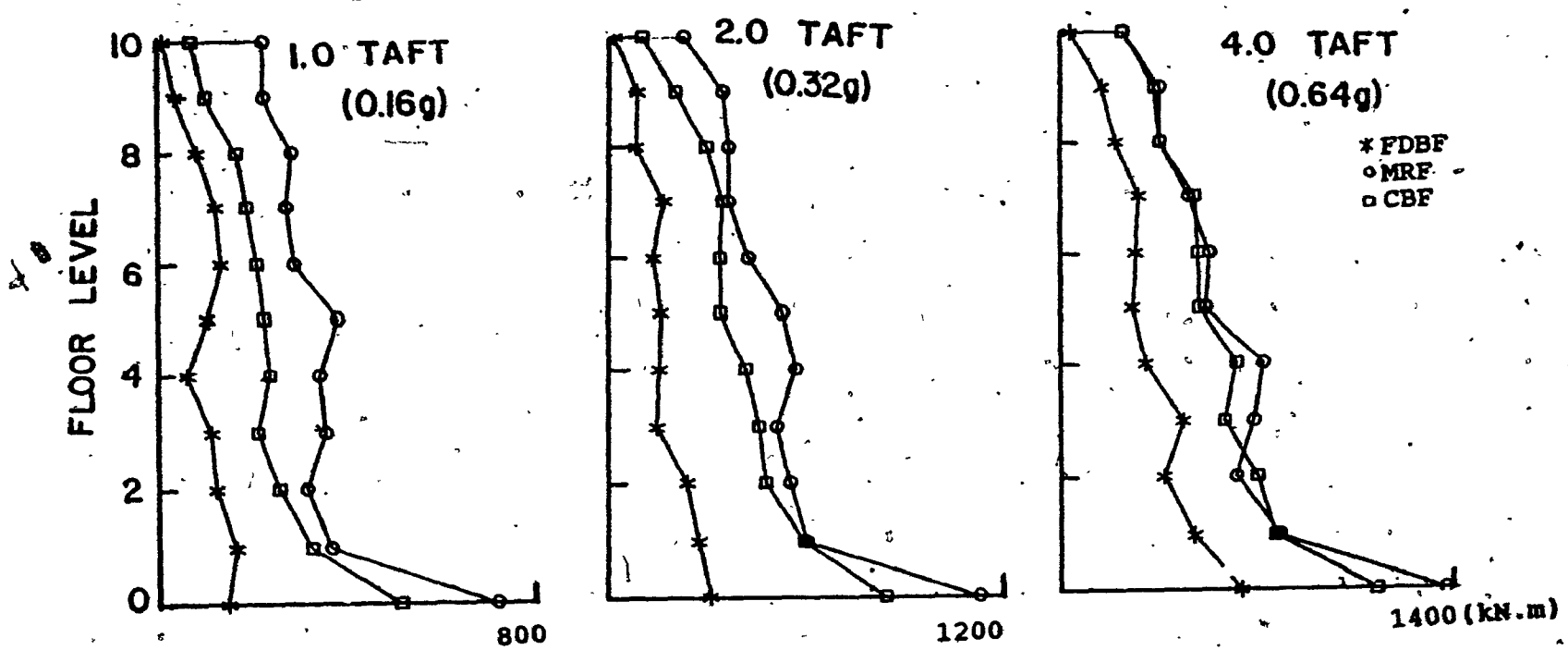

FIG. 3.11 Comparisons between FDBF, MRF, and CBF: Envelope of Moments in Columns for Taft Excitation

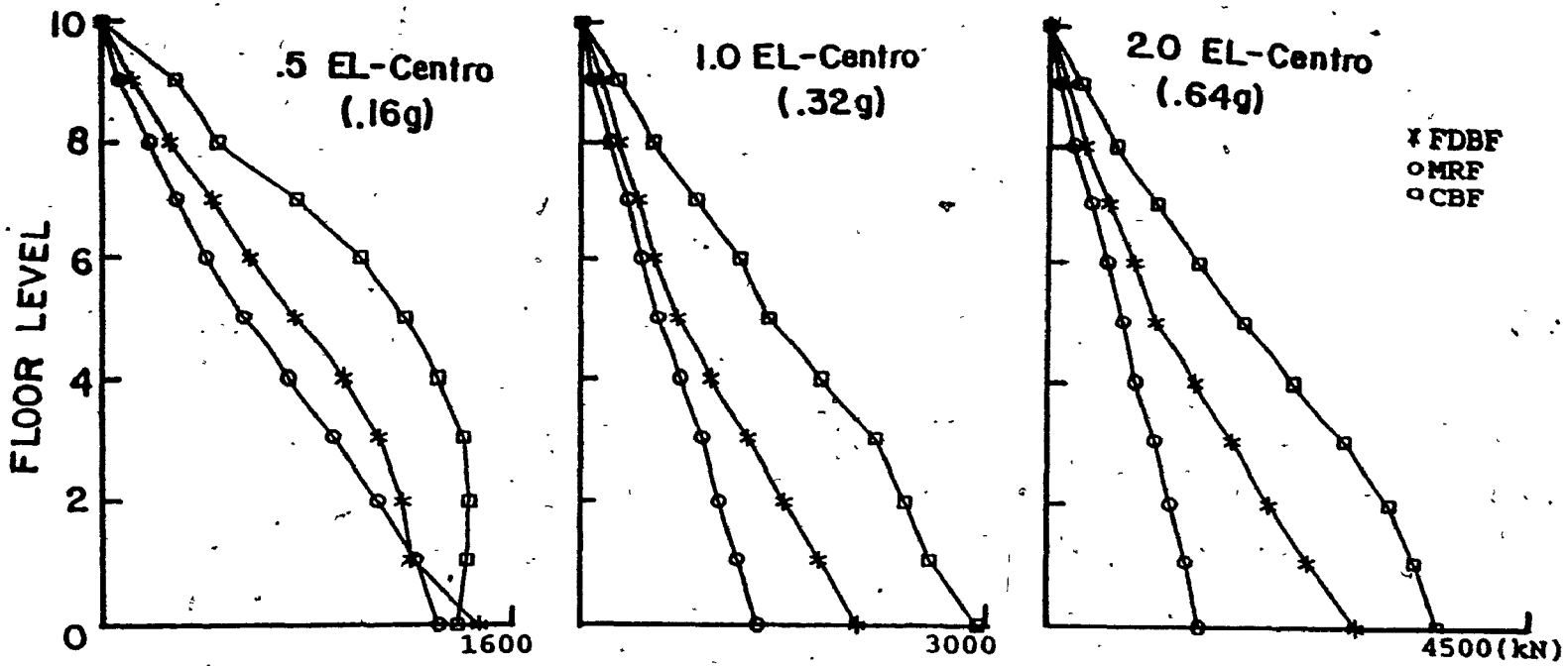

FIG. 3.12 Comparisons between FDBF, MRF, and CBF: Envelope of Axial Forces in Columns for El-Centro Excitation

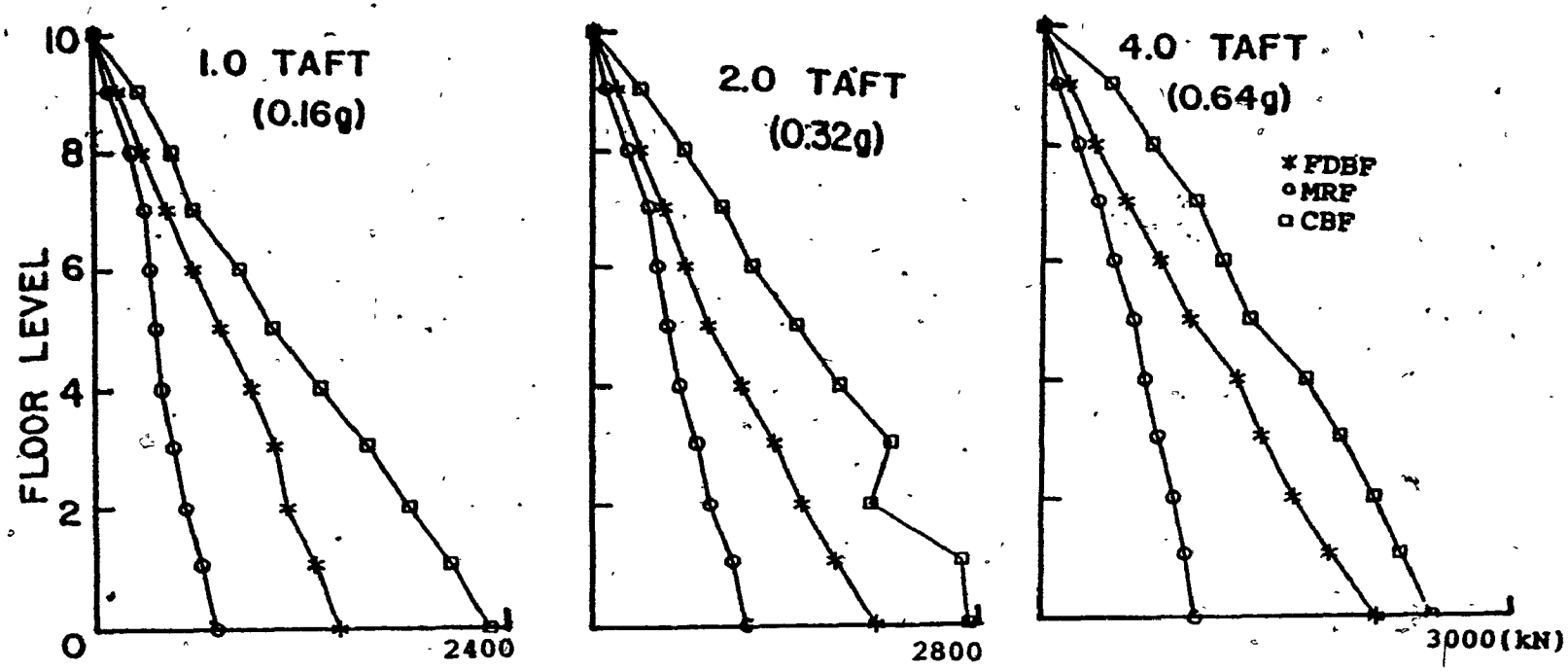

FIG. 3.13 Comparisons between FDBF, MRF, and CBF: Envelope of Axial Forces in Columns for Taft Excitation

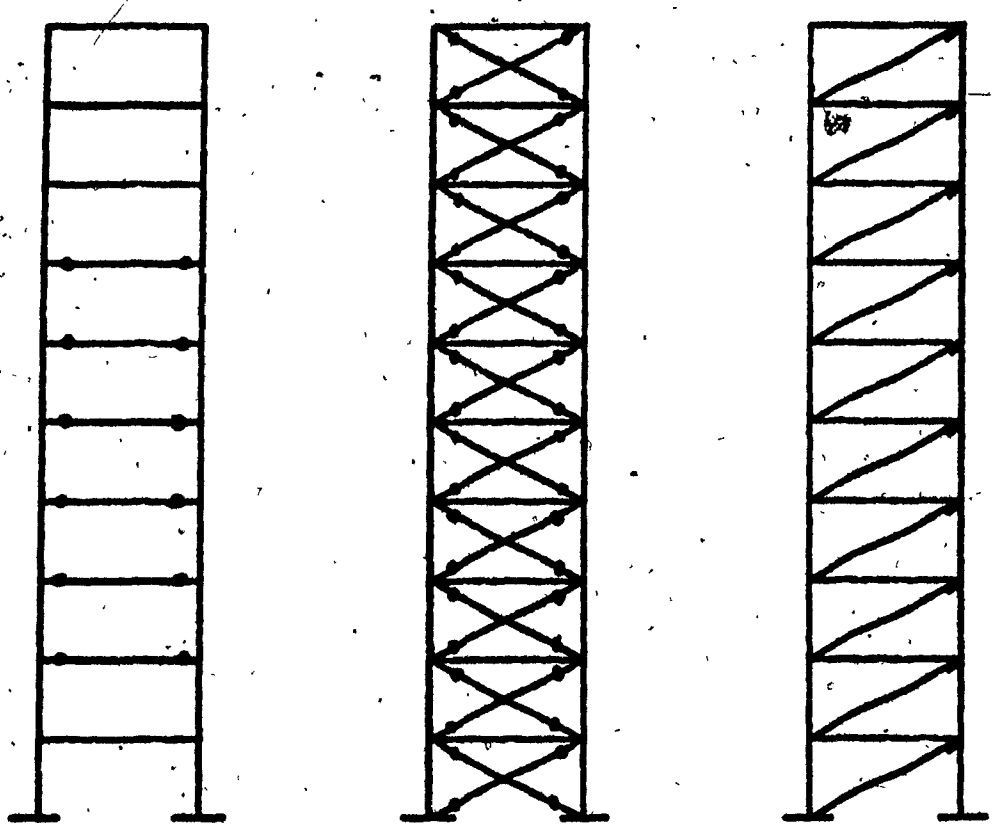

● Plastic Hinge or Yielded Brace

▬ Slipped Joint

FIG. 3.14 Comparisons between FDBF, MRF, and CBF: Structural Damage After Earthquake, 0.5 x El-Centro, (0.16g)

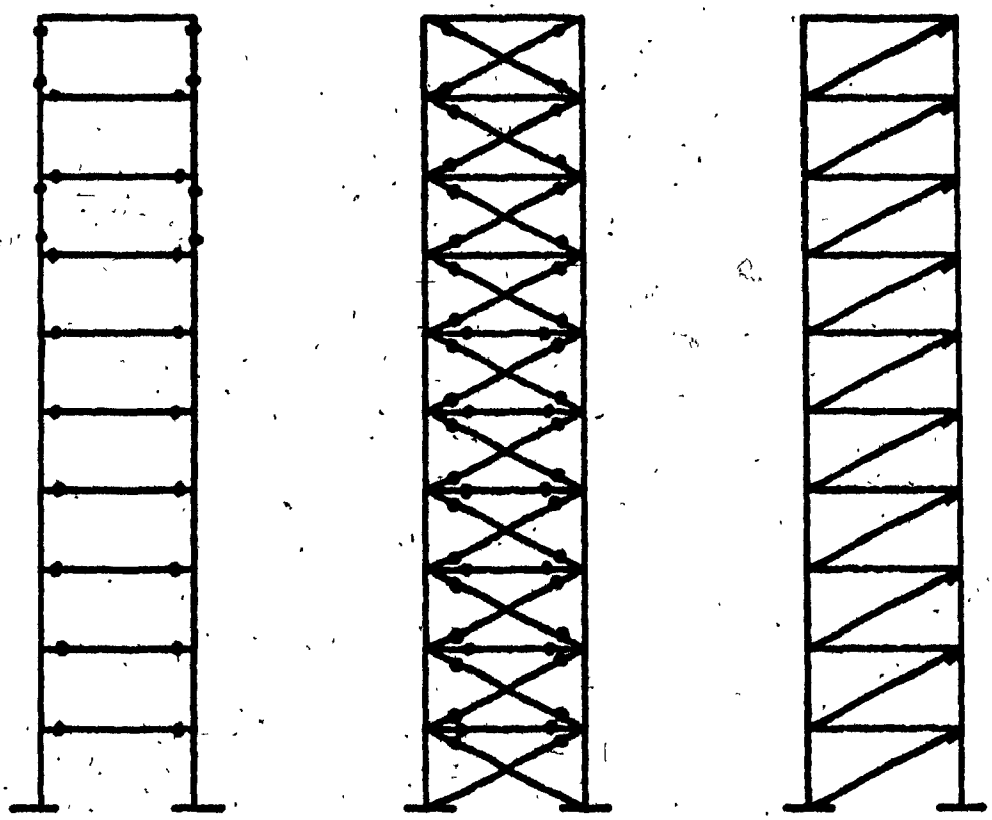

• Plastic Hinge or Yielded Brace

▬ Slipped Joint

FIG. 3.15 Comparisons between FDBF, MRF, and CBF: Structural Damage After Earthquake, 1.0 x El-Centro (0.32g)

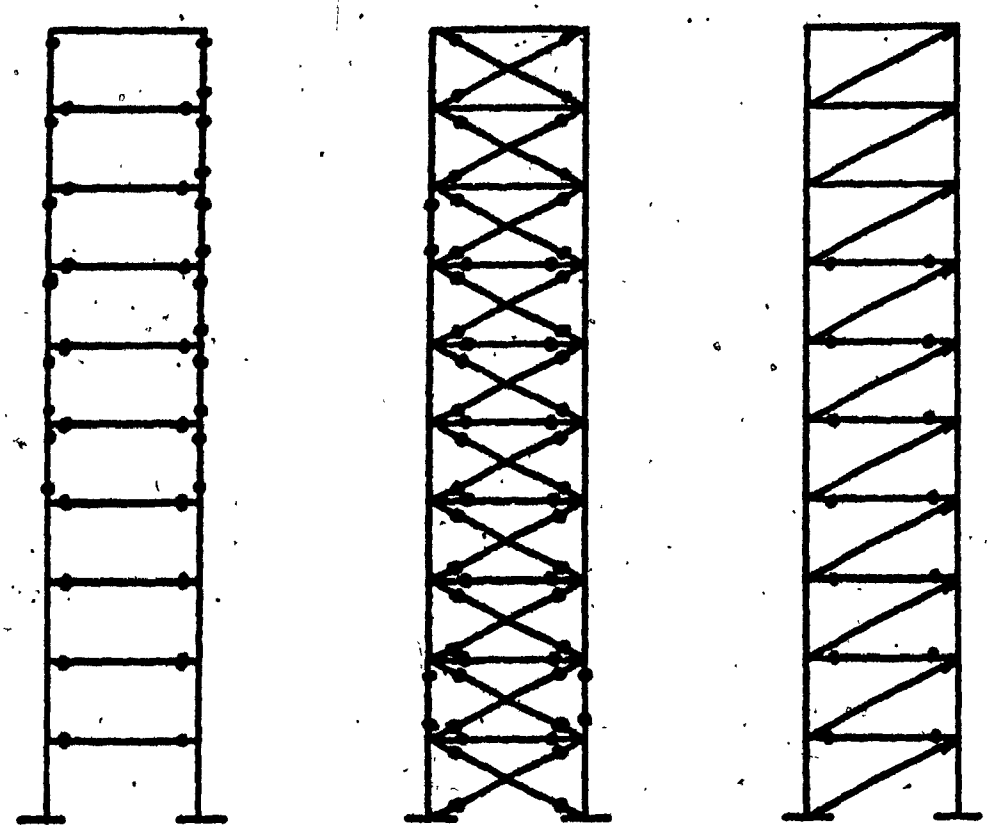

FIG. 3.16 Comparisons between FDBF, MRF, and CBF: Structural Damage After Earthquake, 2.0 x El-Centro, (0.64g)

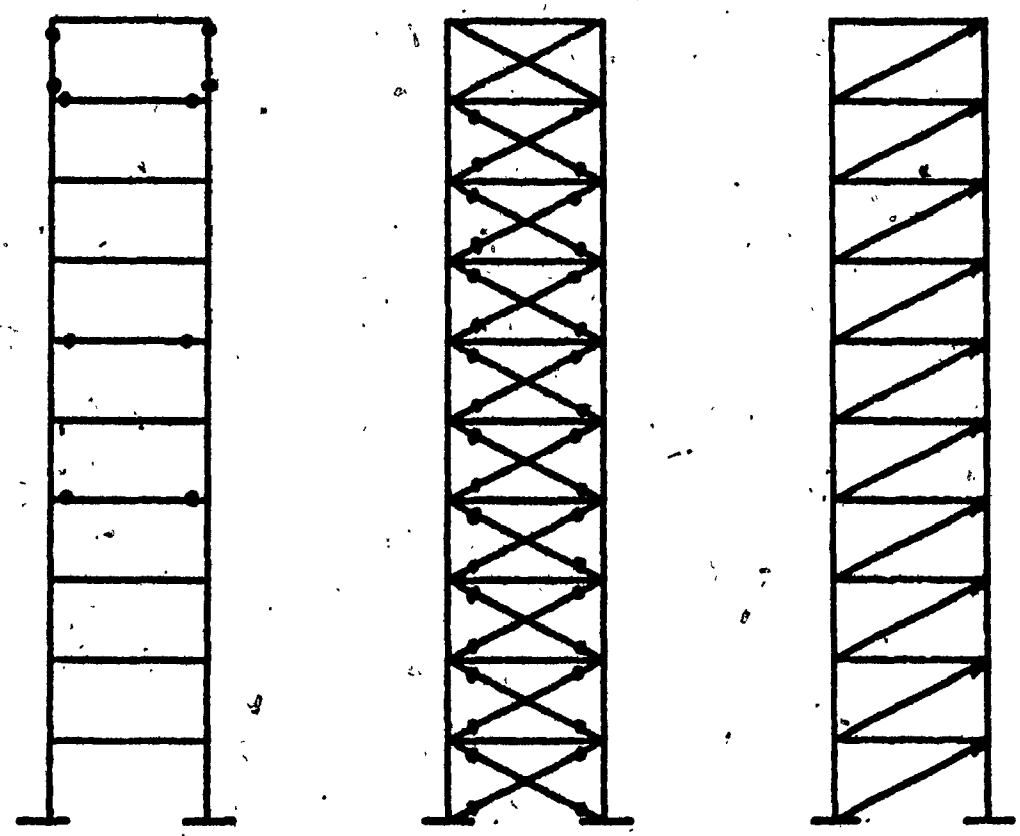

FIG. 3.17 Comparisons between FDBF, MRF, and CBF: Structural Damage After Earthquake, 1.0 x Taft, (0.16g)

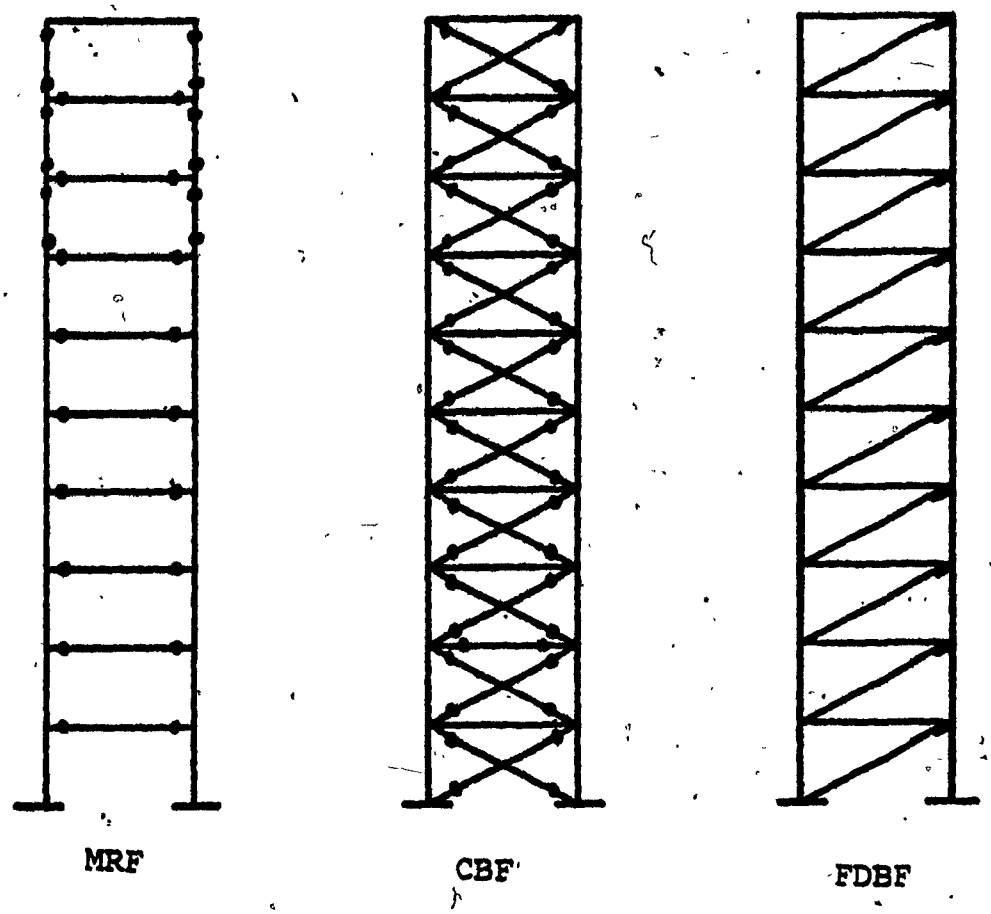

FIG. 3.18 Comparisons between FDBE, MRF, and CBF: Structural Damage After Earthquake, 2.0 x Taft, (0.32g)

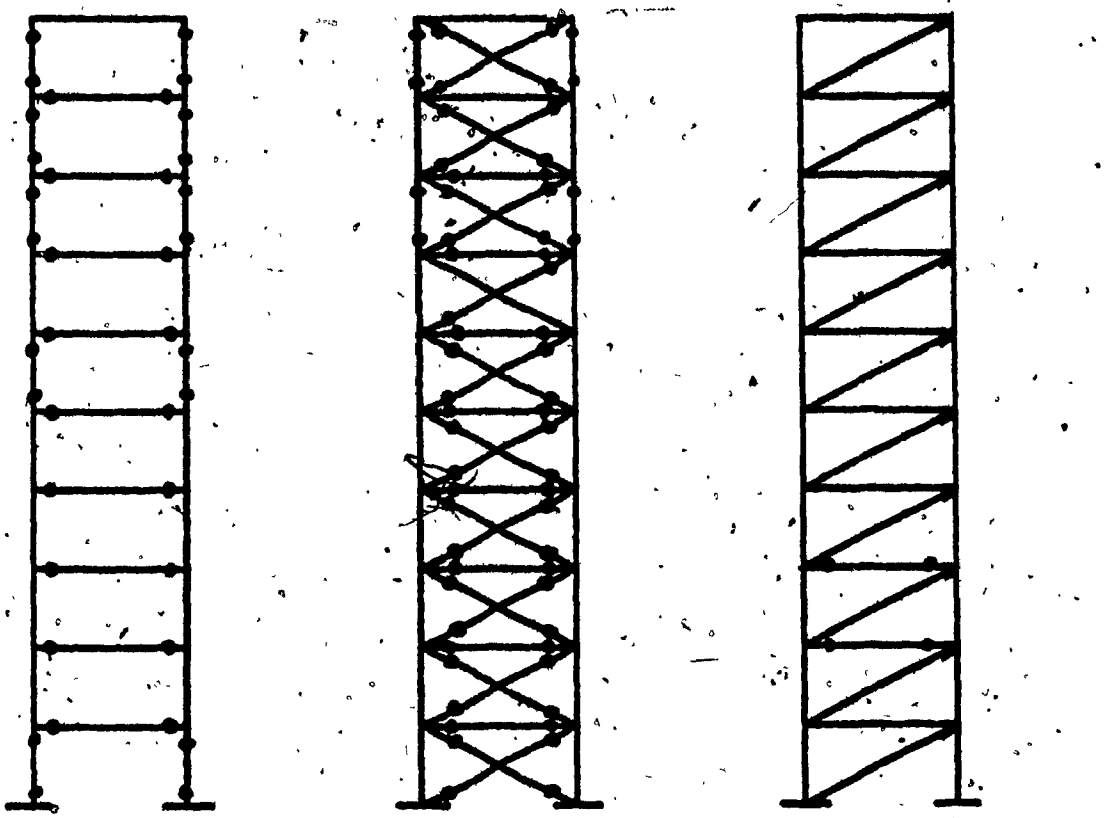

FIG. 3.19 Comparisons between FDBF, MRF, and CBF: Structural Damage After Earthquake, 4.0 x Taft, (0.64g)

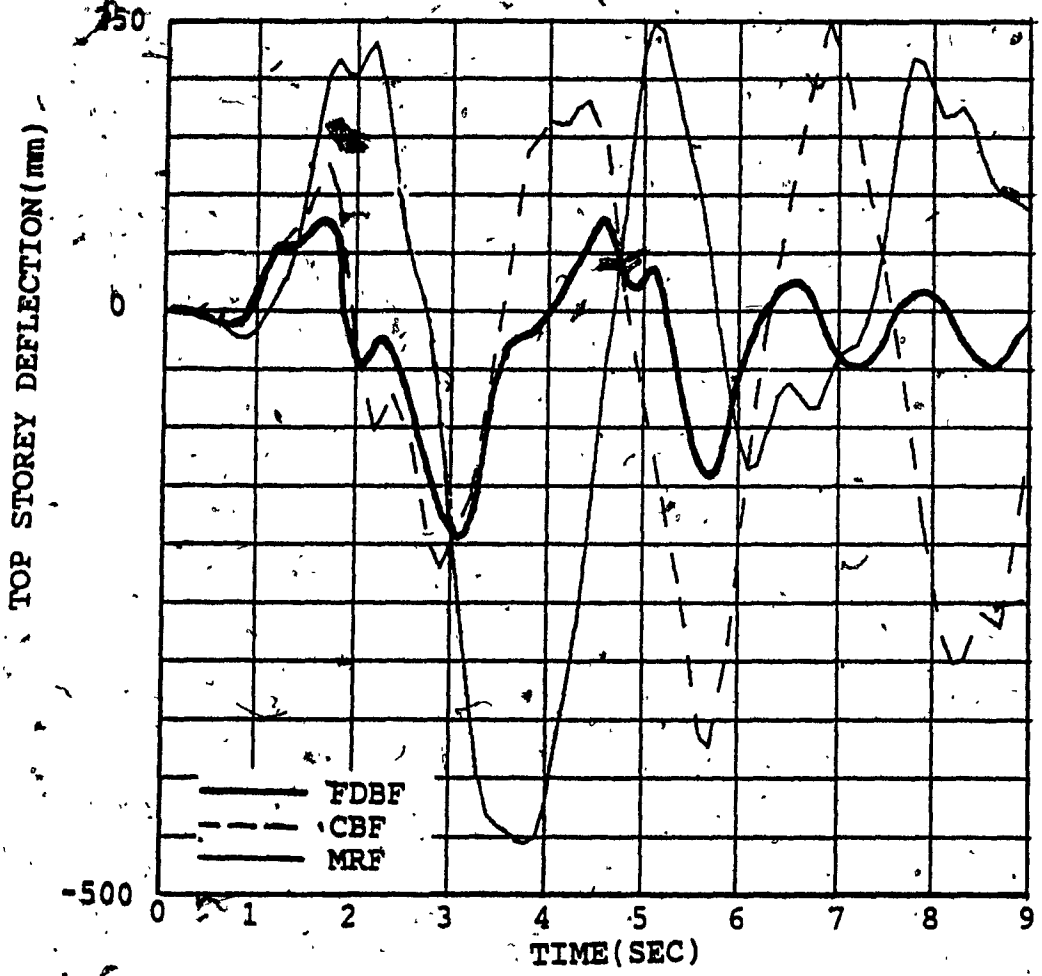

FIG. 3.20 Comparisons between FDBF, MRF, and CBF: Time History of Top Storey Deflections for 1.0 x El-Centro (0.32g)

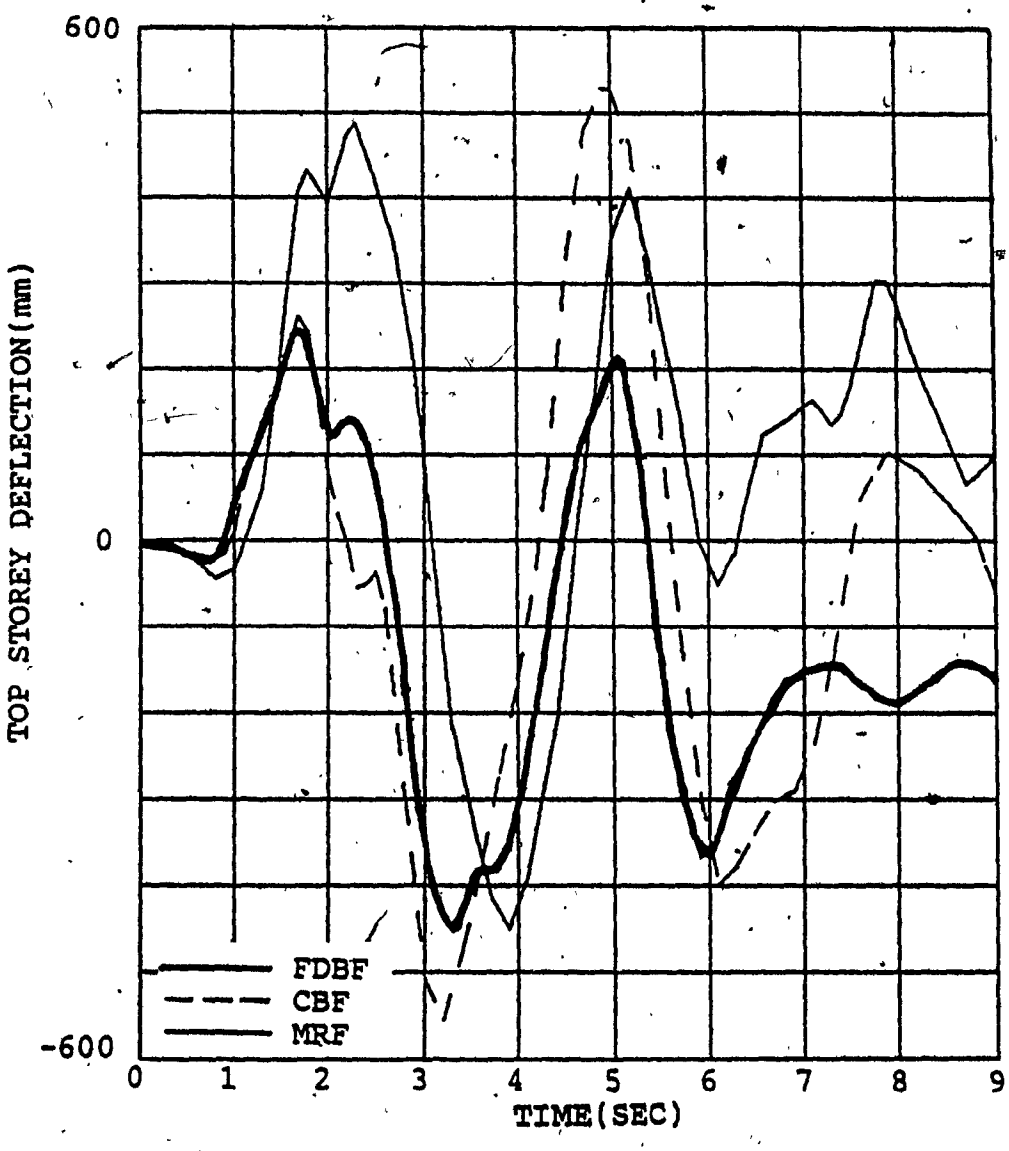

FIG. 3.21 Comparisons between FDBF, MRF, and CBF: Time History of Top Storey Deflections for 2.0 x El-Centro (0.64g)

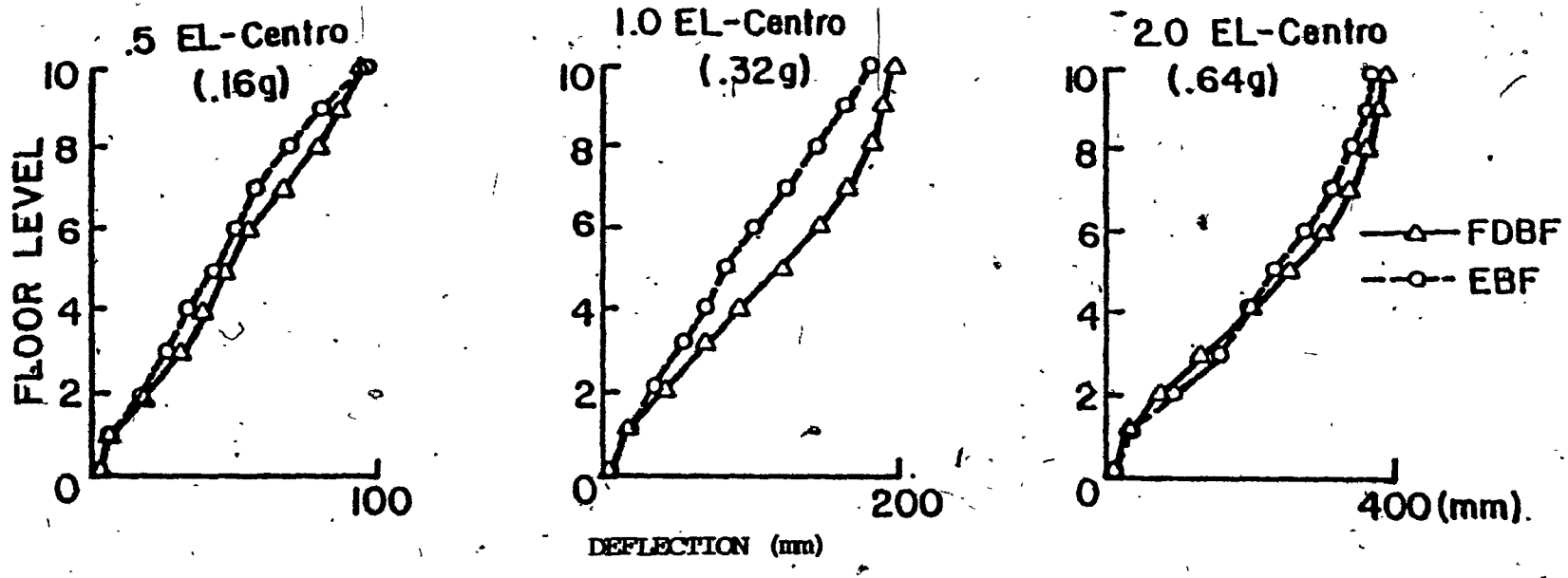

FIG. 3.22 Comparisons between FDBF, and EBF: Deflection Envelope for El-Centro Excitation

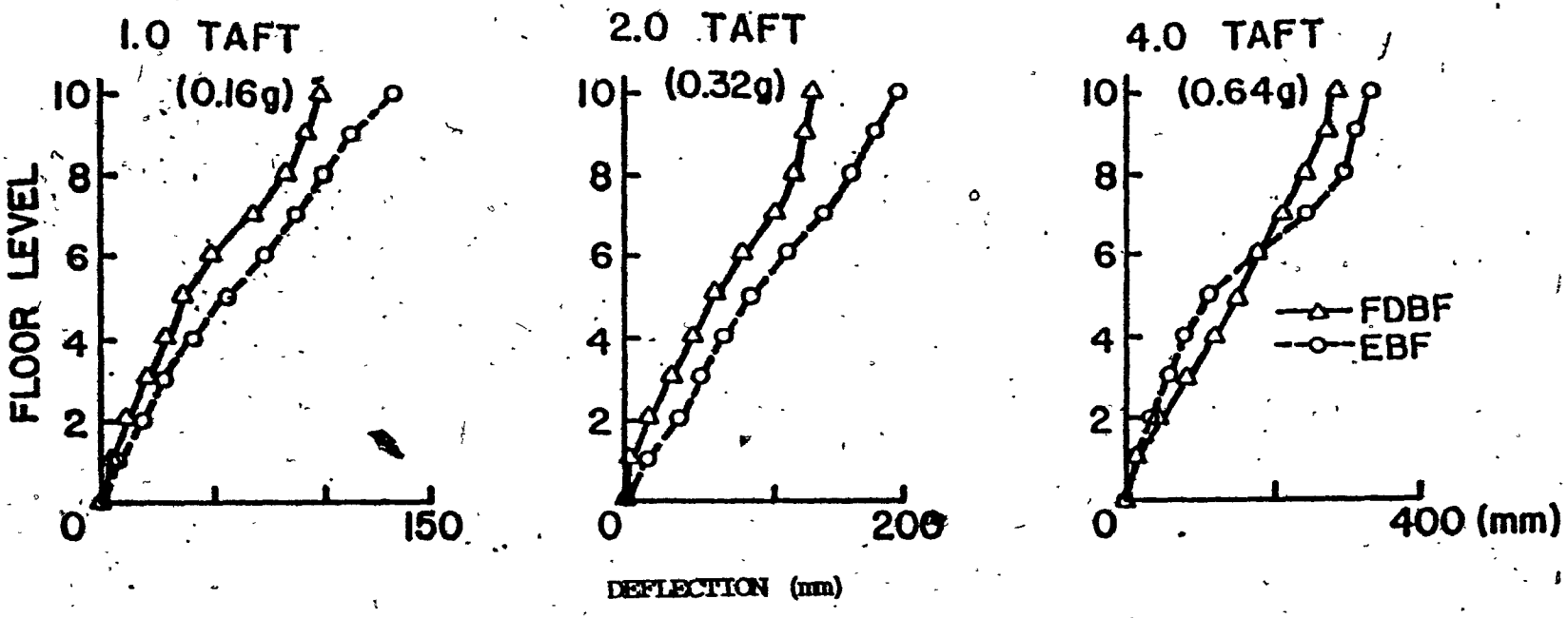

FIG. 3.23 Comparisons between FDBF, and EBF: Deflection Envelope for Taft Excitation

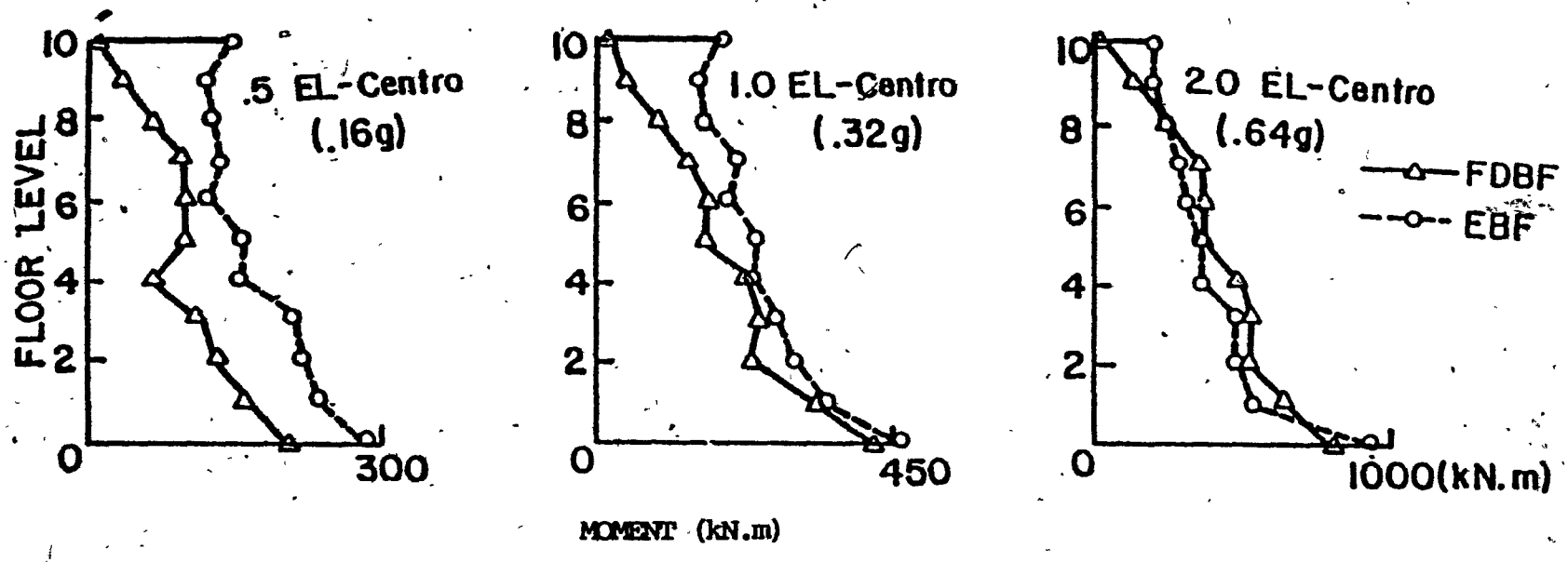

FIG. 3.24 Comparisons between FDBF, and EBF: Envelope of Moments for El-Centro Excitation

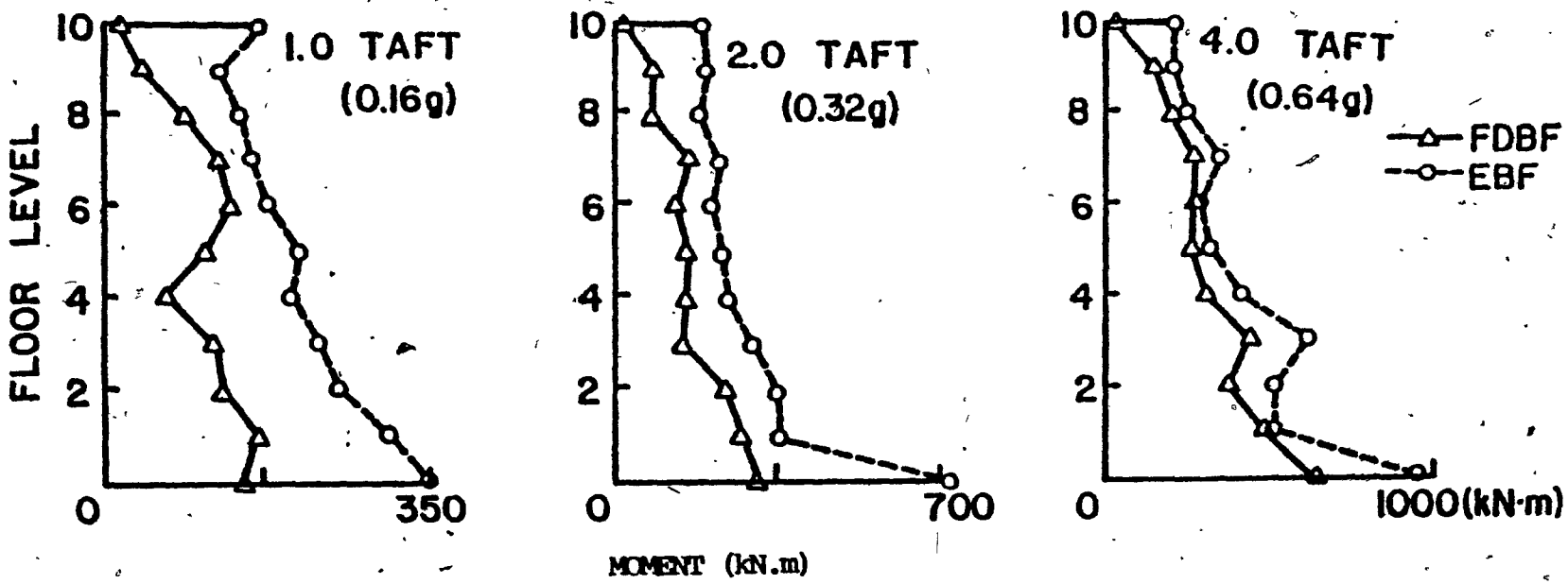

FIG. 3.25 Comparisons between FDBF, and EBF: Envelope of Moments in Columns for Taft Excitation

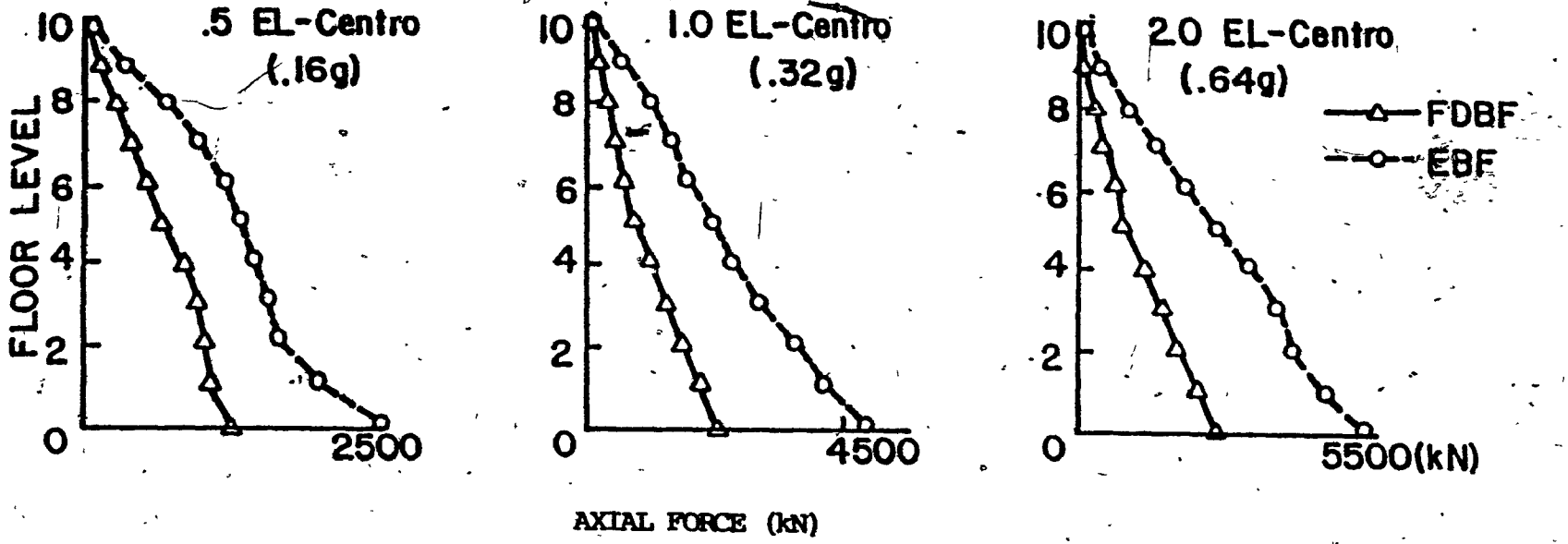

FIG. 3.26 Comparisons between FDBF, and EBF: Envelope of Axial Forces in Columns for El-Centro Excitation

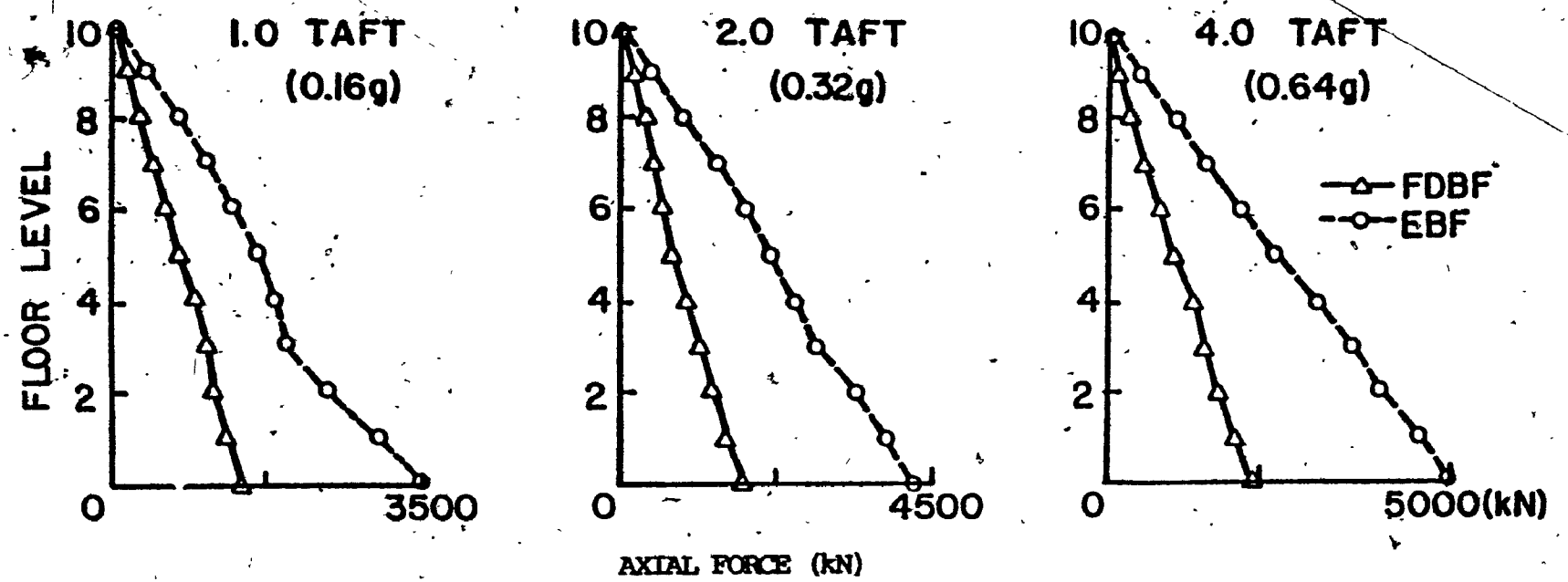

FIG. 3.27 Comparisons between FDBF, and EBF: Envelope of Axial Forces in Columns for Taft Excitation

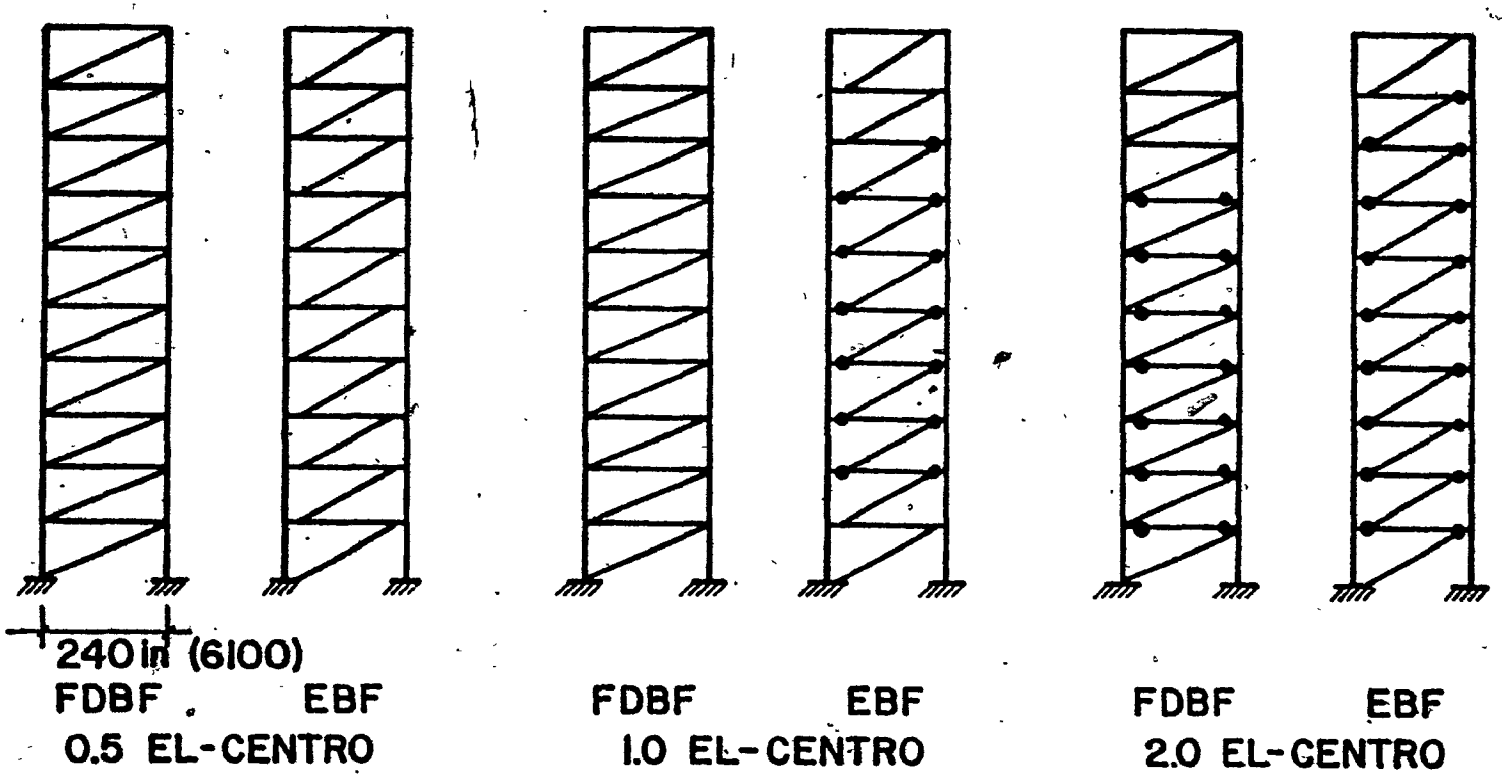

FIG. 3.28 Comparisons between FDBF, and EBF: Structural Damage After Earthquake, (El-Centro)

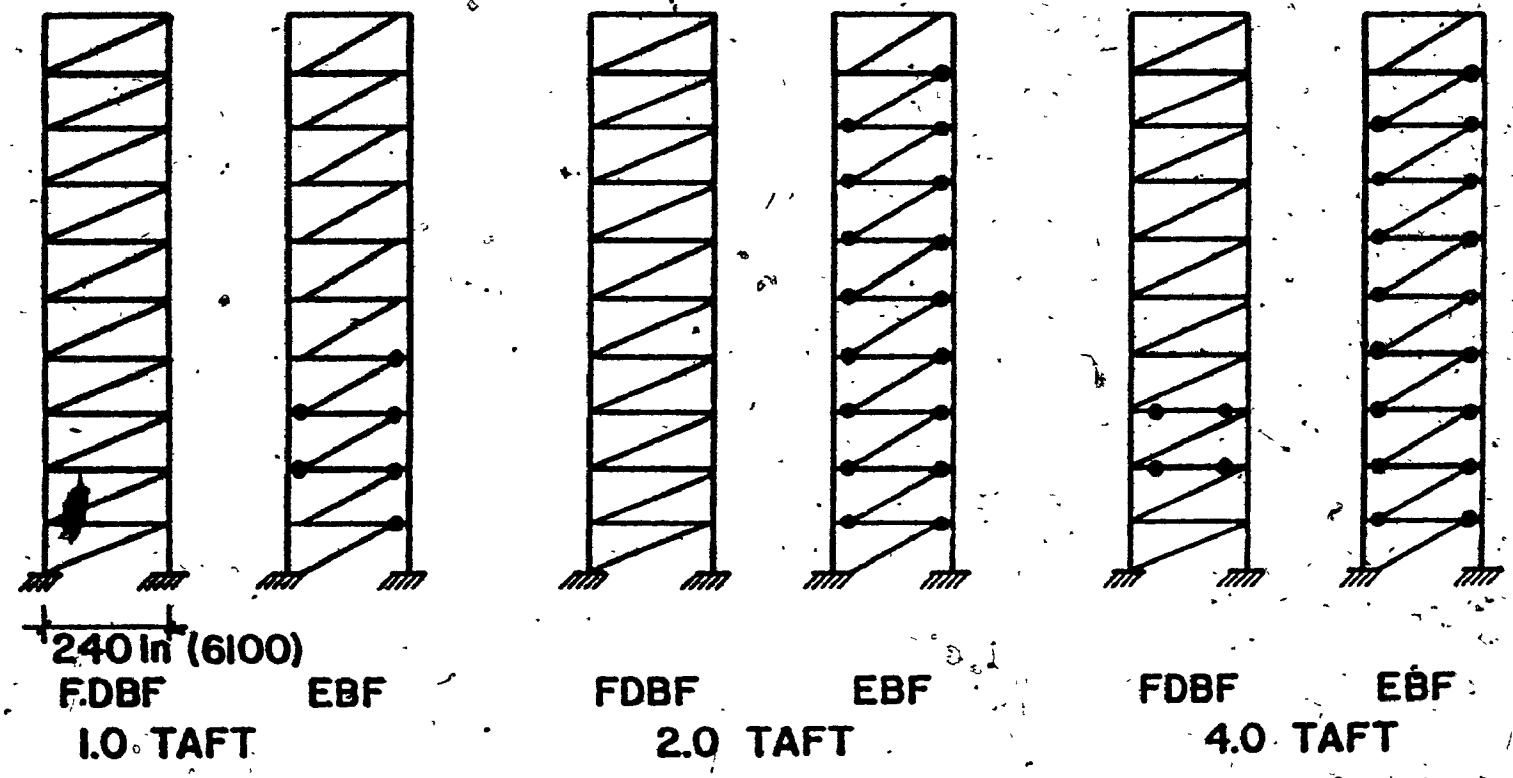

• PLASTIC HINGE

FIG. 3.29 Comparisons between FDBF, and EBF: Structural Damage After Earthquake, (Taft)

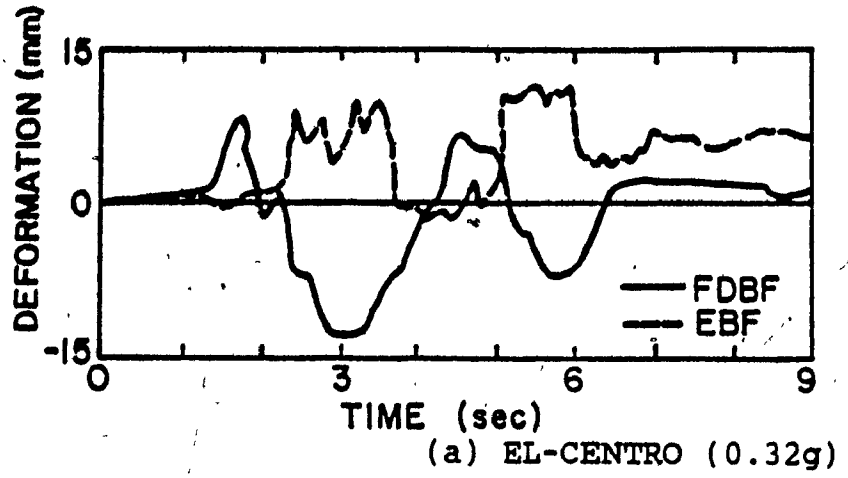

(a) EL-CENTRO (0.32g)

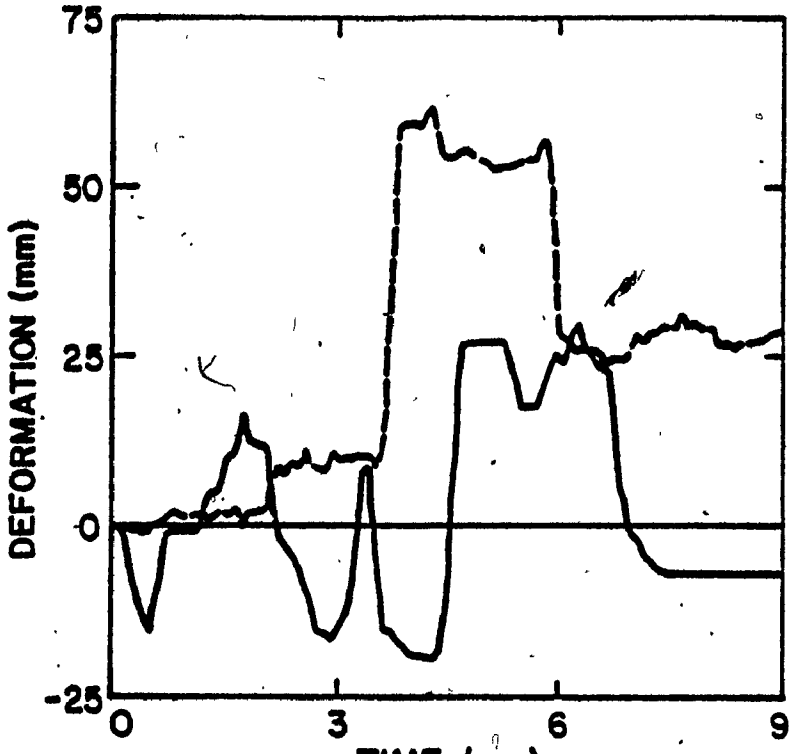

(b) TAFT (0.64g)

FIG. 3.30 Time Histories of the Slipping in the Braces of the FDBF vs. the Vertical Deflection of the Link of EBF (Second Floor)

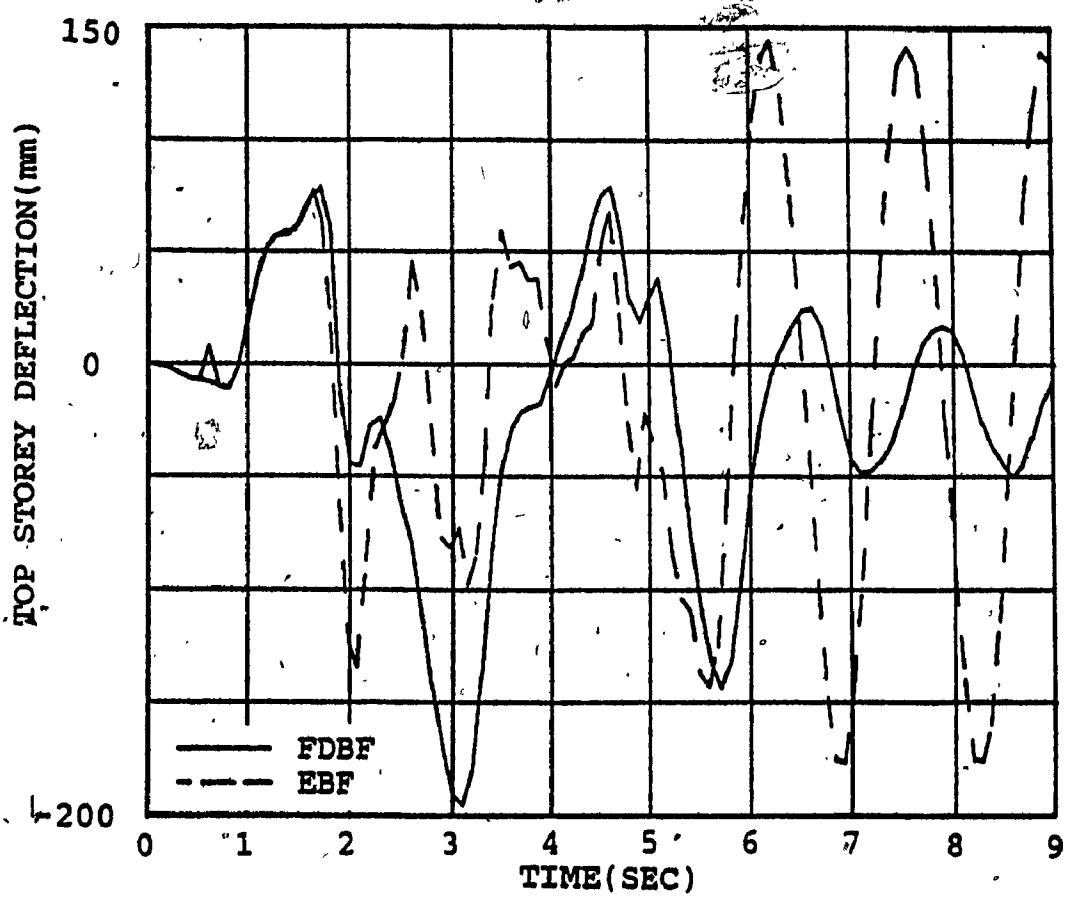

FIG. 3.31 Comparisons between FDBF, and EBF: Time History of Top Storey Deflections for 1.0 x El-Centro Excitation (0.32g)

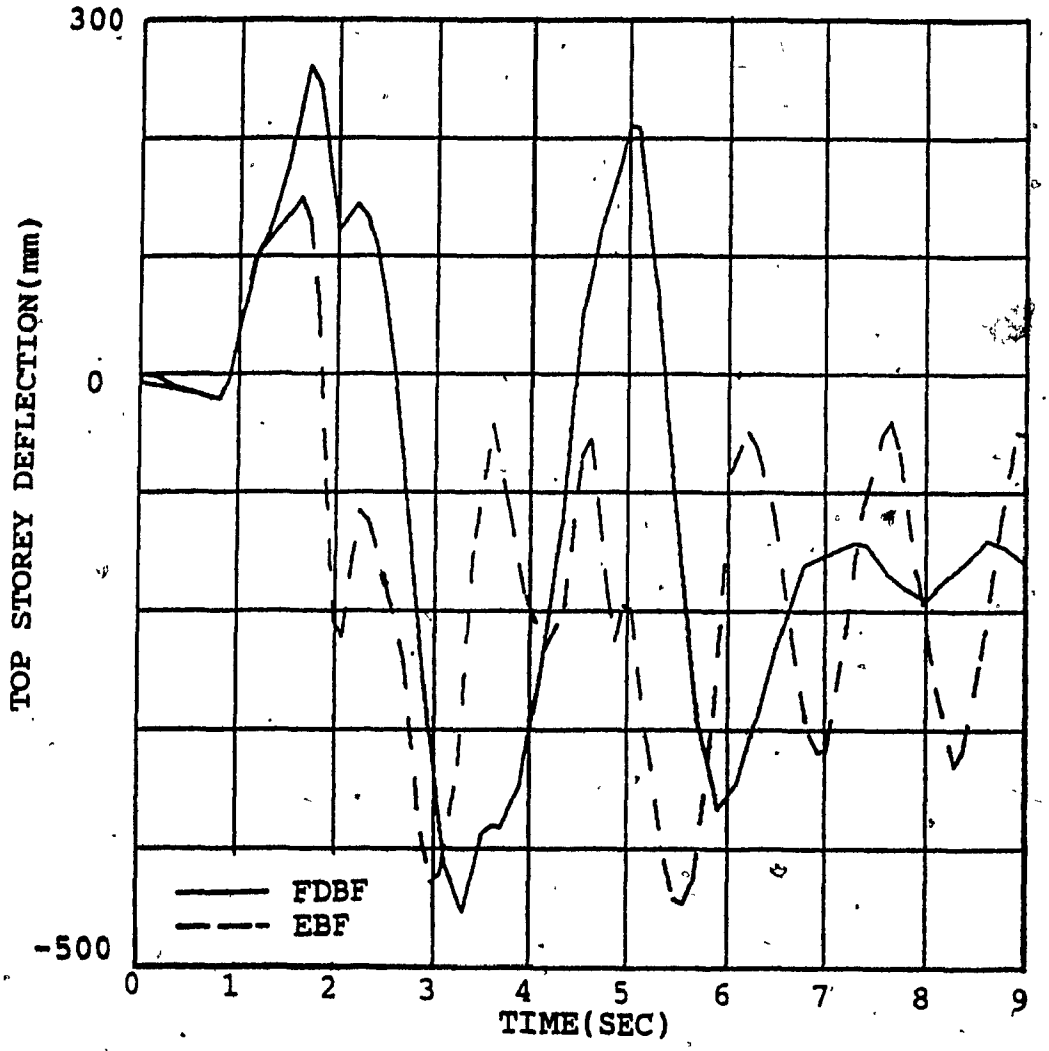

FIG. 3.32 Comparisons between FDBF, and EBF: Time History of Top Storey Deflections for 2.0 x El-Centro (0.64g)

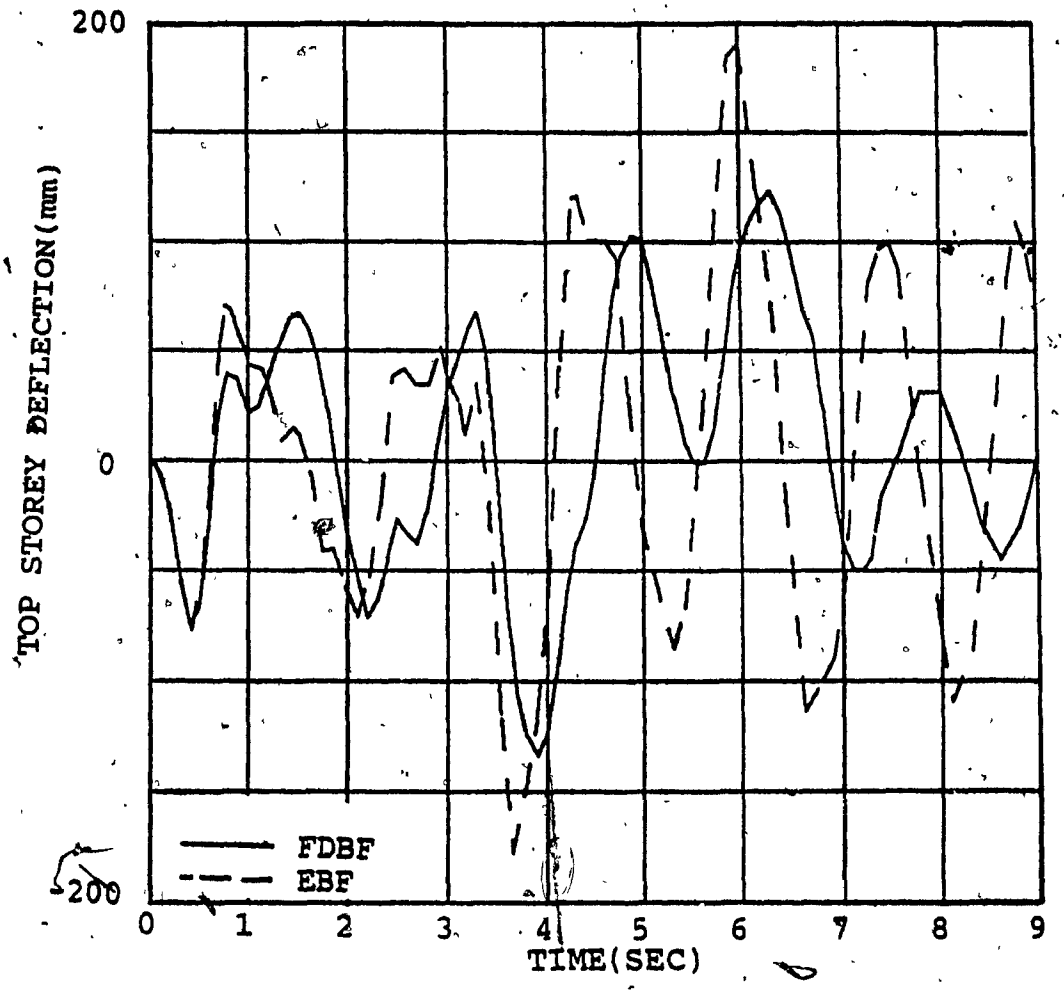

FIG. 3.33 Comparisons between FDBF, and EBF: Time History of Top Storey Deflections for 2.0 x Taft (0.32g)

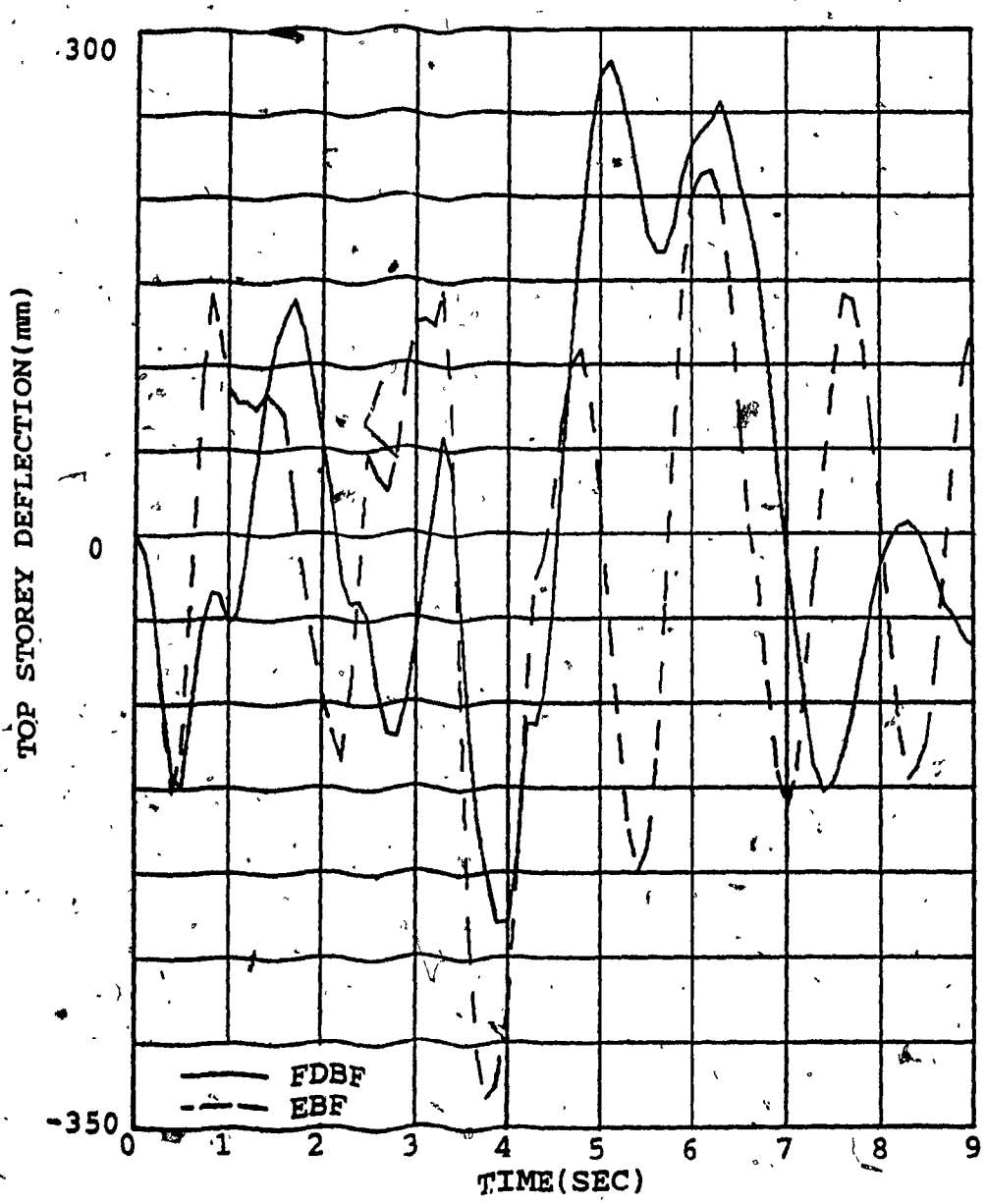

FIG. 3.34 Comparisons between FDBF, and EBF: Time History of Top Storey Deflections for 4.0 x Taft (0.64g)

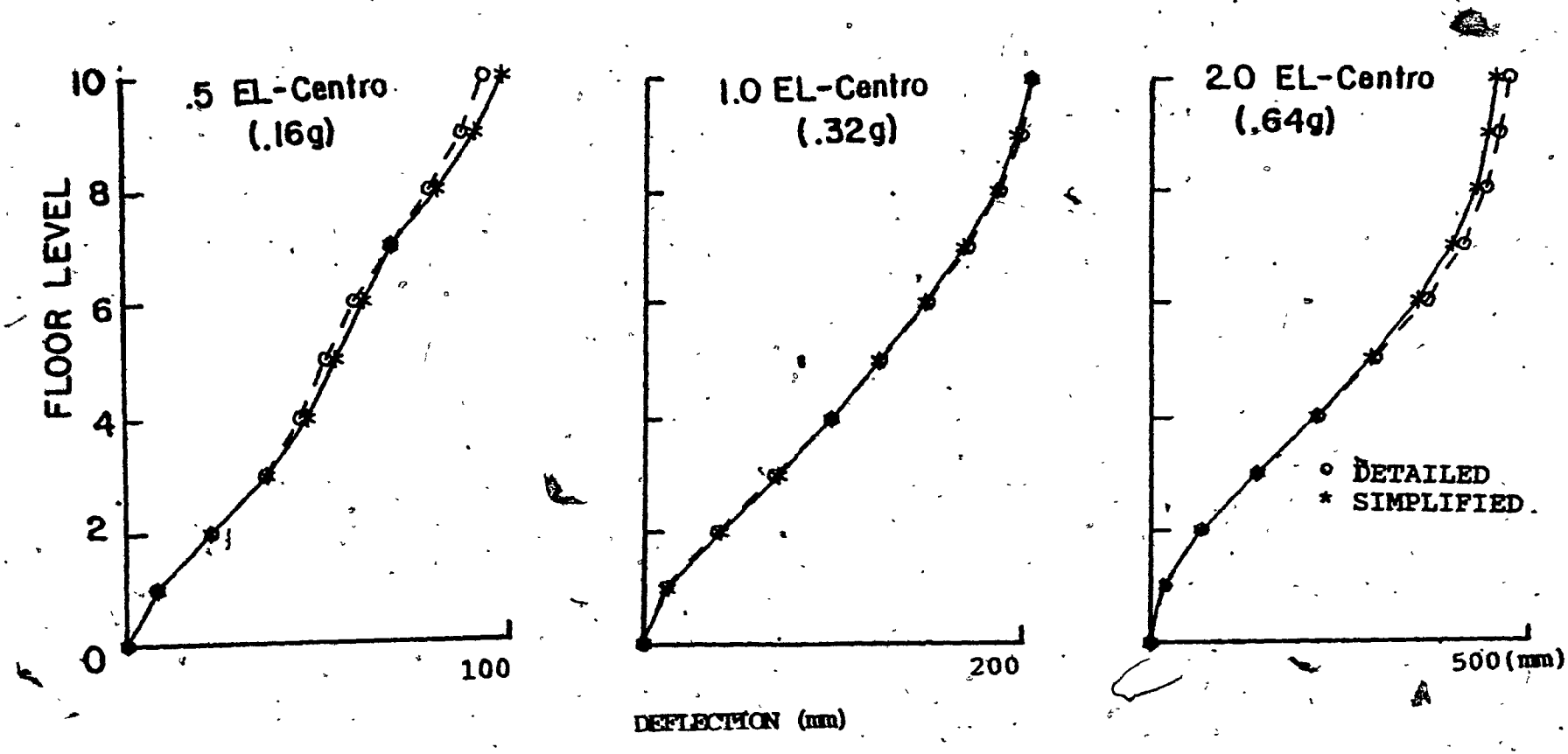

FIG. 3.35 Comparison of Storey Deflections Between the Detailed Analysis and the Simplified Model for Tension Only Bracing (El-Centro Excitation)

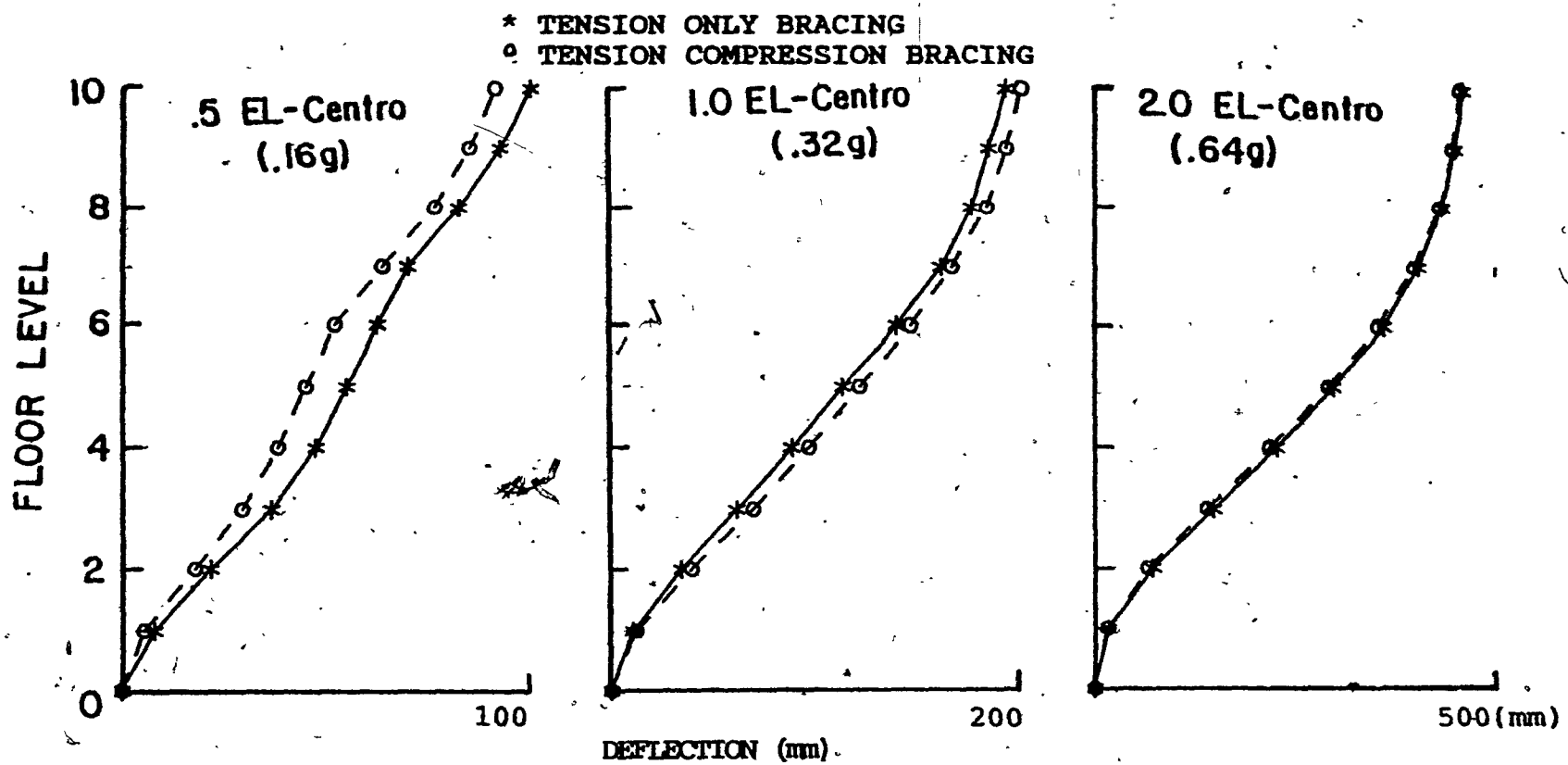

FIG. 3.36 Comparisons between FDBF with Z-Bracing and Pall Mechanism: Deflection Envelope (El-Centro Excitation)

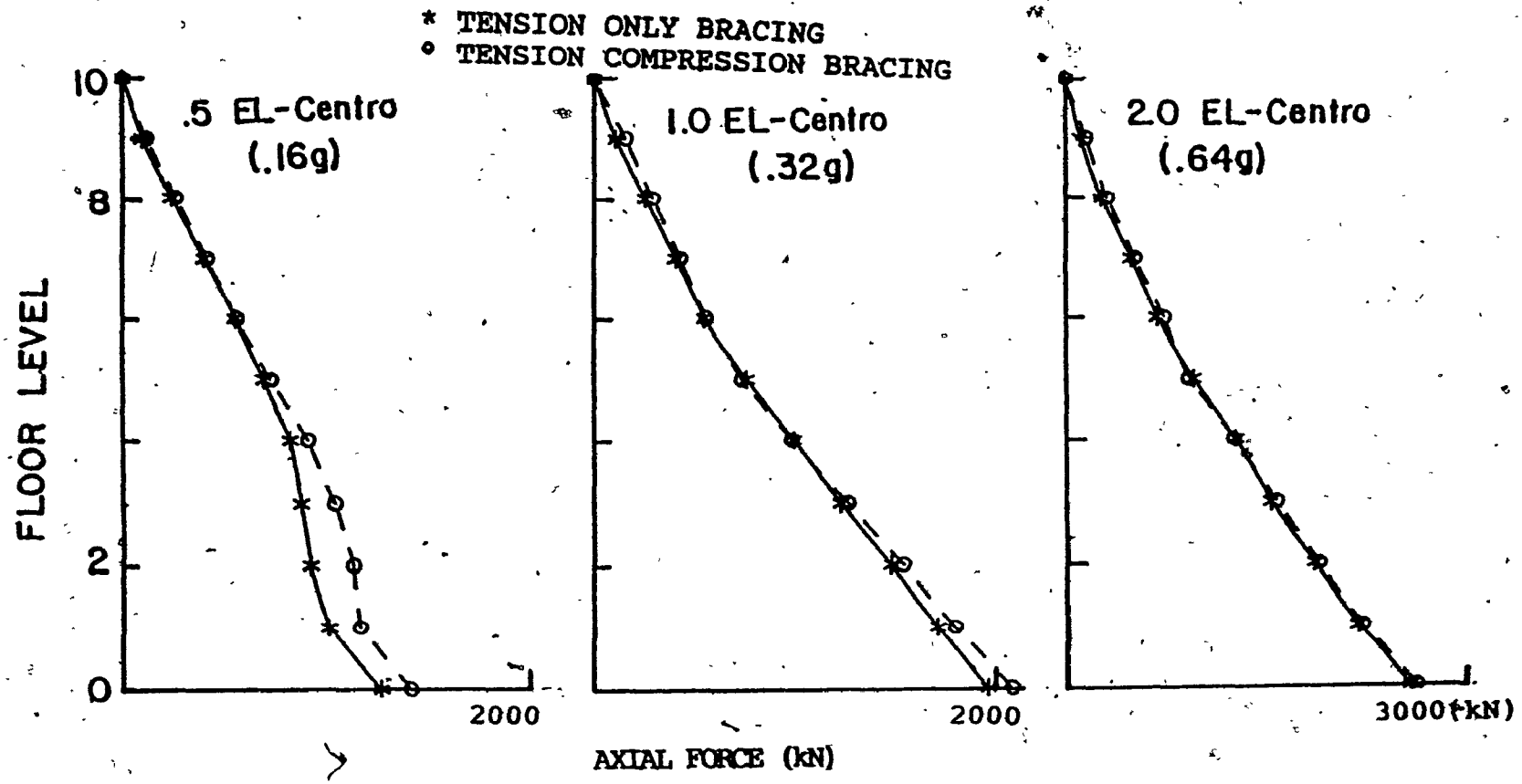

FIG. 3.37 Comparisons between FDBE with Z-Bracing and Pall Mechanism: Envelope of Axial Forces in Columns (El-Centro Excitation)

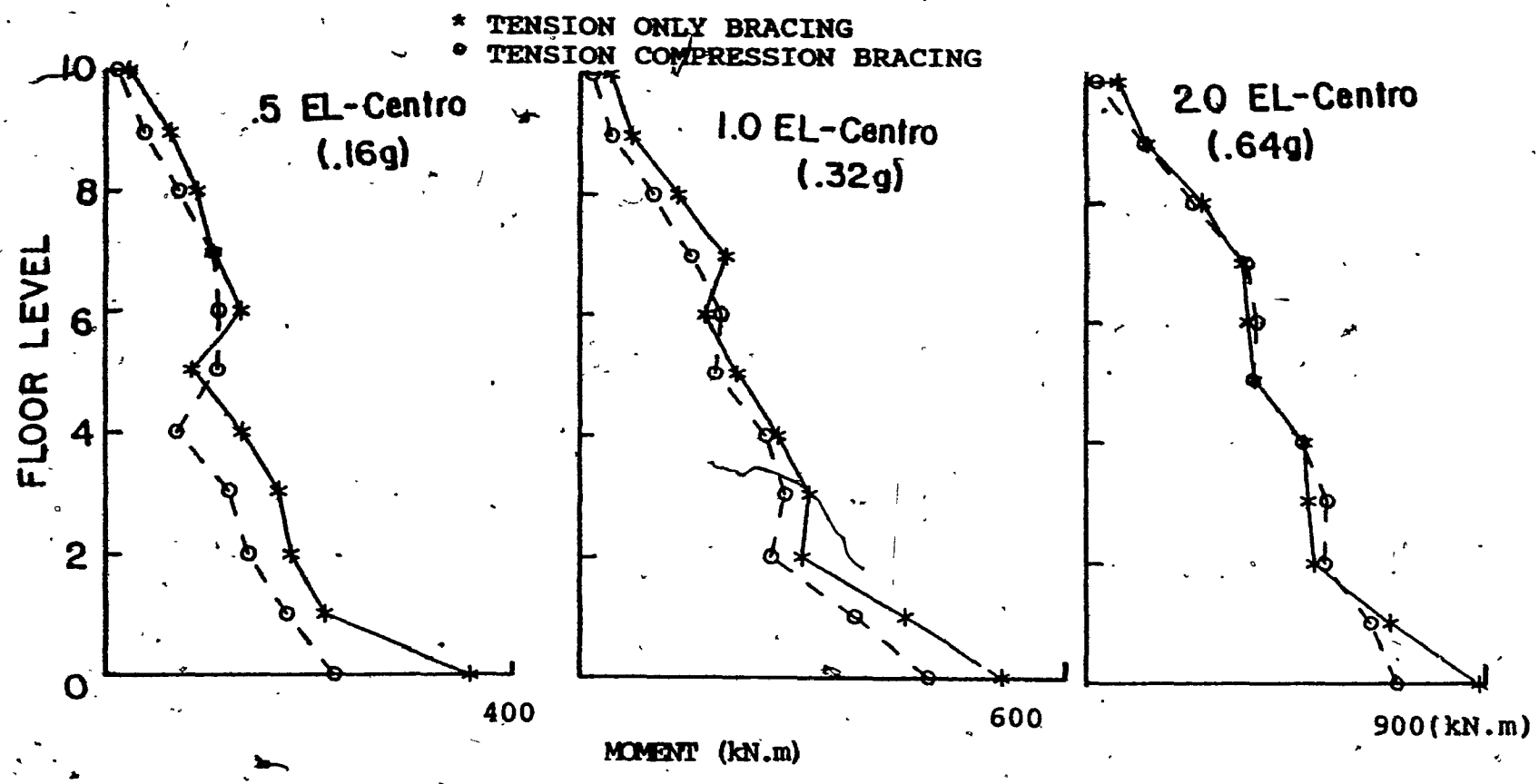

FIG. 3.38 Comparisons between FDBF with Z-Bracing and Pall Mechanism: Envelope of Moments in Columns (El-Centro Excitation)

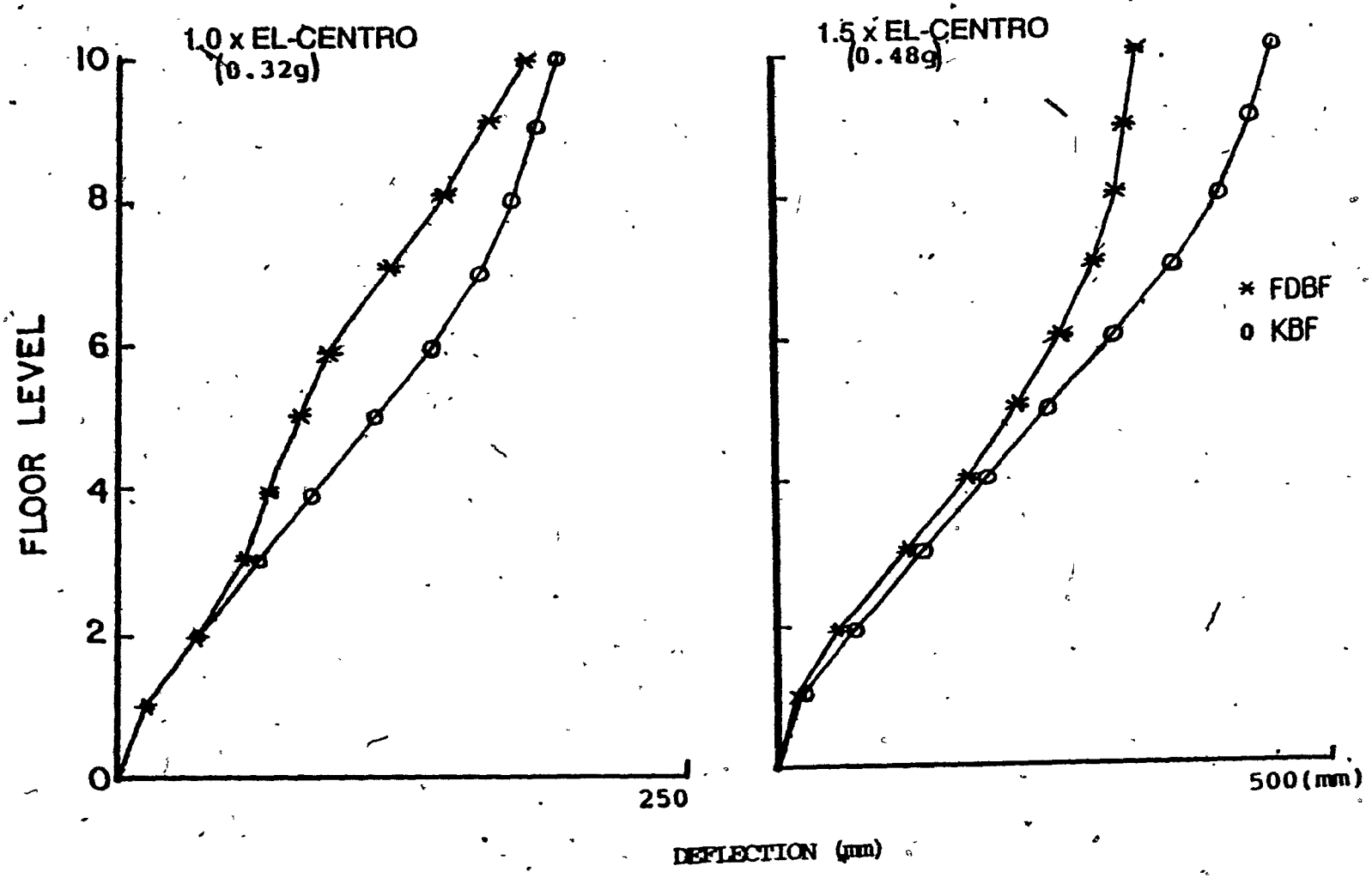

FIG. 3.39 Comparisons between K-Braced Frames: Deflection Envelope

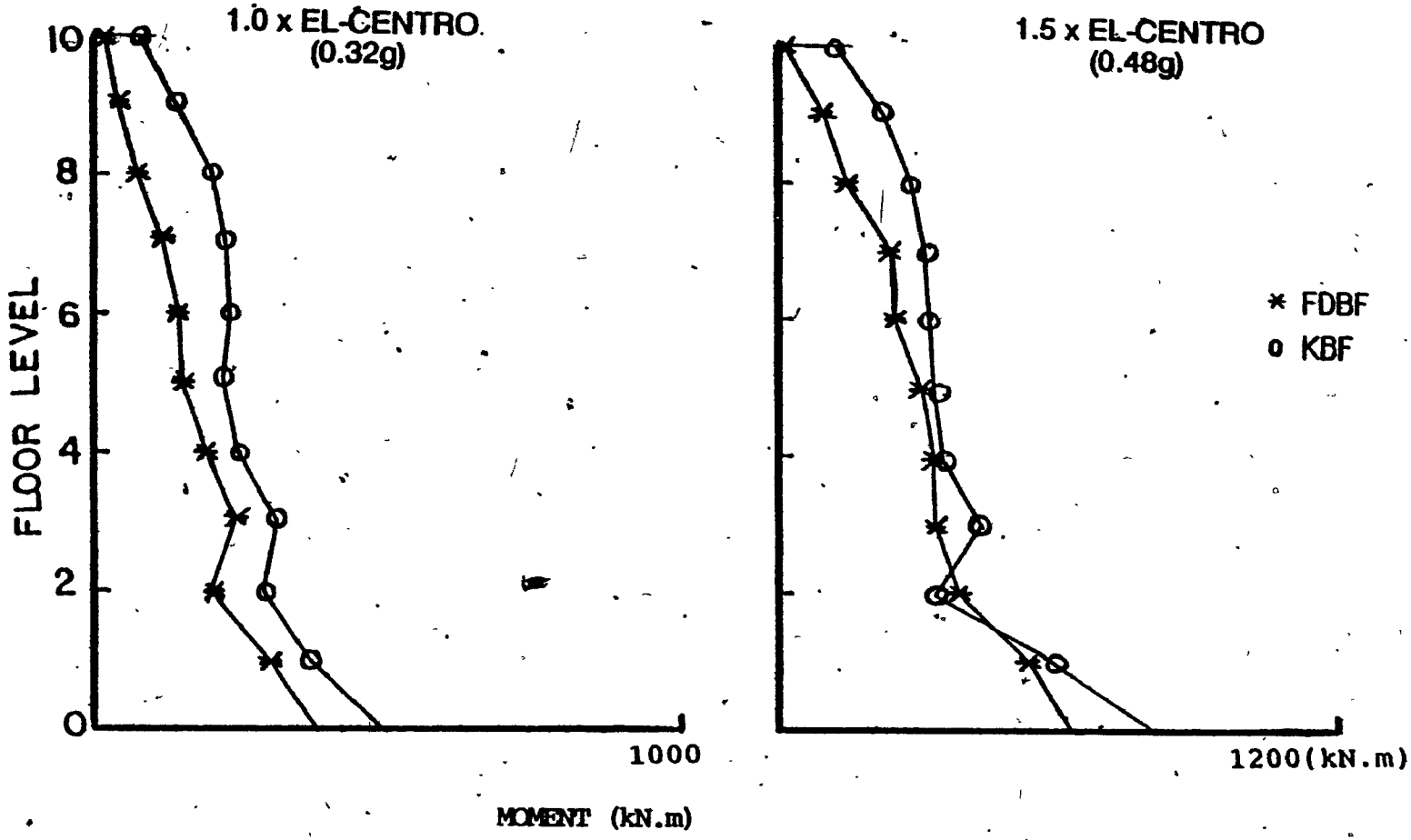

FIG. 3.40 Comparisons between K-Braced Frames: Envelope of Moments in the Columns (El-Centro Excitation)

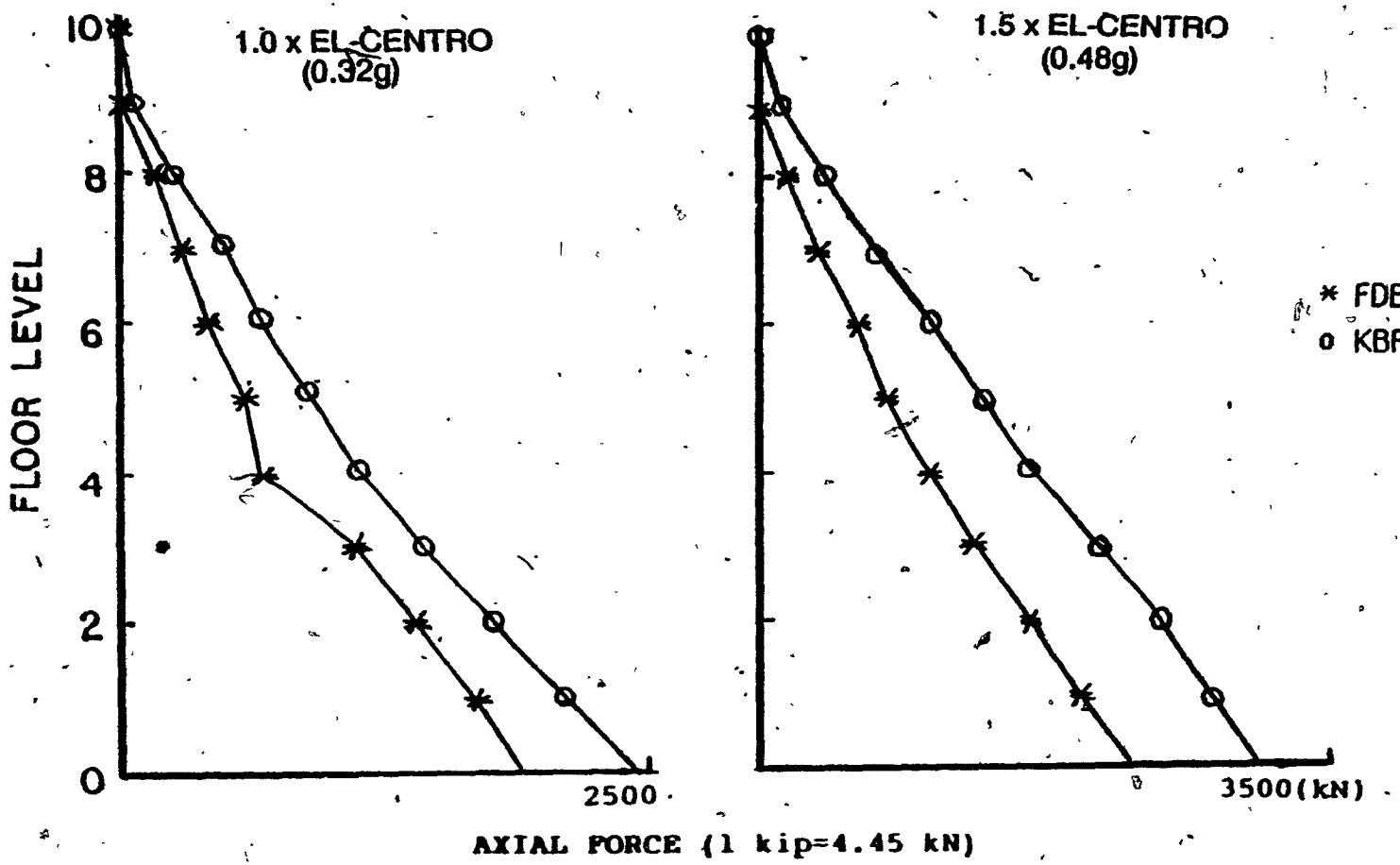

FIG. 3.41 Comparisons between K-Braced Frames: Envelope of Axial Forces in the Columns

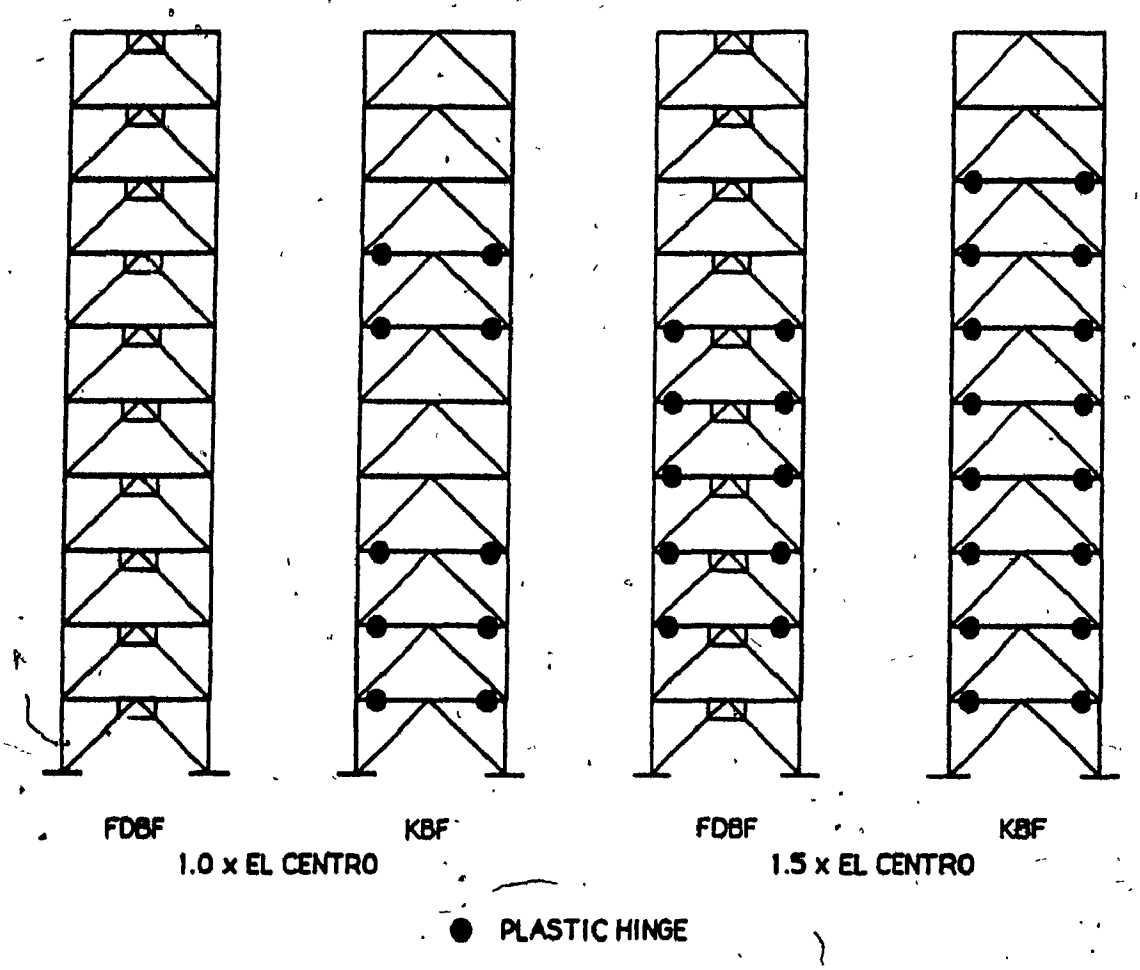

FIG. 3.42 Structural Damage, for K-Braced Frames, After Earthquake

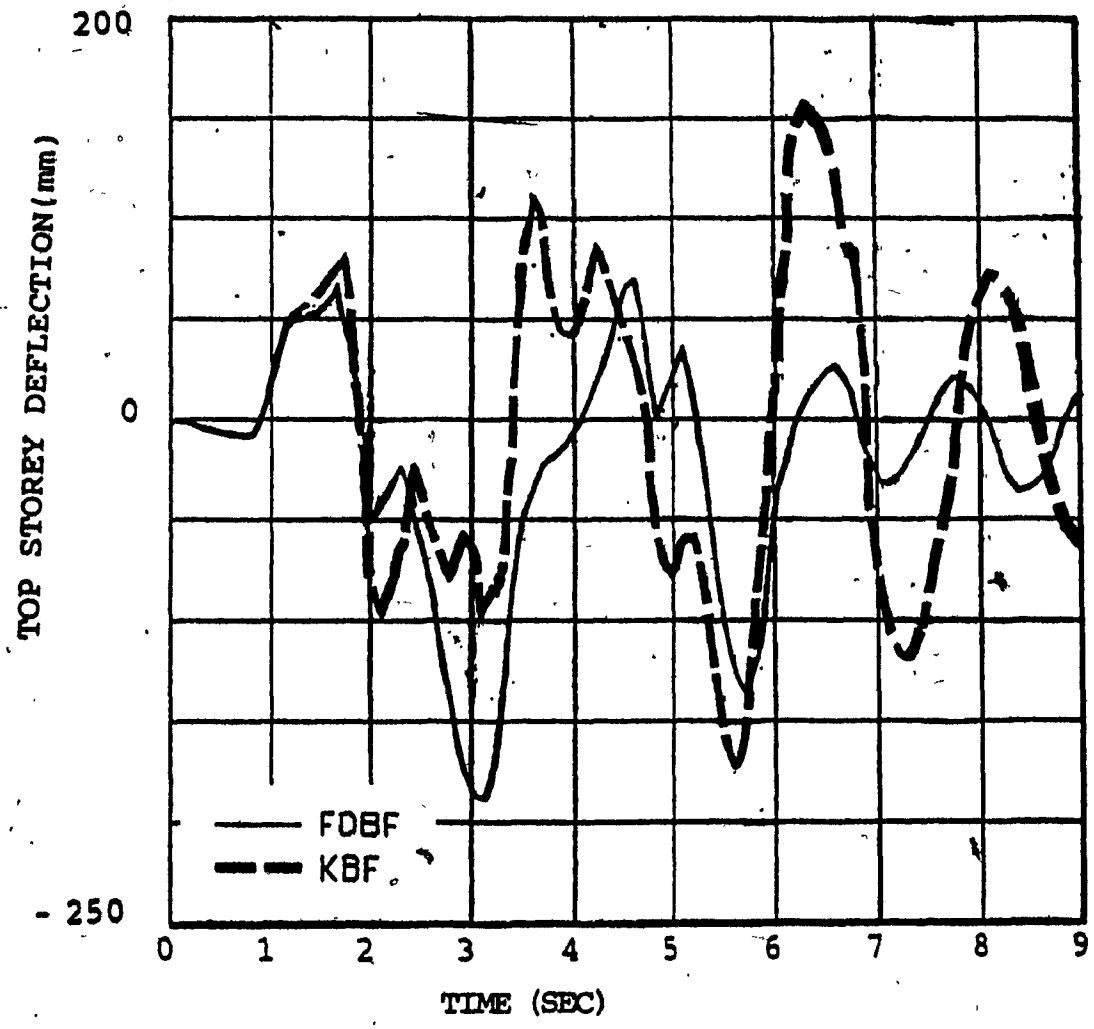

FIG. 3.43 Time Histories of the Top Storey Deflections for K-Braced Frames, 1.0 x El-Centro, (0.32g)

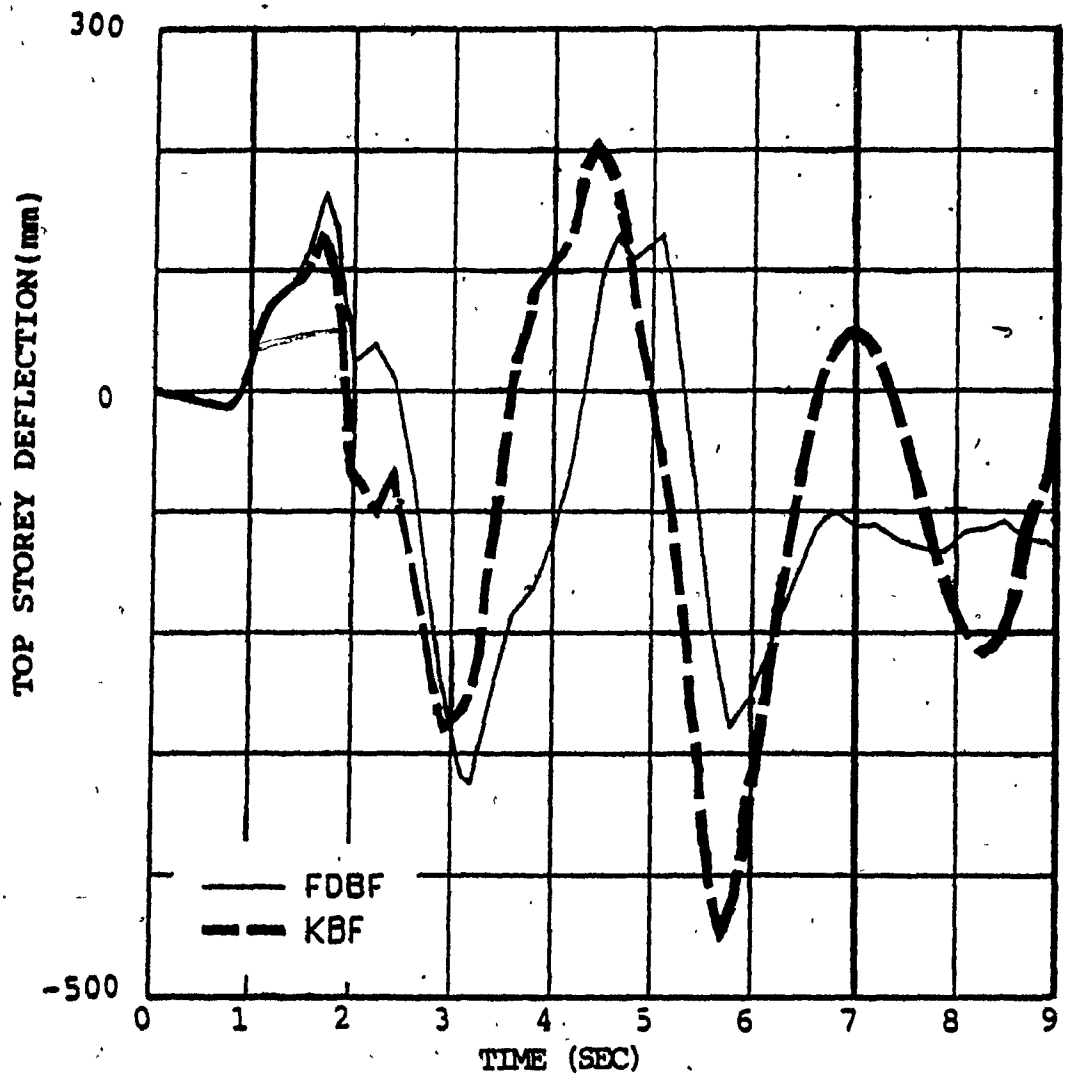

FIG. 3.44 Time Histories of the Top Storey Deflections for K-Braced Frames, 1.5 x El-Centro, (0.48g)

CHAPTER 4

TESTS

TESTS

4.1- INTRODUCTION

In the previous Chapter the analysis of the inelastic dynamic behaviour of friction damped braced frames was examined and its superiority over other existing systems was illustrated. Experimental studies were then necessary to demonstrate that the system behaves as predicted by the analytical models.

4.2- DESIGN OF TEST MODEL

The shaking table at Concordia University has dimensions of 4 m x 6 m (13 ft x 20ft), and a top clearance of 6.5 m (22 ft), which was more than adequate for this type of model. Specifically, the model was designed as a moment resisting frame (MRF) into which bracing was introduced to create a concentric braced frame (CBF) or a friction damped braced frame (FDBF), depending on the value of the slip force in the diagonals.

Two one-meter wide, four storey steel frames, 4m high and spaced 1m apart, were connected together by a cross-bracing to eliminate any torsion in the system, thus ensuring that the two frames deformed together. The details of the model are shown in Figs. 4.1 and 4.2. The columns and the beams consisted of a special light profile, SLP4X4.08, joined together with typical welded moment resistant connections (seen in Fig. 4.2). A steel mass of 910 kg (2000 lb) was added to the top floor in order to ensure that only the fundamental mode of vibration occurred. The bases of the model were welded to the shaking table.

The braces were double channels, 2-C75x6, connected to the structure using steel plates with slotted holes. Brake lining pads were inserted on both sides (between the channel webs and the gusset plate). The details are shown in Fig. 4.3.

The structure is shown on the shaking table in Figs. 4.4 to 4.6.

4.3- SPRING LOADED FRICTION JOINT

A means of creating a known slip force was needed to assure the optimum performance.

To create the pressure to control the slip force in the friction joints, the following methods were tried;

a) The 'turn of the nut' method. In this case the start point was subjected to human error.

b) Coil springs placed under the bolt heads with the shortening calibrated to the slip force. This system was not sufficiently accurate as the forces were not repeatable.

c) Torque meters used to measure the torque applied at each bolt, and calibrated with the slip loads. This again proved to be non-repeatable.

As none of the above methods was sufficiently accurate or repeatable, a new system was developed.

Details of the device developed are shown in Fig. 4.3.

A long bolt passes through the friction joint, in which brake lining pads are trapped between the legs of the double angle diagonals and the gusset plate with slotted holes. The bolt also passes through two arms of a "spring" formed by two spring steel plates, clamped at one end on each side of a spacer. The bolt is held accurately oriented in the holes of the spring steel plate by a conical nut. A strain gauge on the spring plates monitors the force exerted by the bolt on the plates. Because the coefficient of friction is reliable, the slip force relates to the tension force.

Correlation between the strain gauge readings and the slip force were obtained by calibration. They proved to be consistently repeatable. The actual force in the bolt was calculated from the strain gauge values using the elastic properties of the plates. The readings suggested a coefficient of friction of 0.53 for higher forces, rising to 0.6 for small forces. A value of 0.53 was used in calculations.

Figure 4.7 shows the calibration set up and Fig. 4.8 shows the friction device being adjusted.

4.4- QUASI-STATIC TESTS

The behaviour of the structure under slow cyclic loading was initially investigated. The energy dissipated is given by the area of the hysteresis loop and the objective in optimizing the slip force is to maximize this area.

The top of the structure was held in position while the base, which was fixed to the shake table, was moved cyclically over a range of ± 2 kN.

With zero slip force, the frame acts as a moment resisting frame (MRF) and is almost entirely elastic, with full elastic recovery, giving a very narrow hysteresis loop.

At the other extreme it becomes a CBF, which is much more rigid but equally elastic, again with only a small hysteresis loop.

Between these extremes, there is a slip force to give a maximum area of the loop.

The slopes of the lines showing the force displacement relationship, for the friction damped bracing, follow that of the CBF for the initial elastic range and that of the MRF for the slipping range.

It can be readily shown that the maximum area of the loop occurs when P_s = 1.1 kN, which is closely demonstrated in Fig. 4.9(c). In this case, at maximum displacement, almost half the applied shear force is carried by the bracing, while the remainder is carried by the moment resisting frame. This is the relationship derived in Chapter 2.

The hysteresis loops shown are for the sixth to twentieth cycles, but the loops were repeatable for many more cycles. To compare the experimental results with theoretical analysis, "ADINA" Program (37), which is a finite

element program for automatic incremental nonlinear analysis, was chosen since static analysis cannot be performed with the "Drain-2D" program.

The dashed lines in Fig. 4.9 indicate the theoretical results for the nonlinear static analysis obtained using the ADINA program (37), and provide a check on the theoretical analysis.

4.5- DYNAMIC TEST

Sinusoidal base excitation was used to operate the shaking table. The excitation was based on a constant acceleration sweeping through a frequency domain of one to ten cycles per second (Hz). Figure 4.10 shows the variation in the frequency of the shaking table versus time with a constant acceleration of 0.106g. With this type of excitation the occurrence of the resonance frequency is inevitable for different types of structural system. As expected, the natural period of vibration decreases as the slip load increases. Figure 4.11 shows the top storey deflection at different slip forces. Variation in the natural period of vibration is clearly illustrated in this figure.

The results obtained from the tests were compared with the values given by the Drain-2D computer program. Since in the experiments the shaking table gave a sinusoidal motion, the input acceleration in the computer analysis was in sinusoidal form.

In each computer test, the period of vibration for the input acceleration was the same as in the experimental tests, (40.8 in/sec^2 = 0.106 g).

The study was conducted for different slip loads, and the results obtained in the computer analysis are shown in Fig. 4.11. As shown, a close agreement exists between the theoretical and experimental results.

Dynamic tests were repeated over a one year period in order to investigate the long term performance of friction joints. In this manner, it was observed that the behavior of the joints did not change significantly.

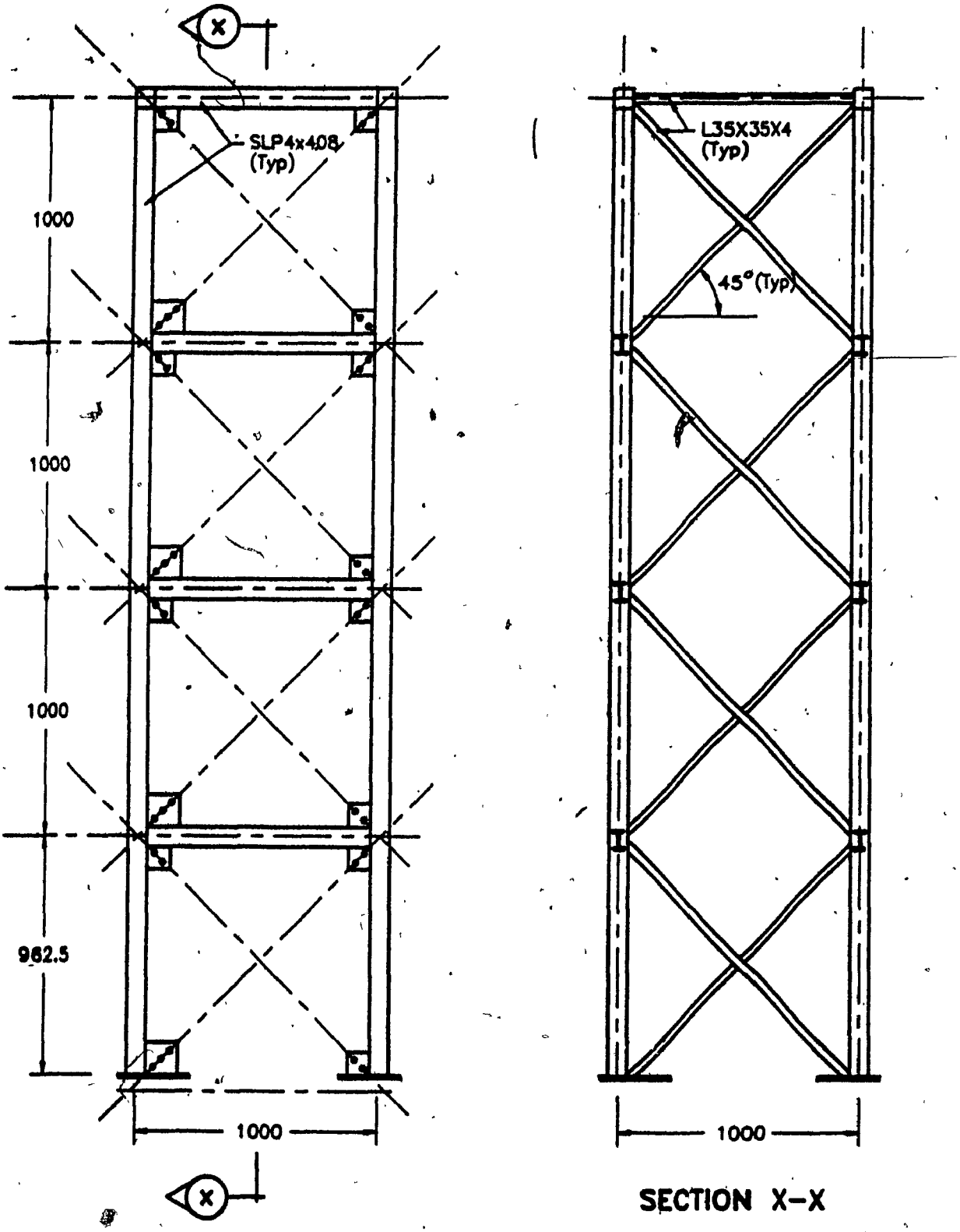

FIG. 4.1 Details of the Model.

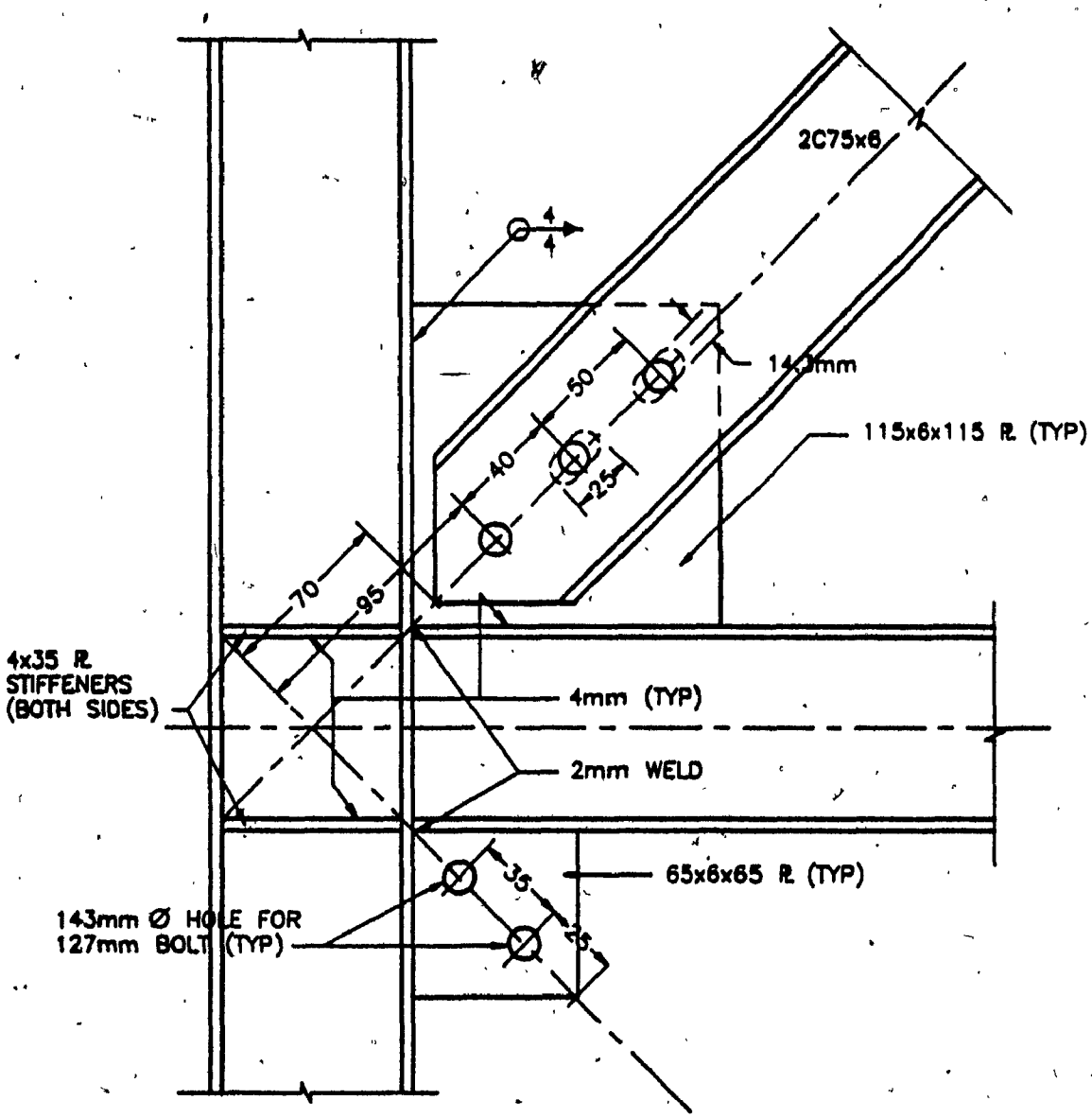

FIG. 4.2 Detail of the Model's Connections.

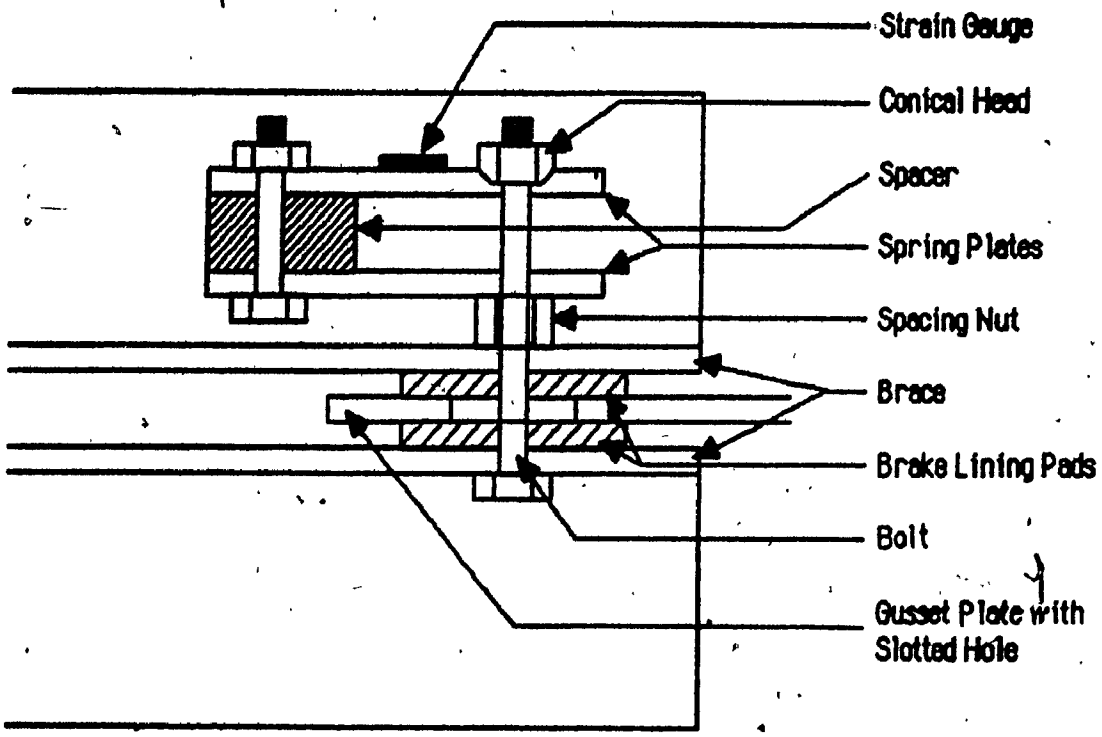

FIG. 4.3 Details of the "Spring Loaded Device" (Sectioned Through Centre Line)

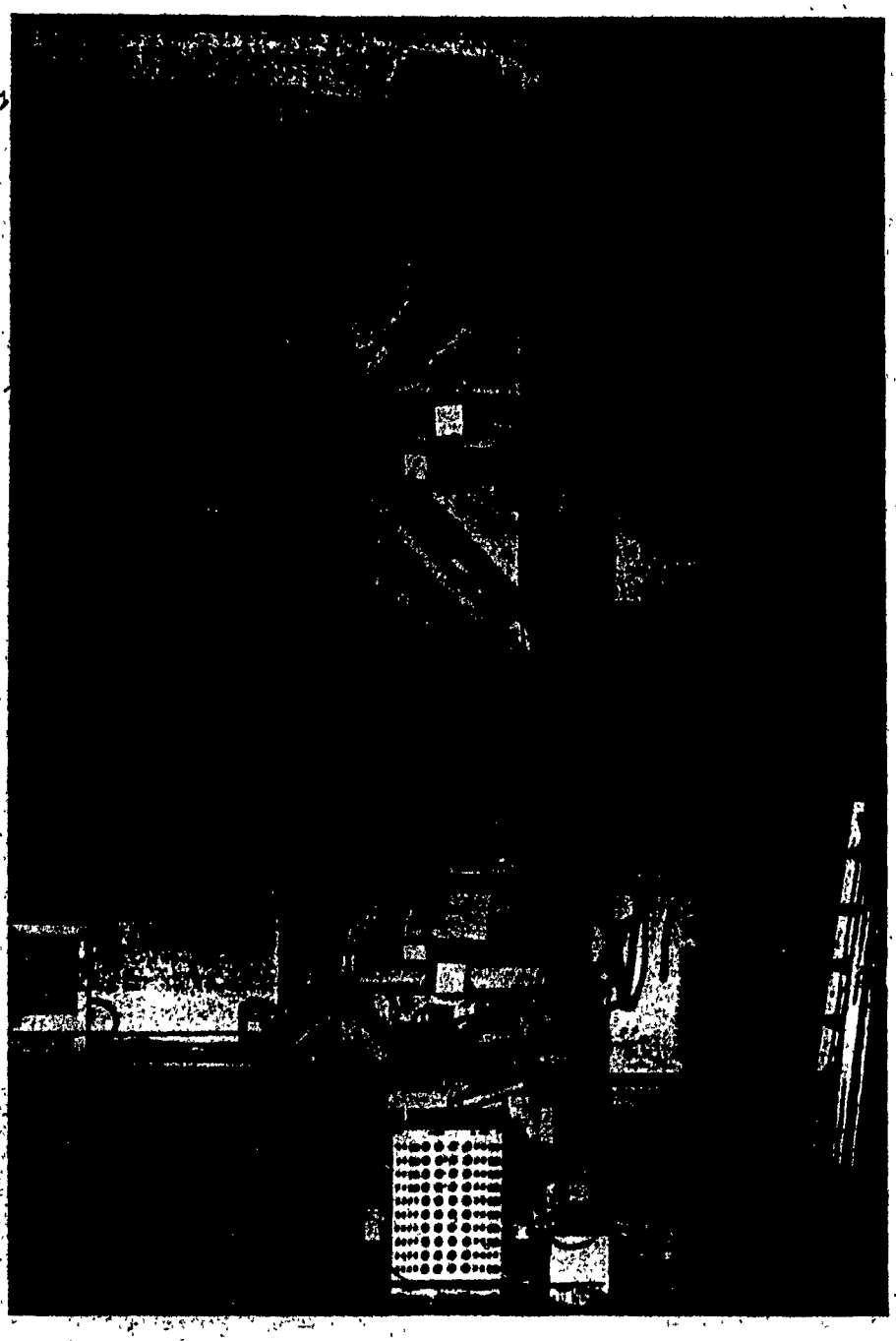

FIG. 4.4 Overall Picture of the Model

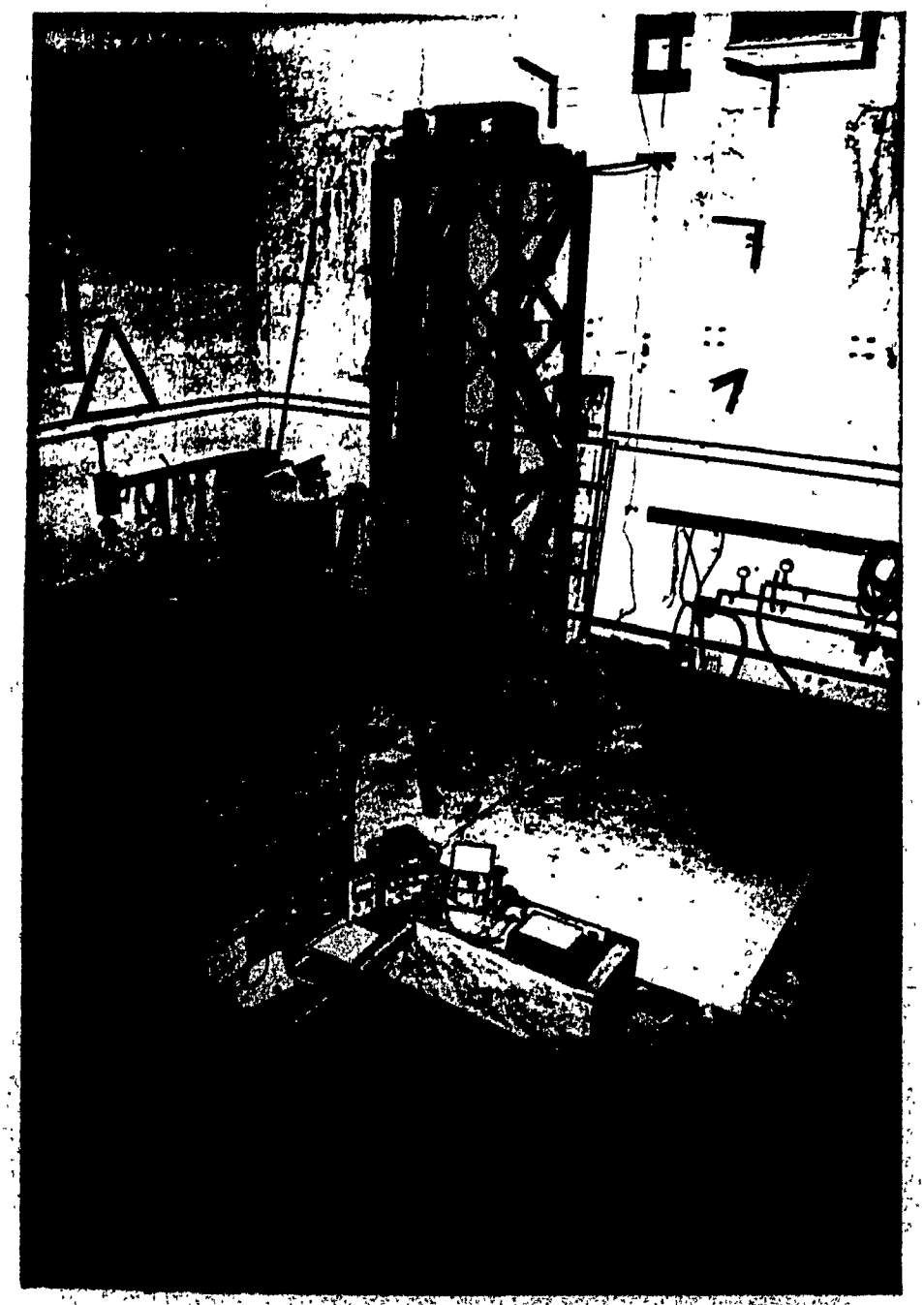

FIG. 4.5 Model on the Shaking Table

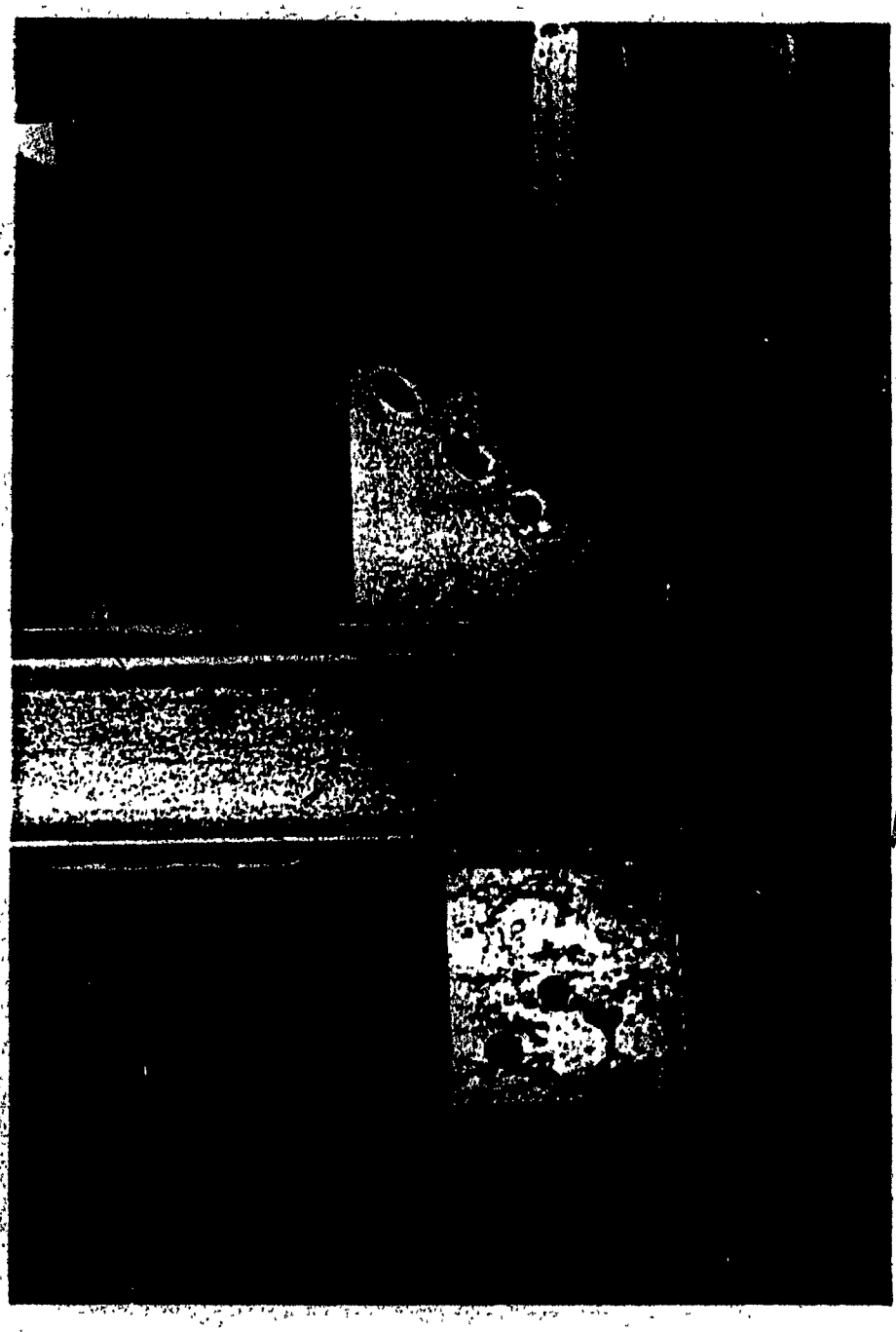

FIG. 4.6 Steel Plates With Slotted Holes

FIG. 4.7 Calibration of the "Spring Loading Device"

FIG. 4.8 Slip Force Adjustment

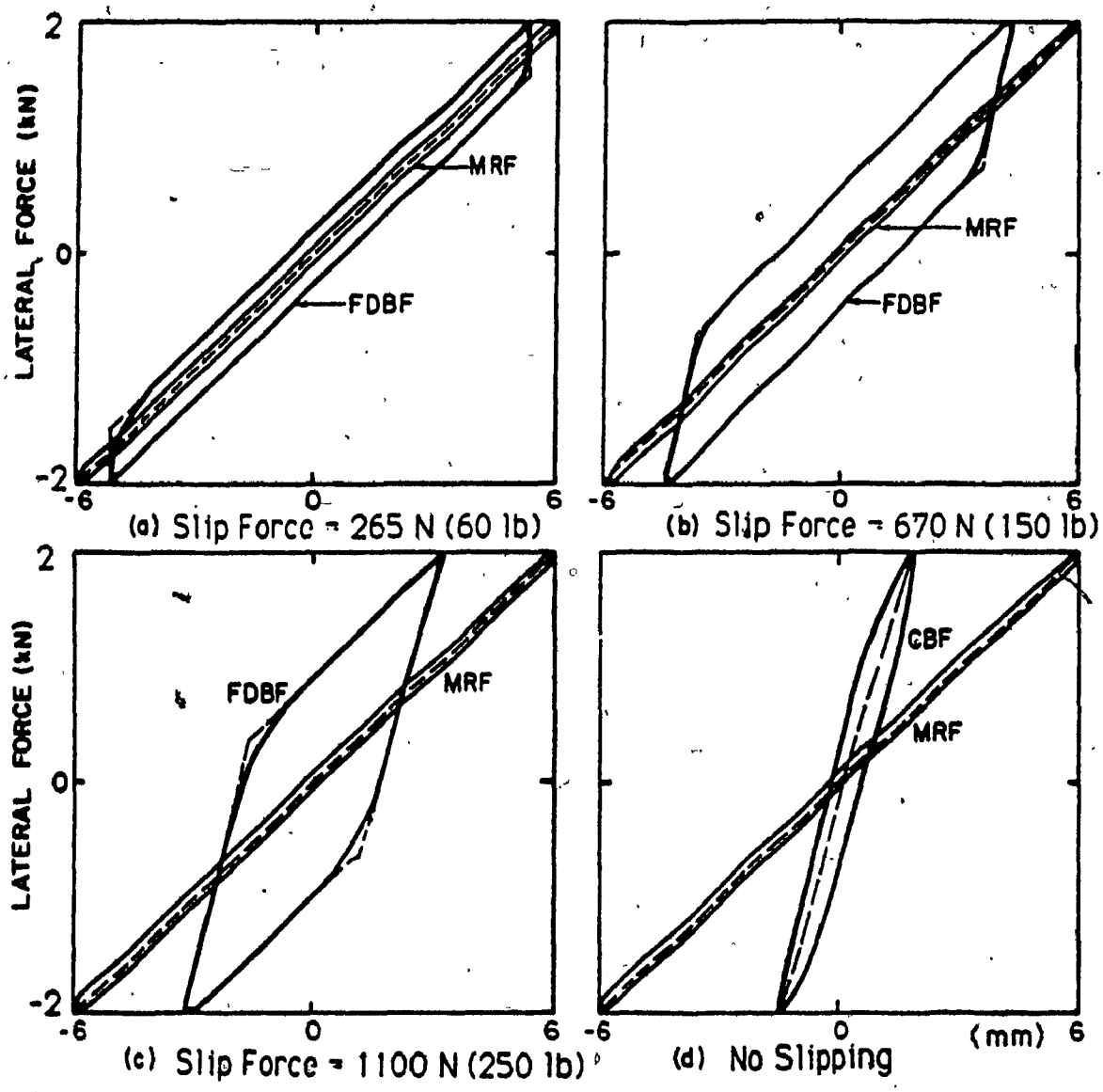

FIG. 4.9 **Lateral Force/Top Storey Deflection Hysteretic Behavior for Different Slip Forces (1in. = 25.4mm, 1lb. = 4.448N)**

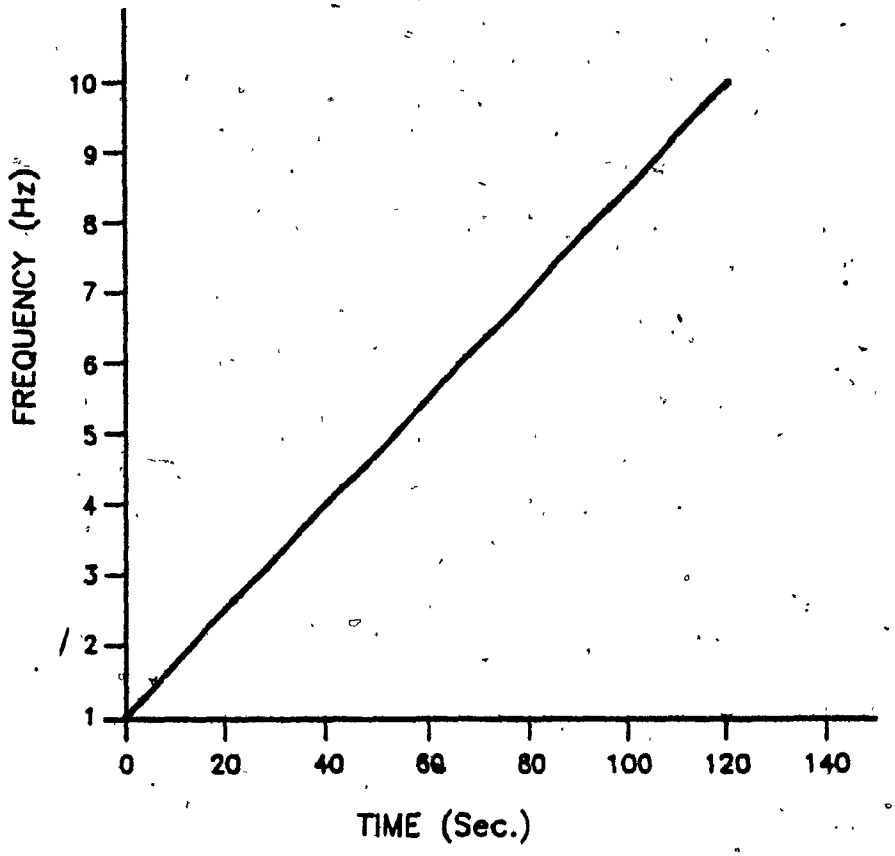

FIG. 4.10 Variation in Frequency of the Shaking Table Versus Time.

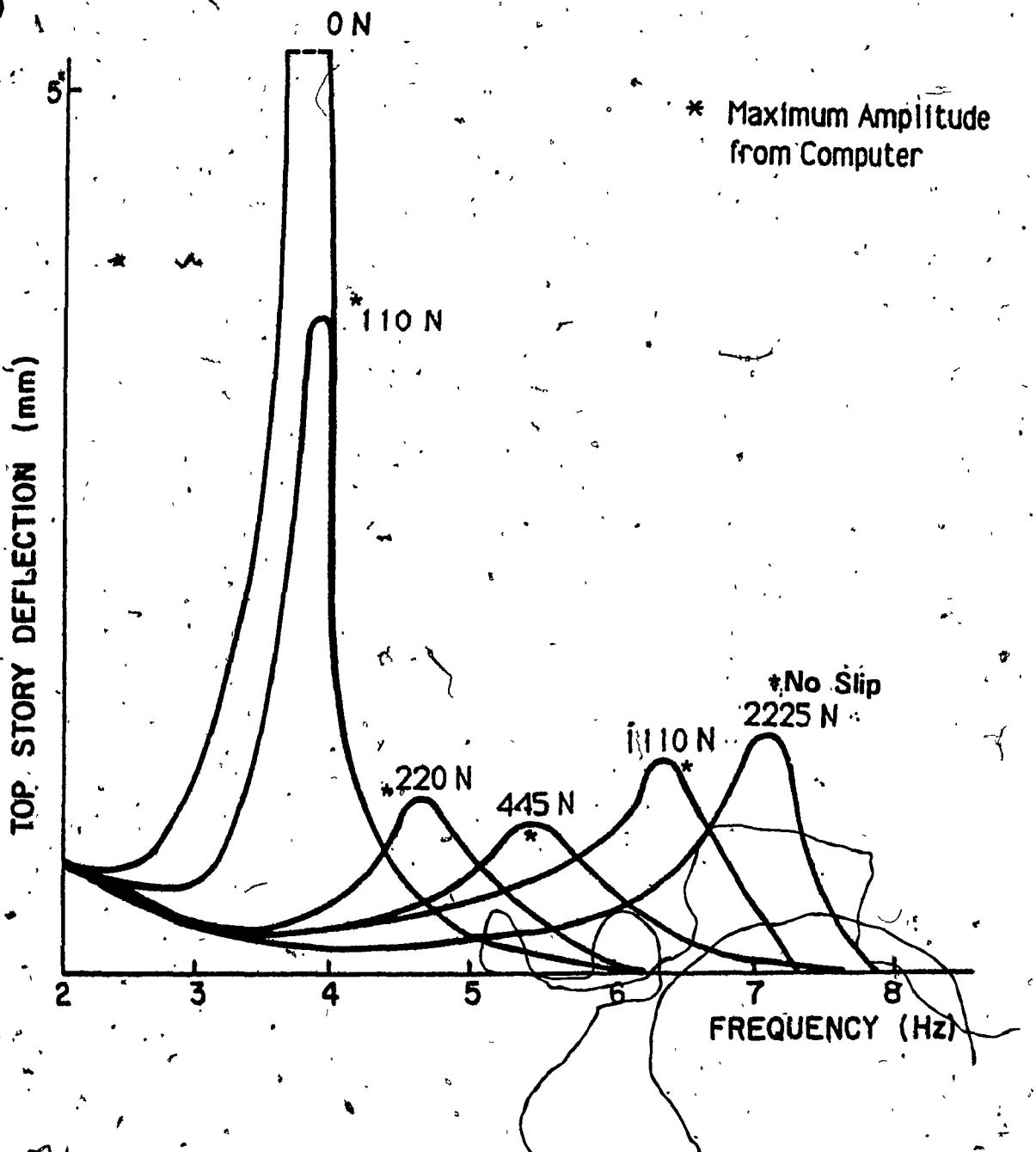

FIG. 4.11 Top Storey Deflection for Different Slip Forces, from Tests and from Computer Analysis (a = 0.106g)

CHAPTER 5

CONCLUSIONS

CONCLUSIONS

5.1- GENERAL

During a major earthquake, steel framed buildings, while capable of remaining standing, may suffer a great deal of permanent and costly damage. For example, a concentric braced frame has a hysteresis behaviour which gives it poor energy dissipating capacity, while the buckling and yielding of the braces cause a rapid decrease in the stiffness of the structure. Moment resisting frames have a stable hysteretic behaviour and good energy dissipating capacity but they tend to become unstable due to excessive lateral displacement resulting in a strong P-Δ effect. Eccentric braced frames combine the merits of concentric braced frames (stiffness), and the energy dissipation of a ductile moment resisting frame, but in a major earthquake the frame would suffer permanent damage to the structural elements.

A structure is required with the energy dissipating capacity of moment resisting frames and the stiffness of braced frames, without relying on permanent damages to the structure to absorb energy. A friction damped braced frame has these characteristics.

This study has shown that friction damped braced frames can absorb energy with little permanent damage, while being readily incorporated into the structural framing.

A simple analysis showed the existence of an optimum slip force based on energy considerations. The results obtained were compared with the results of nonlinear dynamic analysis and were found to be reasonable.

Nonlinear, time history dynamic analyses using Drain-2D were carried out to compare the behaviour of friction damped braced frames, with moment resisting frames, concentric braced frames, and eccentric frames. Friction damped braced frames, with Z and K bracing (effective in tension and compression) and X bracing (or tension only bracing)were also analyzed.

It was shown that for all types of the FDBF, in the optimum arrangement, the acceleration, deflection, and forces in the structural frame are dramatically lower than in traditional framing systems.

For the model steel frame structure that was tested, a "spring loading device" was devised which gave reliable slip forces. Quasi-static tests were conducted and the predicted optimum value of the slip load was demonstrated. It was also shown that a stable and predictable hysteretic loop is achievable. The behaviours were compared with those of nonlinear inelastic analysis using the "ADINA" computer program. The shake table test results were also compared with those of nonlinear dynamic analyses using Drain-2D program. In both cases close agreement was obtained between the experimental value and computer predictions.

It is concluded that:

1. Friction damped braced frames meet the requirements for an efficient energy dissipating mechanism.

2. By simple analysis an optimum slip force can be calculated for a given rigid frame.

3. The slip force can be chosen to suit the moment capacity of the beams, so that all the braces will slip and contribute to the energy dissipation before the frame becomes unstable.

4. Friction joints can be incorporated in many different types of bracing to suit the designer's objectives.

5. The building absorbs energy without permanent damage, the frame remaining elastic for intensities well in excess of those that cause damage in other structural systems.

6. The building becomes more flexible as the braces slip but with no loss of elasticity, resulting in a variable natural frequency, making resonance impossible.

7. The building can be tuned for the optimum response for a specified earthquake.

8. The cost of repairs is minimized.

5.2- RECOMMENDATIONS FOR FUTURE STUDIES:

1 - In the present experimental study the optimization was for a specific model with a specific inputs. Tests with different rigidities, masses, heights and time histories are required to provide fuller information.

2 - Three dimensional analysis could be performed to study the effect of torsional oscillations and to optimize the placing of dampers.

REFERENCES

REFERENCES

1. Pall, A.S., Marsh, C., and Fazio, P., "Friction Joints for Seismic Control of Large Panel Structures," Journal of Prestressed Concrete Institute, Vol. 25, No. 6, November/December, 1980, pp. 38-61.

2. Cardenas, A.E., and Magura, D.D., "Strength of High-rise Shear Walls - Rectangular Cross Sections," ACU Special Publication 26, Response of Multi-story Concrete Structures to Lateral Forces, 1973, pp. 119-147.

3. Bertero, V.V., Popov, E.P. Wang, T.Y., and Vallenas, J., "Seismic Design Implication of the Hysteretic Behaviours of Reinforced Concrete Structural Walls," Proc. Sixth World Conference on Earthquake Engineering, New Delhi, India, 1977, pp. 5-159 to 165.

4. Baktash, P. Marsh, C., and Pall, A.S., "Seismic Tests on a Model Shear Wall with Friction Joints," Canadian Journal of Civil Engineering, Vol. 10, March, 1983, pp. 52-59.

5. Baktash, P., "Experiments on the Seismic Response of a Model of Shear Wall with Friction Joints," Master Thesis, Concordia University, Montreal, September, 1981.

6. Pall, A.S., and Marsh, C., "Friction Damped Concrete Shear Wall," Journal of American Concrete Institute, Proc., Vol, 78, No. 3, May/June, 1981, pp. 187-193.

7. Pall, A.S., "Response of Friction Damped Buildings," Proceedings Eight World Conference on Earthquake Engineering, San Francisco, California, July, 1984.

8. Pall, A.S., and Marsh, C. "Seismic Response of Friction Damped Braced Frames", ASCE, Journal of Strctural Division, No. ST6, June, 1982, pp. 1313-1323.

9. Baktash, P., and Marsh, C., "Seismic Behaviour of Friction Damped Braced Frames", Proceedings Third U.S. National Conference on Earthquake Engineering, Charleston, South Caroline, August, 1986.

10. Baktash, P., and Marsh, C., "Damped Moment Resistant Braced Frames: A Comparative Study," Canadian Journal of Civil Engineering, Vol. 3, No. 3, 1987.

11. Baktash, P., and Marsh, C., "Comparative Seismic Response of Damped Braced Frames," Proceedings of the third Engineering Mechanics Specialty Conference on Dynamic Response of Structures, Los Angeles, California, March/April, 1986.

12. Filiatrault, A., and Cherry, S., "Seismic Tests of Friction Damped Steel Frames," Proceedings of the Third Engineering Mechanics Specialty Conference on Dynamic Response of Structures, Los Angeles, California, March/April, 1986.

13. Austin, M.A., and Pister, K.S., "Optimal Design of Friction Braced Frames under Seismic Loading,: Report No. VCB1EER-83/10, Earthquake Engineering Research Centre, University of California, Berkeley, California, June, 1983.

14. Austin, M.A., and Pister, K.S., "Design of Seismic-Resistant Friction Braced Frames", ASCE, Journal of Structural Divisions, No. 12, Vol. 111,. 1985, pp. 2751-2769.

15. Balling, T.J., and Pister, K.S., Polak, E., "Delight Struct. A Computer Aided Design Environment for Structural Engineering," Report No. EERC 81-19, Earthquake Engineering Research Centre, University of California, Berkeley, California, December, 1981.

16. Popov, E.P., "Seismic Steel Framing Systems for Tall Buildings," AISC Engineering Journal, Vol., 19, No. 3, 1978, pp. 141-149.

17. Goel, S.C., and Hanson, R.D., "Seismic Behaviors of Multistory Braced Steel Frames," ASCE, Journal of Structural Division, Vol. 100, No. ST1, January, 1974, pp. 79-97.

18. Popov, E.P., Takanashi, K., and Roeder, C.W., "Structural Steel Bracing Systems: Behaviors under Cyclic Loading", EERC Report 76-16, Earthquake Engineering Research Centre, University of California, Berkely, California, June, 1976.

19. Roeder, C.E., and Popov, E.P., "Inelastic Behaviors of Eccentrically Braced Steel Frames under Cyclic Loadings," EERC Report No. 77-18, Earthquake Engineering Research Centre, University of California, August, 1977.

20. Roeder, C.W., and Popov, E.P., "Eccentrically Braced Steel Frames for Earthquakes", ASCE, Journal of Structural Division, Vol. 104, No. ST3, March, 1987, pp. 391-411.

21. Popov, E.P., and Black, R., "Steel Struts under Severe Cyclic Loadings," ASCE, Journal of Structural Division, Vol. 107, No. ST9. September, 1981, pp. 1857-1881.

22. Wakabyashi, M., Matsui, C., Minami, K., and Mitani, I., "Inelastic Behaviour of Full Scale Steel Frames with and without Bracing," Bulletin Disaster Prevention Research Institute, Kyoto University, Kyoto, Japan, Vol. 24, Part 1, No. 216, March, 1974.

23. Workman, G.H., "Inelastic Behaviour of Multistory Braced Frame Structures Subjected to Earthquake Excitation," Ph.D. Thesis, University of Michigan, Ann Arbor, Michigan, 1969.

24. Jain, A.K., and Goel, S.C., "Hysteresis Models for Steel Members Subjected to Cyclic Buckling or Cyclic End Moments and Buckling," Report No. UMEE 78R6, University of Michigan, Ann Arbor, Michigan, 1969.

25. Popov, E.P., and Bertero, V.V., "Seismic Analysis of Some Steel Building Frames," ASCE, Journal of Engineering Mechanic Division, No. EM1, February, 1980, pp. 75-92.

26. Fujimoto, M. Aoyagi, T., Ukai, K., Wada, A., and Saito, K., "Structural Characteristics of Eccentric K-Brace Frames," Tran. AIJ, No. 195, May, 1972.

27. Hisatoku, T., et al, "Experimental Study on the Static Behaviours of the Y-Typed Bracings, Report of Takenaka Technical Institute, No. 12, August, 1974.

28. Popov, E.P., and Roeder, C.W., "Design of Eccentrically Braced Steel Frame", AISC Engineering Journal, Vol. 15, No. 3., 1978, pp. 77-81.

29. Kanaan, A.E., and Powell, G.H., "Drain-2D, A General Purpose Computer Program of Dynamic Analysis of Inelastic Plane Structures", College of Engineering, University of California, Berkeley, California, 1973.

30. Nilforoushan, R., "Seismic Behaviors of Multistory K-Braced Frame Structures," Research Report, UMEE 73R9, University of Michigan, Ann Arbor, Michigan, November, 1973.

31. Clough, R.W., and Penzien, J., "Dynamics of Structures," McGraw-Hill Book Co., 1975.

32. Higginbotham, A.B., "The Inelastic Cyclic Behaviours of Axially loaded Steel Members", Ph.D. Thesis, University of Michigan, Ann Arbor, Michigan, 1973.

33. Singh, P., "Seismic Behaviour of Braces and Braced Steel Frames", PhD. Thesis, University of Michigan, Ann Arbor, Michigan, July, 1977.

34. Marshall, P.W., "Design Consideration for Offshore Structures Having Nonlinear Response to Earthquakes," ASCE Annual Convention and Exposition, Chicago, October, 1978, Preprint No. 3302, pp. 148-172.

35. Jain, A.K., "Hysteresis Behaviors of Bracing Members and Seismic Response of Braced Frames with Different Proportions," Ph.D. Thesis, University of Michigan, Ann Arbor, Michigan, July, 1978.

36. Wilson, E.L. and Dovey, H.H., "Three Dimensional Analysis of Building Systems, TABS," Report No. EERC 72-8, University of California, 1972.

37. ADINA, "A Finite Element Program for Automatic Incremental Nonlinear Analysis," Report AE81-1, ADINA Engineering, September, 1981.

APPENDIX A

LISTING OF THE MODIFIED SUBROUTINES FOR TENSION ONLY BRACING

```
      SUBROUTINE INEL1 (KCONT,FCONT,NDOF,NINFC,ID,X,Y,NN)
C
C
      COMMON /IFLAG/ FLAG(40)
      COMMON /INFEL/ IMEM,KST,LM(4),KGEOM,EALEP,EALE,FL,COSA,SINA,
     -               KODYX,KODY,SEP,SEL,VTOT,VPACP,VPACN,VBUCK,VENP,
     -               TVENP,VENN,TVENN,SENP,TSENP,SENN,TSENN,SDFO,
     -               NODI,NODJ,KOUTDT,KBUCK,PYP,PYN,IMEMI,BK,REST(163)
      COMMON /WORK/ FTYP(40,5),KBUC(40),FEF(40,4),KDFEF(40),DD(4),
     -              GA(4,4),FFEF(4),SFF(4),SSFF(4),NMEM,NMBT,NFEF,
     -              GNEL,INEL,INODI,INODJ,INC,IINC,IMBT,IIMBT,IKGM,
     -              IKDT,KFDL,IKFDL,KFLL,IKFLL,FDL,FFDL,FLL,FFLL,
     -              FINIT,FFINIT,XL,YL,PSH,PPSH,AREA,W(1505)
      COMMON /THIST/ ITHOUT(10),THOUT(20),ITHP,ISAVE,NELTH,NSTH,NF7,
     -               ISE
C
      DIMENSION KCONT(1),ID(NN,1),X(1),Y(1),COM(1)
      DIMENSION AST(2),YESNO(2)
      EQUIVALENCE (IMEM,COM(1))
      DATA AST /2H  ,2H */
      DATA YESNO /4H YES,4H NO /
C
C  CONTROL VARIABLES
C
      NDOF=4
      NINFC=37
      NMEM=KCONT(2)
      NMBT=KCONT(3)
      NFEF=KCONT(4)
      WRITE (9,10) (KCONT(I),I=2,4)
   10 FORMAT (' TRUSS ELEMENTS (TENSION ONLY BRACING)'////
     -        ' NO. OF ELEMENTS          =',I4/
     -        ' NO. OF STIFFNESS TYPES =',I4/
     -        ' NO. OF F.E.F. PATTERNS =',I4)
C
C  INPUT STIFFNESS PROPERTIES
C
      WRITE (9,20)
   20 FORMAT (////' STIFFNESS TYPES'//
     -        ' TYPE',7X,'YOUNGS    HARDENING',6X,'SECTION    ',
     -        'POS. YIELD   NEG. YIELD    BUCKLING'/
     -        '  NO.',6X,'MODULUS      RATIO',10X,'AREA',7X,
     -        'STRESS',7X,'STRESS',8X,'CODE'/)
C
      DO 30 IT=1,NMBT
         READ (8,40) I,(FTYP(IT,J),J=1,5),KBUC(IT)
         WRITE (9,50) IT,(FTYP(IT,J),J=1,5),KBUC(IT)
   40    FORMAT (I5,5F10.0,I5)
   50    FORMAT (I4,E14.4,E13.4,3F13.2,I10)
   30 CONTINUE
C
C  FIXED END FORCE PATTERNS
C
      IF (NFEF.EQ.0) GO TO 100
      WRITE (9,60)
```

```
   60 FORMAT (/////' FIXED END FORCE PATTERNS'//
     -       ' PATTERN   AXIS',2(7X,'AXIAL',7X,'SHEAR')/
     -       '    NO.    CODE',2(7X,'AT  I'),2(7X,'AT  J')//)
      DO 70 NF=1,NFEF
         READ (8,80) I,KDFEF(NF),(FEF(NF,J),J=1,4)
         WRITE (9,90) NF,KDFEF(NF),(FEF(NF,J),J=1,4)
   80    FORMAT (2I5,4F10.0)
   90    FORMAT (I6,I8,1X,4F12.2)
   70 CONTINUE
C
C  ELEMENT DATA
C
  100 WRITE (9,110)
  110 FORMAT (////' ELEMENT SPECIFICATION'//
     -       3X,'ELEM  NODE  NODE  NODE  STIF  GEOM  TIME',
     -       3X,'FEF PATTERNS    FEF SCALE FACTORS',5X,'INITIAL'/
     -       3X,' NO.     I     J   DIFF  TYPE  STIF  HIST',
     -       3X,'  DL    LL',8X,'DL        LL',7X,' FORCE'/)
      KODYX=0
      KODY=0
      KST=0
      DO 120 J=15,29
  120 COM(J)=0.
      DO 125 JJ=1,40
  125 FLAG(JJ)=0.
      BK=0.
      IMEM=1
  130 READ (8,140) INEL,INODI,INODJ,IINC,IIMBT,IKGM,IKDT,IKFDL,
     -             IKFLL,FFDL,FFLL,FFINIT,IIMEM1,IINC1
  140 FORMAT (9I5,3F5.0,2I5)
      IF (INEL.GT.IMEM) GO TO 170
  150 NODI=INODI
      NODJ=INODJ
      INC=IINC
      IF (INC.EQ.0) INC=1
      IMEM1=IIMEM1
      INC1=IINC1
      IF(INC1.EQ.0) INC1=1
      IMBT=IIMBT
      KGEOM=IKGM
      KOUTDT=IKDT
      YNG=YESNO(2)
      IF (KGEOM.NE.0) YNG=YESNO(1)
      YNT=YESNO(2)
      IF (KOUTDT.NE.0) YNT=YESNO(1)
      KFDL=IKFDL
      KFLL=IKFLL
      FDL=FFDL
      FLL=FFLL
      FINIT=FFINIT
      AST=AST(1)
      IF (INEL-NMEM) 130,170,130
  160 NODI=NODI+INC
      NODJ=NODJ+INC
      IMEM1=IMEM1+INC1
```

```
      ASTT=AST(2)
  170 WRITE (9,180) ASTT,IMEM,NODI,NODJ,INC,IMBT,YNG,YNT,KFDL,KFLL,
     -                  FDL,FLL,FINIT,IMEM1
  180 FORMAT (A2,I4,I7,3I6,3X,A4,2X,A4,I7,I6,F11.2,F10.2,F11.2,I5)
C
C  COUNT NUMBER OF ELEMENT TIME HISTORIES
C
      IF (KOUTDT.NE.0) NELTH=NELTH+1
C
C  LOCATION MATRIX
C
      DO 190 L=1,2
         LM(L)=ID(NODI,L)
         LM(L+2)=ID(NODJ,L)
  190 CONTINUE
      CALL BAND
C
C  ELEMENT PROPERTIES
C
      XL=X(NODJ)-X(NODI)
      YL=Y(NODJ)-Y(NODI)
      FL=SQRT(XL**2+YL**2)
      COSA=XL/FL
      SINA=YL/FL
      KBUCK=KBUC(IMBT)
      PSH=FTYP(IMBT,2)
      PPSH=1.-PSH
      AREA=FTYP(IMBT,3)
      EALEP=FTYP(IMBT,1)*PPSH*AREA/FL
      EALE=EALEP*PSH/PPSH
      PYP=AREA*FTYP(IMBT,4)*PPSH
      PYN=AREA*(-ABS(FTYP(IMBT,5)))*PPSH
C
C  LOADS DUE TO FIXED END FORCES
C
      SFEF=0.
      IF (KFDL+KFLL.EQ.0) GO TO 310
      DO 200 I=1,NDOF
      DO 200 J=1,NDOF
  200 GA(I,J)=0.
      GA(1,1)=COSA
      GA(1,2)=SINA
      GA(2,1)=-SINA
      GA(2,2)=COSA
      GA(3,3)=COSA
      GA(3,4)=SINA
      GA(4,3)=-SINA
      GA(4,4)=COSA
      DO 210 I=1,4
         SFF(I)=0.
         SSFF(I)=0.
  210 CONTINUE
      IF (KFDL.EQ.0) GO TO 250
      DO 220 I=1,4
  220 FFEF(I)=FEF(KFDL,I)*FDL
```

```
      IF (KDFEF(KFDL).EQ.0) GO TO 230
      CALL MULT (GA,FFEF,SFF,4,4,1)
      GO TO 250
  230 DO 240 I=1,4
  240 SFF(I)=FFEF(I)
  250 IF (KFLL.EQ.0) GO TO 290
      DO 260 I=1,4
  260 FFEF(I)=FEF(KFLL,I)*FLL
      IF (KDFEF(KFLL).EQ.0) GO TO 270
      CALL MULT (GA,FFEF,SSFF,4,4,1)
      GO TO 290
  270 DO 280 I=1,4
  280 SSFF(I)=FFEF(I)
  290 DO 300 I=1,4
  300 SSFF(I)=SSFF(I)+SFF(I)
      CALL MULTT (GA,SSFF,DD,4,4,1)
      CALL SFORCE (DD)
C
C  INITIALIZE ELEMENT FORCE
C
      SFEF=(SSFF(3)-SSFF(1))*0.5
  310 FF=FINIT+SFEF
      SEP=PPSH*FF
      SEL=PSH*FF
      IF (FINIT.LT.0.) GO TO 320
      SENP=FINIT
      SENN=0.
      GO TO 330
  320 SENN=FINIT
      SENP=0.
  330 CALL FINISH
C
C  GENERATE MISSING ELEMENTS
C
      IF (IMEM.EQ.NMEM) RETURN
      IMEM=IMEM+1
      IF (IMEM:EQ.INEL) GO TO 150
      GO TO 160
C
      RETURN
      END
```

```
      SUBROUTINE STIF1 (MSTEP,NDOF,NINFC,COMS,FK,DFAC)
C
C
      COMMON /IFLAG/ FLAG(40)
      COMMON /INFEL/ IMEM,KST,LM(4),KGEOM,EALEP,EALE,FL,COSA,SINA,
     -               KODYX,KODY,SEP,SEL,VTOT,VPACP,VPACN,VBUCK,VENP,
     -               TVENP,VENN,TVENN,SENP,TSENP,SENN,TSENN,SDFO,
     -               NODI,NODJ,KOUTDT,KBUCK,PYP,PYN,IMEM1,BK,REST(163)
      COMMON /WORK/ SST(2,2),AA(2,4),AATK(4,2),FFK(4,4),W(1969)
C
      DIMENSION COM(14),COMS(14),FK(4,4)
      EQUIVALENCE (IMEM,COM(1))
C
C  TRUSS ELEMENT STIFFNESS FORMULATION
C
      DO 10 J=3,14
   10 COM(J)=COMS(J)
C
C  ELASTOPLASTIC COMPONENT, WITHOUT YIELD
C
      FK(1,1)=EALEP*COSA**2
      FK(1,2)=EALEP*SINA*COSA
      FK(1,3)=-FK(1,1)
      FK(1,4)=-FK(1,2)
      FK(2,2)=EALEP*SINA**2
      FK(2,3)=FK(1,4)
      FK(2,4)=-FK(2,2)
      FK(3,3)=FK(1,1)
      FK(3,4)=FK(1,2)
      FK(4,4)=FK(2,2)
      DO 20 I=2,4
      JJ=I-1
      DO 20 J=1,JJ
   20 FK(I,J)=FK(J,I)
C
C  CHANGE SIGN IF YIELDS
C
      IF (KODY.EQ.0) GO TO 40
      DO 30 I=1,16
   30 FK(I,1)=-FK(I,1)
      GO TO 90
C
C  INITIAL STIFFNESS FOR STEP 0, BETA-0 ALLOWANCE FOR STEP 1
C
   40 IF (MSTEP.GT.1) GO TO 90
      CC=1.
      IF (MSTEP.EQ.1) CC=DFAC
      CC=(1.+EALE/EALEP)*CC
      DO 50 I=1,16
   50 FK(I,1)=FK(I,1)*CC
C
C  ADD GEOMETRIC STIFFNESS
C
      IF (MSTEP.EQ.0.OR.KGEOM.EQ.0) GO TO 90
      PFL=(COMS(15)+COMS(16))/FL
```

```
      DO 60 I=1,4
   60 SST(I,1)=PFL
      DO 70 I=1,8
   70 AA(I,1)=0.
      AA(1,1)=-SINA
      AA(1,2)=COSA
      AA(2,3)=SINA
      AA(2,4)=-COSA
      CALL MULTST (AA,SST,AATK,FFK,4,2)
      DO 80 I=1,16
   80 FK(I,1)=FK(I,1)+FFK(I,1)
C
   90 RETURN
      END
```

```
      SUBROUTINE RESP1 (NDOF,NINFC,KBAL,KPR,COMS,DDISM,DD,TIME,VELM,
     -                  DFAC,DELTA)
C
      COMMON /IFLAG/ FLAG(40)
      COMMON /INFEL/ IMEM,KST,LM(4),KGEOM,EALEP,EALE,FL,COSA,SINA,
     -               KODYX,KODY,SEP,SEL,VTOT,VPACP,VPACN,VBUCK,VENP,
     -               TVENP,VENN,TVENN,SENP,TSENP,SENN,TSENN,SDFO,
     -               NODI,NODJ,KOUTDT,KBUCK,PYP,PYN,IMEM1,BK,REST(163)
      COMMON /WORK/ EAL,DSL,DSEP,DSNL,FAC,FACTOR,FACACC,DSUB,
     -              POUT(1997)
      COMMON /THIST/ ITHOUT(10),THOUT(20),ITHP,ISAVE,NELTH,NSTH,NF7,
     -               ISE
C
      DIMENSION COM(14),COMS(14),DDISM(1),DD(1),VELM(1)
      EQUIVALENCE (IMEM,COM(1))
C
C   STATE DETERMINATION FOR TRUSS ELEMENTS
C
      DO 10 I=1,NINFC
   10 COM(I)=COMS(I)
      KODYX=KODY
      BK=FLAG(IMEM)
      IF (IMEM.EQ.1) IHED=0
      BT=FLAG(IMEM1)
      IF (BT.EQ.0.) GO TO 11
      KBUCK=0
      P=-PYNN
      IF (P.GT.PYP) PYN=-PYP
      IF (P.LE.PYP) PYN=PYNN
      GO TO 12
   11 KBUCK=1
      PYN=PYNN
   12 CONTINUE
C
C  EXTENSION INCREMENT
C
      DV=COSA*(DDISM(3)-DDISM(1))+SINA*(DDISM(4)-DDISM(2))
      VTOT=VTOT+DV
C
C  LINEAR FORCE INCREMENT
C
      EAL=EALEP
      IF (KODY.NE.0) EAL=0.
      SLIN=SEP+EAL*DV
C
C  INITIALIZE
C
      FACAC=0.
   20 FACTOR=1.-FACAC
C
C  ELASTIC, GET FACTOR FOR STATUS CHANGE
C
      IF (KODY.NE.0) GO TO 60
      DSEP=EALEP*DV
      IF (DSEP) 30,110,40
```

```
   30 FAC=(PYN-SEP)/DSEP
      IF (FAC.GE.FACTOR) GO TO 50
      FACTOR=FAC
      SEP=PYN
      KODY=1
      VBUCK=0.
      GO TO 110
   40 FAC=(PYP-SEP)/DSEP
      IF (FAC.GE.FACTOR) GO TO 50
      FACTOR=FAC
      SEP=PYP
      KODY=1
      BK=1
      GO TO 110
   50 SEP=SEP+FACTOR*DSEP
      GO TO 110
C
C  YIELDED OR BUCKLING, AND CONTINUING
C
   60 IF (SEP*DV.LT.0.) GO TO 80
C
C  UPDATE PLASTIC DEFORMATIONS
C
      IF (KBUCK.NE.0.AND.SEP.LT.0.) GO TO 70
      DVP=FACTOR*DV
      IF (DVP.GT.0.) VPACP=VPACP+DVP
      IF (DVP,LT.0.) VPACN=VPACN+DVP
   70 VBUCK=VBUCK-FACTOR*DV
      GO TO 120
C
C  YIELDED BUT UNLOADING
C
   80 IF (KBUCK.NE.0.AND.SEP.LT.0.) GO TO 90
      KODY=0
      GO TO 20
C
C  BUCKLING AND REVERSING
C
   90 FAC=VBUCK/DV
      IF (FAC.GE.FACTOR) GO TO 100
      FACTOR=FAC
      KODY=0
  100 VBUCK=VBUCK-FACTOR*DV
C
C  CHECK FOR COMPLETION OF CYCLE
C
  110 FACAC=FACAC+FACTOR
      IF (FACAC.LT.0.9999999) GO TO 20
C
C  NEW FORCE, UNBALANCED FORCE DUE TO YIELD
C
  120 SEL=SEL+EALE*DV
      ST=SEP+SEL
      DSUB=SLIN-SEP
      IF (ABS(DSUB).GT.1.E-8) KBAL=1
```

```
C
C  DEFORMATION RATE FOR DAMPING
C
      IF (DFAC.EQ.0.0.AND.DELTA.EQ.0.0) GO TO 140
      IF (TIME.EQ.0.) GO TO 150
      KBAL=1
      DV=COSA*(VELM(3)-VELM(1))+SINA*(VELM(4)-VELM(2))
C
C  BETA-O DAMPING FORCE
C
      IF (DFAC.EQ.0.) GO TO 130
      DSUB=DSUB+DFAC*(EALE+EALEP)*DV
C
C  STRUCTURAL DAMPING FORCE
C
  130 IF (DELTA.EQ.0.) GO TO 140
      DSL=DELTA*SIGN(ABS(ST),DV)
      DSUB=DSUB-DSL+SDFO
      SDFO=DSL
C
C  UNBALANCED LOAD VECTOR
C
  140 IF (KBAL.EQ.0) GO TO 150
      DD(3)=DSUB*COSA
      DD(4)=DSUB*SINA
      DD(1)=-DD(3)
      DD(2)=-DD(4)
C
C  ACCUMULATE ENVELOPES
C
  150 IF (SENP.GE.ST) GO TO 160
      SENP=ST
      TSENP=TIME
      GO TO 170
  160 IF (SENN.LE.ST) GO TO 170
      SENN=ST
      TSENN=TIME
  170 IF (VENP.GE.VTOT) GO TO 180
      VENP=VTOT
      TVENP=TIME
      GO TO 190
  180 IF (VENN.LE.VTOT) GO TO 190
      VENN=VTOT
      TVENN=TIME
C
C  PRINT TIME HISTORY
C
  190 ISAVE=0
      IF (KPR.LT.0) GO TO 200
      IF (KPR.EQ.0.OR.KOUTDT.EQ.0) GO TO 250
      IF (ITHP.GT.1) GO TO 240
  200 IF (IHED.NE.0) GO TO 220
      KKPR=IABS(KPR)
      WRITE (9,210) KKPR,TIME
  210 FORMAT (///' RESULTS FOR GROUP',I3,', TRUSS ELEMENTS, TIME =',
```

```
     -        F8.3//5X,' ELEM   NODE   NODE   YIELD',8X,'AXIAL',6X,
     -        'TOTAL',5X,'ACCUM. PLASTIC EXTENSIONS'/
     -        7X,'NO.     I      J     CODE',8X,'FORCE',4X,
     -        'EXTENSION     POSITIVE     NEGATIVE'/)
      IHED=1
  220 WRITE (9,230) IMEM,NODI,NODJ,KODY,ST,VTOT,VPACP,VPACN
  230 FORMAT (I9,2I7,I8,F14.2,3F13.5)
C
C  SET TIME HISTORY IN /THIST/
C
  240 IF (ITHP.LT.1.OR.KOUTDT.EQ.0) GO TO 250
      KKPR=IABS(KPR)
      ITHOUT(1)=KKPR
      ITHOUT(2)=1
      ITHOUT(3)=IMEM
      ITHOUT(4)=NODI
      ITHOUT(5)=NODJ
      ITHOUT(6)=KODY
      THOUT(1)=ST
      THOUT(2)=VTOT
      THOUT(3)=VPACP
      THOUT(4)=VPACN
      THOUT(5)=TIME
      ISAVE=1
C
C  SET INDICATOR FOR STIFFNESS CHANGE
C
  250 KST=0
      IF (KODYX.NE.KODY) KST=1
      IF (BK.NE.FLAG(IMEM)) FLAG(IMEM)=BK
C
C  UPDATE INFORMATION IN COMS
C
      DO 260 J=1,NINFC
  260 COMS(J)=COM(J)
C
      RETURN
      END
```

```
      SUBROUTINE OUT1 (COMS,NINFC)
C
C
      COMMON /IFLAG /FLAG(40)
      COMMON /INFEL/ IMEM,KST,LM(4),KGEOM,EALEP,EALE,FL,COSA,SINA,
     -               KODYX,KODY,SEP,SEL,VTOT,VPACP,VPACN,VBUCK,VENP,
     -               TVENP,VENN,TVENN,SENP,TSENP,SENN,TSENN,SDFO,
     -               NODI,NODJ,KOUTDT,KBUCK,PYP,PYN,IMEM1,BK,REST(163)
C
      DIMENSION COM(1),COMS(1)
      EQUIVALENCE (IMEM,COM(1))
C
C  ENVELOPE OUTPUT, TRUSS ELEMENTS
C
      DO 10 J=1,NINFC
   10 COM(J)=COMS(J)
      IF (IMEM.EQ.1) WRITE (9,20)
   20 FORMAT (' TRUSS ELEMENTS (TENSOIN ONLY BRACING)'///
     -        ' ELEM   NODE   NODE',11X,'MAXIMUM AXIAL FORCES',19X,
     -        'MAXIMUM EXTENSIONS',12X,'ACCUM. PLASTIC EXTENSIONS'/
     -        '  NO.     I      J',6X,'TENSION   TIME',6X,
     -        'COMPN   TIME     POSITIVE   TIME   NEGATIVE   ',
     -        'TIME',7X,'POSITIVE     NEGATIVE'/)
      WRITE (9,30) IMEM,NODI,NODJ,SENP,TSENP,SENN,TSENN,VENP,TVENP,
     -             VENN,TVENN,VPACP,VPACN
   30 FORMAT (I4,I7,I7,2X,2(F11.2,F7.2),2X,2(F11.5,F7.2),2X,2F13.5)
C
      RETURN
      END
```

```
      SUBROUTINE THPR1 (NS)
C
      COMMON /THIST/ ITHOUT(10),THOUT(20),ITHP,ISAVE,NELTH,NSTH,NF7,
     1               ISE
C
C  REORGANIZED TIME HISTORY OUTPUT, TRUSS ELEMENTS
C
      IF (NS.GT.1) GO TO 20
      WRITE (9,10) ITHOUT(1),ITHOUT(3)
   10 FORMAT ('1RESULTS FOR GROUP',I3,', TRUSS ELEMENTS, ELEMENT ',
     -        'NO.',I4//5X,' TIME   NODE   NODE   YIELD',8X,'AXIAL',
     -        6X,'TOTAL      ACCUM. PLASTIC EXTENSIONS'/15X,
     -        'I      J      CODE',8X,'FORCE    EXTENSION',5X,
     -        'POSITIVE      NEGATIVE'/)
   20 WRITE (9,30) THOUT(5),(ITHOUT(I),I=4,6),(THOUT(I),I=1,4)
   30 FORMAT ('0',F8.3,2I7,I8,F14.2,3F13.5)
      IF (ISE.EQ.0) GO TO 40
      WRITE (NF7) THOUT(5),(ITHOUT(I),I=4,6),(THOUT(I),I=1,4)
C
   40 RETURN
      END
```